SPATIO-TEMPORAL CHANGES OF LAKE WATER EXTENTS IN LAKES REGION (TURKEY) USING REMOTE SENSING

A THESIS SUBMITTED TO
THE GRADUATE SCHOOL OF NATURAL AND APPLIED SCIENCES
OF
MIDDLE EAST TECHNICAL UNIVERSITY

BY

EMIN ATABEY PEKER

IN PARTIAL FULFILLMENT OF THE REQUIREMENTS
FOR
THE DEGREE OF MASTER OF SCIENCE
IN
GEODETIC AND GEOGRAPHIC INFORMATION TECHNOLOGIES

JUNE 2019

Approval of the thesis:

SPATIO-TEMPORAL CHANGES OF LAKE WATER EXTENTS IN LAKES REGION (TURKEY) USING REMOTE SENSING

submitted by **EMIN ATABEY PEKER** in partial fulfillment of the requirements for the degree of **Master of Science in Geodetic and Geographic Information Technologies Department, Middle East Technical University** by,

Prof. Dr. Halil Kalıpçılar
Dean, Graduate School of **Natural and Applied Sciences** ________________

Prof. Dr. Zuhal Akyürek
Head of Department, **Geodetic and Geographic Information Technologies** ________________

Assoc. Prof. Dr. Koray K. Yılmaz
Supervisor, **Geological Engineering Dept., METU** ________________

Prof. Dr. M. Lütfi Süzen
Co-Supervisor, **Geological Engineering Dept., METU** ________________

Examining Committee Members:

Prof. Dr. Elçin Kentel Erdoğan
Civil Engineering Dept., METU ________________

Assoc. Prof. Dr. Koray K. Yılmaz
Geological Engineering Dept., METU ________________

Prof. Dr. M. Lütfi Süzen
Geological Engineering Dept., METU ________________

Prof. Dr. İsmail Yücel
Civil Engineering Dept., METU ________________

Assoc. Prof. Dr. Özlem Yağbasan
Geography Education Dept., Gazi University ________________

Date: 17.06.2019

I hereby declare that all information in this document has been obtained and presented in accordance with academic rules and ethical conduct. I also declare that, as required by these rules and conduct, I have fully cited and referenced all material and results that are not original to this work.

Name, Surname: Emin Atabey Peker

Signature:

ABSTRACT

SPATIO-TEMPORAL CHANGES OF LAKE WATER EXTENTS IN LAKES REGION (TURKEY) USING REMOTE SENSING

Peker, Emin Atabey
Master of Science, Geodetic and Geographic Information Technologies
Supervisor: Assoc. Prof. Dr. Koray K. Yılmaz
Co-Supervisor: Prof. Dr. M. Lütfi Süzen

June 2019, 125 pages

Monitoring inland water bodies has been one of the most popular practices in remote sensing. Changes in water extents of lakes are especially important due to strong links to sustainable water resources management and ecosystem services. Considering that the Mediterranean region is a hot spot of climate change (IPCC, 2013), monitoring of lakes become more crucial. This study investigates the spatio-temporal changes in water extents of 16 lakes in the Lakes Region, Turkey using remote sensing techniques for the 1984-2018 time period. The analysis was performed within Google Earth Engine® - a cloud-based geospatial data processing platform. The remotely sensed imagery utilized consisted of all the cloud free (less than 10%) images from Landsat and Sentinel-2 platforms available for the study area and period. Normalized Difference Water Index (NDWI) was used to delineate water extent from the image inventory. Bathymetry data was used with lake level measurements to calculate variation in area and volume of lakes. Areas calculated with remote sensing images were than compared with areas calculated via in-situ measurements. Results showed that lake extents obtained from in-situ lake level measurements were generally higher than those estimated from remotely sensed images, with correlation coefficient values ranging between 0.04 and 0.93. Furthermore, the relationship between spatio-temporal variations in the lake extents and hydrometeorological variables, such as precipitation and evaporation, were investigated. According to these analysis in Lake Eber, Lake Ilgin, Lake Beysehir, Lake Acigol, Lake Karatas, Lake Akgol, Lake Karamik and Lake Gavur; water extents have a positive correlation with precipitation and negative correlation with evaporation. Analysis indicated that In Lake Burdur and Lake Aksehir water extents decreased continuously since 1984. Seasonal fluctuations in water extents were identified for Lake Salda, Lake Beysehir, Lake Yarisli, Lake Kovada, Lake Acigol, Lake Ilgın, Lake Karatas, Lake Karamik, Lake Eber and Lake Akgol. In Lake Egirdir, Lake Salda, Lake Beysehir and Lake Sugla water extent did not fall below %90 of their maximum extent at the end of the study period (2017).

Keywords: Lakes, Lake Water Extent, Lakes Region in Turkey, Google Earth Engine, Landsat, Sentinel-2

ÖZ

GÖLLER YÖRESİNDEKİ GÖLLERİN SU SINIRININ ZAMANSAL DEĞİŞİMLERİNİN UZAKTAN ALGILAMA İLE TESPİTİ

Peker, Emin Atabey
Yüksek Lisans, Jeodezi ve Coğrafik Bilgi Teknolojileri
Tez Danışmanı: Doç. Dr. Koray K. Yılmaz
Ortak Tez Danışmanı: Prof. Dr. M. Lütfi Süzen

Haziran 2019, 125 sayfa

Göllerin su sınırılarının izlenmesi uzaktan algılamanın en popüler alanlarından birisidir. Göllerin su sınırı değişimi, sürdürülebilir su kaynakları yönetimi ve ekosistem ile ilişkisinden ötürü önem arz etmektedir. Akdeniz Bölgesi'nin iklim değişikliğinde etkilenecek önemli bir noktada olduğu düşünüldüğünde göl gözlemleri daha da önemli bir hale gelmektedir. Bu çalışmada Göller Yöresi'nde bulunan 16 göle ait su sınır çizgisindeki alansal ve zamansal değişim 1984 2018 döneminde uydu görüntüleri kullanılarak izlenmiştir. Analizler bulut tabanlı coğrafi veri işleme platformu olan Google Earth Engine'de gerçekleştirilmiştir. Çalışmada %10'dan daha az bulutluluk içeren Landsat ve Sentinel 2 görüntüleri kullanılmıştır. Uydu görüntülerinden su sınırı tespiti için Normalize Edilmiş Su Fark İndeksi (NDWI) kullanılmıştır. Batimetri verileri göl su seviyesi ölçümleriyle beraber kullanılarak göllerin alan ve hacimleri hesaplanmış ve sonuçlar uzaktan algılama yöntemleriyle elde edilen alan verileriyle karşılaştırılmıştır. Yersel ölçümlerden elde edilen alan değerleri uzaktan algılama yöntemleriyle elde edilen alan değerlerinden yüksek çıkmıştır. Korelasyon katsayısı 0.04-0.93 arası değerler almıştır. Göllerin su sınırı değişimleri yağış ve buharlaşma verileriyle beraber incelenmiştir. Bu analizler

sonucunda Eber, Ilgin, Beysehir, Acigol, Karatas, Akgol, Karamik ve Gavur göllerinde su sınırlarıyla yağış değerleri arasında pozitif korelasyon, buharlaşma değerleri arasında ise negative korelasyon tespit edilmiştir. Analizler sonucunda Akşehir ve Burdur göllerinde düzenli olarak su sınırının azaldığı , Salda, Beyşehir, Yarışlı, Kovada, Acigol, Ilgın, Karataş, Karamık, Eber ve Akgöl için ise alan da mevsimsel dalgalanmalar olduğu tespit edilmiştir. Egirdir, Salda, Beyşehir, Suğla göllerinde 2017 sonu itibariyle su sınırı maksimum seviyelerine oranla %90 ın altına düşmemiştir.

Anahtar Kelimeler: Göller, Göl Su Sınırı, Göller Bölgesi, Google Earth Engine, Landsat, Sentinel 2

This thesis work is dedicated to my family and my friends

ACKNOWLEDGEMENTS

I would like to present my sincere gratefulness to my thesis supervisor Assoc. Prof. Dr. Koray K. Yilmaz for his scientific lead during all process of the thesis. I also would like to thank my co-supervisor Prof. Dr. M. Lutfi Suzen for his critical support. It's such a great chance to work with them.

I would like to thank to Turkish State Meteorological Service for providing me the meteorological data.

I would like to thank to General Directorate of State Hydraulic Works for providing me the hydrological data.

I would like to thank Geomatics Engineer Murat Caliskan for his teaching on coding.

TABLE OF CONTENTS

LIST OF TABLES

TABLES

LIST OF FIGURES

FIGURES

LIST OF ABBREVIATIONS

AWEI : Automated Water Extraction Index

DEM : Digital Elevation Model

ETM+ : Enhanced Thematic Mapper Plus

GEE : Google Earth Engine

IDE : Integrated Development Environment

MSI : Multi Spectral Instrument

NDVI : Normalized Difference Vegetation Index

NDWI : Normalized Difference Water Index

NIR : Near Infrared

NOAA : National Oceanic and Atmospheric Administration

OLI : The Landsat Operational Land Imager (OLI)

PCP : Potential Cloud Pixels

RS : Remote Sensing

SLC : Scan Line Corrector

SWIR : Short-wave Infrared

TIN : Triangular Irregular Networks

TIRS : The Landsat Thermal Infra-Red Scanner

TM : Thematic Mapper

TOA : Top of Atmosphere

CHAPTER 1

INTRODUCTION

1.1. Purpose and Scope

Monitoring of inland water bodies is one of the major research topics in remote sensing considering the negative consequences due to both anthropogenic impacts and climatic change. According to the Intergovernmental Panel on climate change report, Mediterranean region is one of the most vulnerable regions in the world to the impacts of global warming (IPCC, 2013). Hence, monitoring of water resources in the Mediterranean region becomes critical. Lakes are one of the most important water resources in terms of benefits for the environment, ecosystem and economy. It is crucial to monitor the variation in lake water extent and lake volumes to understand the lake water budget and to develop sustainable water management plans. Remote sensing techniques provide inexpensive and objective means to monitor lake water extents at regional scales for a long period of time with ever increasing spatio-temporal scales.

Lakes Region, located in the Mediterranean region, consists of 16 lakes mostly of tectonic origin. Lakes, which are located in the inner (northern) part of the Western Taurus Mountains are important for sustaining ecosystem services, biodiversity and socio-economic development in the region. However, rapid population growth together with increasing drought periods in the region put additional stress on the lakes (Ozden, 2010).

The objectives of this study are as follows; (1) Time series analysis of lake water extents by remotely sensed imagery in Lakes Region (2) Comparison of areas determined by remotely sensed imagery and in-situ lake level measurements through bathymetry information, and (3) Investigating the potential relationships between water extents and meteorological variables. The scope of this work includes calculation of lake water extents for the study lakes using Normalized Difference Water Index (NDWI), calculated from all the available imagery between 1984 and 2018 and to compare spatio-temporal changes in lake water extents with meteorological variables.

In this study, Google Earth Engine® (GEE) platform is used to investigate the variation of water extents in the lakes over time (1984-2018). By using GEE platform available Landsat and Sentinel imageries for the study period was queried, NDWI values were calculated and the water extents were obtained, all in the cloud - without downloading the imageries.

1.2. Study Area

Lakes Region (Figure 1.1) is located in the Western Mediterranean region in Turkey, situated between N 37° 01' – N 38° 30' latitudes and E 29° 33' - 32° 21' longitudes. The region consists of 16 lakes and spreads over the borders of five cities namely Denizli, Afyonkarahisar, Konya, Burdur and Isparta as seen in Figure 1.2 and approximately covers an area of 1.711.250 ha. The elevation ranges between 1000 meters and 1500 meters in the region. Lakes Region is actually a collection of basins. The western part of the region consists of many closed basins mainly Lake Acigol and Lake Burdur basin, the eastern part (Lake Beysehir and Lake Sugla basin) comprises the sub-basins of the larger Konya basin. The central part of the region is connected to the Mediterranean Sea because it can discharge the excess water of Lake Egirdir to Aksu River with a natural strait over Lake Kovada. Basins forming the Lakes Region are mostly formed through combined effect of karstic landscape and tectonic events. For this reason, fracture systems control the flow of water over and under the ground and substantially limit the surface flow (Gorcelioglu, 1976).

The area between the Mediterranean and the Inner Anatolian regions is evaluated under the Mediterranean Transitional Region eco-region. Climate of this region has dry and hot summers, cold winters and rainy springs and the mean annual temperature at 1000 meters is between 11º and 14º C (Atalay & Efe, 2008). In the region which has the most precipitation in spring and winter (72.69%), the mean annual precipitation is 551.8 mm. Summer and autumn which is comparatively dry have 29.31% of total precipitation (Taylan & Aydin, 2018).

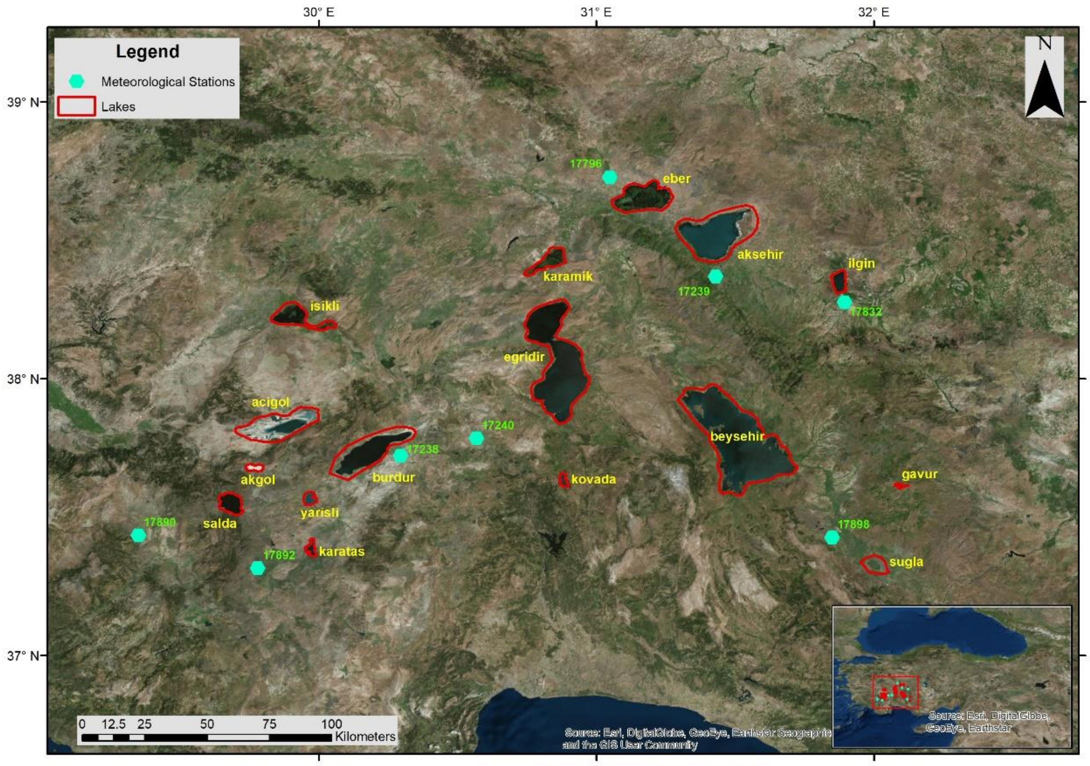

Figure 1.1. *Location Map of the Study Area*

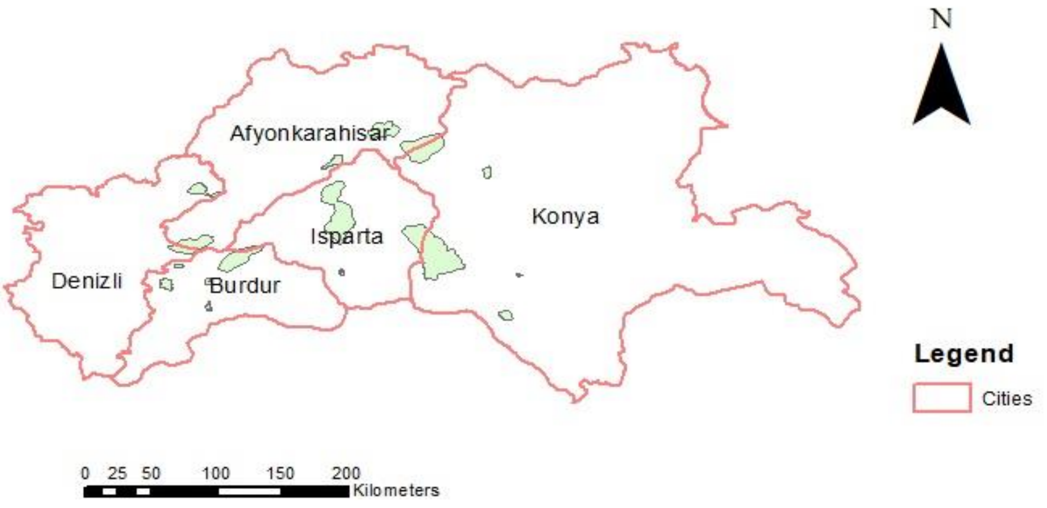

Figure 1.2. *Lakes and Cities*

1.2.1. Studied Lakes

Lake Aksehir: Lake Aksehir is located in the provinces of Afyonkarahisar and Konya that is in the southwestern part of Turkey. It is a tectonic freshwater lake (Altinsacli, 2000).

Lake Eber: Lake Eber is located in the province of Afyonkarahisar. The lake is a freshwater marsh and due to the reeds on the large part of the lake is seen as a meadow (Ozturk, 2005)

Lake Ilgin: Lake Ilgin is located in the province of Konya. It is a tectonic freshwater lake (Wetlands of Turkey, 2016). The lake was declared a natural protected area in 1992.

Lake Beysehir: Lake Beyşehir is Turkey's second largest lake. It is a freshwater lake and located in the province of Konya. The lake is located in a tectonic setting (Cevik, 2009). The lake was declared a natural protected area in 1992.

Lake Egirdir: Lake Eğirdir is a freshwater lake located in the province of Isparta and formed by tectonic and karstic effects (Kesici, 2015). The lake was declared a natural protected area in 1992

Lake Sugla: Lake Sugla is a tectonic freshwater lake located in the province of Konya (Doganer, 2015).

Lake Karamik: Lake Karamik is located in the province of Afyonkarahisar. The lake is very shallow, and generally swamp conditions prevail. Many migratory birds were observed in the lake (Uzun, 2007).

Lake Kovada: Lake Kovada is a freshwater lake formed by tectonism and karstic dissolution (Sener S. , 2016). The lake was declared a national park in 1970.

Lake Burdur: Lake Burdur is saline lake of tectonic origin and located in the provinces of Burdur and Isparta. Lake Burdur that has been a Ramsar Site since 1993 and Wildlife Reserve since 1994 is harbouring nearly 100 bird species. (Burdur Governor of the Republic of Turkey, 2019).

Lake Acigol: Lake Acigol is a tectonic lake and located in the province of Denizli and Afyonkarahisar. There are 176 bird species belonging to 20 families in the vicinity of the lake (Uyan, 2014).

Lake Isikli: Lake Isikli is a freshwater lake located in the province of Denizli and Afyonkarahisar. Lake Isikli is a breeding site for waterbirds and wintering wildfowl (Wetlands of Turkey, 2016).

Lake Salda: Lake Salda is a crater lake located in the province of Burdur. There are endemic algae fish in the lake. Hydromagnesite mineral formed in the lake is one of the most beautiful and contemporary examples of 'biological mineralization'. (Zedef, 1995). The lake was declared a natural protected area in 1989.

Lake Yarisli: Lake Yarisli is a karstic lake and located in the province of Burdur. Flamingos use the lake area during migration (Wetlands of Turkey, 2016).

Lake Karatas: Lake Karatas is a freshwater lake located in the province of Burdur. The reeds in the lake are nesting spaces for 122 bird species (Lake Karatas, 2013). The lake was declared a wildlife conservation area in 1985.

Lake Akgol: Lake Akgol is a karstic lake and located in the province of Burdur. In Akgol, which is too salty, fish cannot live, bird watching can be done (Burdur Province Nature Tourism Master Plan 2013 - 2023, 2013).

The maximum extent, elevation and maximum depth data of the 16 studied lakes are shown in the Table 1.1.

Table 1.1. Maximum Extent, Elevation and Max Depth of Lakes

	Maximum Extent (km^2)	Elevation (m)	Maximum Depth (m)
Acigol	143	842	1.5
Akgol	10.4	987	NA
Aksehir	332	966	7
Beysehir	670.1	1115	10
Burdur	205.5	845	110
Eber	100	967	21
Egirdir	469.5	915	17
Gavur	3	1836	NA
Ilgin	26.9	1026	2 - 10
Isikli	62.1	813	8.7
Karamik	28	1001	3
Karatas	12	1050	2
Kovada	8.4	908	6
Salda	46.2	1316	184
Sugla	39.8	1084	NA
Yarisli	14.8	930	4

1.3. Literature Review

1.3.1. Characteristics of Landsat TM, ETM+, OLI/TIRS and Sentinel MSI Sensors

Remote sensing sensors record the brightness of an area in electromagnetic spectrum. All sensors have a spectral sensitivity intervals (bands) which refers to spectral resolution. Recorded wavelengths are presented as bands (blue, green, red, near infrared, etc…). The number of bands varies depending on the sensor system (Lucas, 1998).

In this study Landsat 5 TM, Landsat 7 ETM+, Landsat 8 OLI/TIRS and Sentinel-2 imagery were used. Landsat 4 and 5 have thematic mapper (TM) sensor. Thematic Mapper sensor was designed to achieve higher image resolution than the MSS sensor which was used in Landsat 3 and earlier platforms (Landsat Science, 2019). Landsat 4 and 5 have thematic mapper (TM) sensor. The thematic mapper has a spatial resolution of 30 meter that refers a measure of the smallest object that can be resolved by the sensor and its spectral range is between 0.45 and 12.5 μm and the temporal resolution is 16 days refers to the frequency of the same location. The thematic mapper consists of 7 bands and has an image size of 185 km * 172 km. The Enhanced Thematic Mapper Plus (ETM+) has a high-resolution band in addition to TM sensors and it is carried by Landsat 7. The Landsat Operational Land Imager (OLI) sensor has two new spectral bands with respect to the ETM+ sensor, one for detecting cirrus clouds (band 9) and the other for coastal zone observations (band 1). The Landsat Thermal Infra-Red Scanner (TIRS) has two more bands in the thermal spectrum which was covered by one single band in TM and ETM+ sensors. OLI/TIRS sensors are carried by Landsat 8 (Landsat Science, 2019). The spatial and spectral resolution properties of TM, ETM+ and OLI/TIRS sensors are listed in Table 1.2. Google Earth Engine includes a cloud masking algorithm, called Fmask (Zhu & Woodcock, 2012), for Landsat 5, Landsat 7 and Landsat 8 is available in.

Sentinel-2 is a wide-swath, high-resolution, multi-spectral imaging mission supporting Copernicus Land Monitoring studies. Multispectral Instrument (MSI) sensor have 13 bands. There are three QA bands and one (QA60) is a bitmask band with cloud mask information (ESA Sentinel Online, 2019) and it is carried by Sentinel-2 platform. Sentinel-2 bands are listed in Table 1.2

Table 1.2. Spectral and Spatial Resolutions of TM, ETM+, OLI/TIRS and MSI sensors

Band	**TM (Landsat 5)**			**ETM+ (Landsat 7)**		
		Spectral Resolution (μm)	Spatial Resolution (m)		Spectral Resolution (μm)	Spatial Resolution (m)
1	Blue	0.45-0.52	30	Blue	0.45-0.52	30
2	Green	0.52-0.60	30	Green	0.53-0.60	30
3	Red	0.63-0.69	30	Red	0.63-0.69	30
4	Near Infrared (NIR)	0.76-0.90	30	Near Infrared (NIR)	0.77-0.90	30
5	Shortwave Infrared (SWIR) 1	1.55-1.75	30	Shortwave Infrared (SWIR) 1	1.55-1.75	30
6	Thermal	10.40-12.50	120	Thermal	10.40-12.50	60
7	Shortwave Infrared (SWIR) 2	2.08-2.35	30	Shortwave Infrared (SWIR) 2	2.09-2.35	30
8				Panchromatic	0.52-0.90	15
Band	**OLI/TIRS (Landsat 8)**			**MIS (Sentinel-2)**		
		Spectral Resolution (μm)	Spatial Resolution (m)		Spectral Resolution (μm)	Spatial Resolution (m)
1	Coastal Aerosol	0.435 - 0.451	30	Coastal Aerosol	0.421-0.457	60
2	Blue	0.452 - 0.512	30	Blue	0.439-0.535	10
3	Green	0.533 - 0.590	30	Green	0.537-0.582	10
4	Red	0.636 - 0.673	30	Red	0.646-0.685	10
5	Near Infrared (NIR)	0.851 - 0.879	30	Vegetation Red Edge	0.694-0.714	20
6	Short-wave Infrared (SWIR) 1	1.566 - 1.651	30	Vegetation Red Edge	0.731-0.749	20
7	Short-wave Infrared (SWIR) 2	2.107 - 2.294	30	Vegetation Red Edge	0.768-0.796	20
8	Panchromatic	0.503 - 0.676	15	Near Infrared (NIR)	0.767-0.908	10
8a				Near Infrared (NIR)	0.848-.0.881	20
9	Cirrus	1.363 - 1.384	30	Water Vapor	0.931-0.958	60
10	TIRS 1	10.60 – 11.19	100	SWIR - Cirrus	1.338-1.414	60
11	TIRS 2	11.50 - 12.51	100	SWIR	1.539-1.681	20
12				SWIR	2.072-2.312	20

1.3.2. Indices Used in Water Body Mapping

Water body mapping has an important place in remote sensing applications. Index methods are used to separate water from the background based on a threshold value. This threshold value is mostly fixed except noises in the image such as shadow, forest, built-up areas, snow, and clouds (Acharya , Subedi & Lee, 2018).

Normalized Difference Vegetation Index (NDVI) quantifies vegetation by using near-infrared and red bands (Eqn. 1). Vegetation reflects near-infrared and green light besides absorbs red and blue light. Although the main objective of this index, which was developed by Kriegler et al. (1969), was to detect vegetation, the index was also successful in the determination of water bodies. Rokni et al. (2014) shows that accuracy of NDVI as 99.06 % and 98.91 % in 2000 and 2010 for comparing different indices in mapping the extent of Lake Urmia.

$$\text{NDVI} = (\text{NIR} - \text{Red}) / (\text{NIR} + \text{Red}) \tag{1}$$

Automated Water Extraction Index (AWEI) detects water bodies using Landsat imagery time series by a single threshold. This index introduced by Feyisa, Meilby, Fensholt, & Proud (2014) includes two indices; AWEI_{nsh} (Eqn. 2) works well in case of no shadows in the image and AWEI_{sh} (Eqn. 3) is a further improvement of AWEI_{nsh} and distinguishes water pixels from shadow pixels. According to study of Rokni accuracy of AWEI is 96.63 % and 94.06 % in 2000 and 2010.

$$\text{AWEI}_{\text{nsh}} = 4 \times (\text{Green} - \text{SWIR1}) - (0.25 \times \text{NIR} + 2.75 \times \text{SWIR2}) \tag{2}$$

$$\text{AWEI}_{\text{sh}} = \text{Blue} + 2.5 \times \text{Green} - 1.5 \times (\text{NIR} + \text{SWIR1}) - 0.25 \times \text{SWIR2} \tag{3}$$

Normalized Difference Water Index (NDWI) was proposed by McFeeters (1996) (Eqn. 4). NDWI is an index that minimizes the reflectance of water in NIR band and maximize the reflectance of the water in green band (Xu H. , 2006). NDWI varies between -1 to +1. NDWI > 0 is a water class and NDWI ≤ 0 designates non-water. Rokni calculated the accuracy of NDWI as 99.35 % and 99.64 % in 2000 and 2010 and determined that the NDWI provides the highest accuracy among water indices.

Ayhan (2016) states that NDWI is the best method to differentiate wet, moist and dry classes and selected as the water extent extraction method for Lake Tuz. Despite the fact that the NDWI > 0 is water class, Du, et al., (2016) states that when the threshold value of 0 is used to identify water, some built-up pixels could be wrongly assigned as water. In this study NDWI is used to identify water pixels within study lakes.

NDWI= (Green – NIR) / (Green + NIR) (*4*)

Thus, NDWI can be calculated for each platform used in this study as (ρ denotes the band):

Landsat 5 and Landsat 7 $\mathrm{NDWI} = \frac{\rho_2 - \rho_4}{\rho_2 + \rho_4}$

Landsat 8 $\mathrm{NDWI} = \frac{\rho_3 - \rho_5}{\rho_3 + \rho_5}$

Sentinel 2 $\mathrm{NDWI} = \frac{\rho_3 - \rho_8}{\rho_3 + \rho_8}$

Modified Normalized Difference Water Index (MNDWI) uses shortwave infrared (SWIR) band instead of near infrared band used in NDWI (Eqn. 5). Xu (2006) proposed this index to overcome the inseparability of built-up areas. Li et al. (2013) found that the MNDWI is the most efficient index for detecting water body in a study to find the best performing NDWI model at three different study sites in the Yangtze River Basin. Chang et al. (2018) also found that the MNDWI is performing best in delineating water from land while comparing with NDWI by Landsat OLI image covering Poyang Lake, China.

MNDWI= (Green – SWIR) / (Green + SWIR) (*5*)

Donchyts, Giesen, & Gorelick (2017) demonstrates that NDWI can be effectively used for accurate water detection in combination with geospatial parallel processing platforms, such as Google Earth Engine. Their results indicated a very high correlation (R^2=0.99) between remotely sensed surface area and observations for the study dam reservoir in Prosser Creek Reservoir, CA, USA. Buma, Lee, & Seo (2018) shows that

Modified NDWI (MDNWI) and NDWI performed well in extracting water pixels for examining the aerial changes in the Lake Chad over the 13-year period (2003–2016) using Landsat imagery with an overall accuracy greater than 90%. Yang, Zhao, Qin, Zhao, & Liang (2017) used panchromatic high-resolution bands to sharpen short wave infrared (SWIR) bands for enhancing water indices and found that NDWI index was the most feasible index for delineating water bodies. Liu, Yang, Chen, Fang, & Li (2018) used more than 400 Landsat images with NDWI to extract the lake surface area separately and compared the variations in lakes extents with climate variables in the northwest of China. Sisay (2016) implemented NDWI and Automated Water Extraction Index (AWEI) to extract and quantify the water surface area changes by downloaded Landsat images belong to 6 different years between 1973 and 2014 in the Central Rift Valley Region of Ethiopia. Wang, Jia, Chen, & Wang (2018) identified through obtaining the minimal and maximal surface water extent in the year of 1990, 2000, 2010 and 2017 by removing non-water pixels with NDWI masking procedures by using the Landsat images within GEE platform in the Middle Yangtze River Basin. Wendleder, Friedl, & Mayer (2018) mapped supraglacial lakes forming on the downstream Baltoro Glacier which is located in the Karakoram Range in Northern Pakistan in summer with multi-spectral Landsat and ASTER images by using NDWI threshold of 0.1 in an effort to minimize the misclassification of snow.

Many studies have been carried out in Lakes Region in the past. Yagmur et al. (2018) analysed temporal changes of Lake Beysehir and Lake Tuz extents in Konya Closed Basin using only 7 Landsat images in a period of about 30 years (1987-2017) within GEE platform and determined that water surface area in the Konya Closed Basin has decreased nearly 23.5% within the past 3 decades. Karaman et al. (2013) determined the area of Lake Acigol as 69 km² in May 2010 using MNDWI and Landsat 5 imagery. Ozdemir & Bahadir (2010) applied controlled classification to Landsat images and calculated the area of Lake Acigol as 50 km² in 1987, 31 km² at 2000 and 2002 and 32 km² in 2005. Kole et al. (2016) determined that the area of Lake Aksehir was reduced from 287 km² to 82 km² from 1990 to 2016 by using Landsat imageries. Bahadir (2013) investigated the spatial changes in Lake Aksehir with digitized 5 Landsat images between 1975 and 2010 and determined lake area decreased by 66.38%. Kaplan, Avdan, Yavdan, & Yildiz (2016) used 4 Landsat satellite images, two from Landsat TM, and one from Landsat ETM+ and one from Landsat 8 that were collected in April. Their analysis utilizing Normalized Difference Water Index (NDWI) and Normalized Difference Vegetation Index (NDVI) revealed that the water extent of Lake Aksehir was reduced from 324.5 km^2 in 1987 to 99.7 km^2 in 2016. Sener et al. (2010) found that the surface area of Lake Aksehir decreased from 342 km^2 to 85 km^2 from 1975 to 2006 by digitizing Landsat and ASTER images. Fethi, Ileri, Avci, & Kocadere (2015) determined the area of Lake Beysehir as 652 km^2 in 1984, 617 km^2 in 2005, 639 km^2 in 2014 using Landsat images. By using Landsat and Spot images it was determined that the area of Lake Burdur decreased 203 km^2 to 146 km^2 from 1987 to 2008 (Ataol, 2010). Yildirim, Erdogan, & Uysal (2011) determined that the surface area of Lake Eber decreased by 28.4% and lake water level declined by 2.03 m by digitized 9 Landsat images between 1975 to 2009. Fethi, Ileri, Avci, & Kocadere (2015) determined the area of Lake Egirdir as 463 km^2 in 1984, 455 km^2 in 1990, 458 km^2 in 2004, 454 km^2 in 2013 using Landsat images.

CHAPTER 2

DATASETS

2.1. Satellite Data

In this study, multiple satellite platforms including Landsat 5 TM, Landsat 7 ETM+, Landsat 8 OLI/TIRS and Sentinel 2 MSI, have been utilized to cover as much as possible the study period spanning 1984 through 2018. Landsat 5 TM covers the period 1984-2012, Landsat 7 ETM+ covers the period 1999 through 2003, Landsat 8 OLI/TIRS covers the period 2013 to 2018, Sentinel 2 MIS is available from 2015 to 2018. All these image collections were queried and analyzed within the Google Earth Engine® (GEE) Platform. Landsat 7 ETM+ scenes were only utilized until May 30, 2003 due to Scan Line Corrector (SLC) failure of the sensor causing data gaps which could not be filled in GEE platform. As seen in Figure 2.1 the lowest precipitation values between 1981 and 2016 were reached in 2008 (Ministry of Forestry and Water Affairs, 2018). For this reason, the period between 2003 and 2008 certain number of Landsat 7 ETM+ images were downloaded from U.S. Geological Survey website (USGS, 2019) and the scan line gaps were filled using values of neighboring pixels. NDWI values were then calculated for these images. Both gap filling and NDWI calculation operations were carried out in ArcGIS Software version 10.1. This manual operation enabled inclusion of 181 Landsat 7 ETM+ images for the 2003-2008 period. Table 2.1 lists the number of images used for each study lake. Figure 2.2 shows the dates (y-axis) when an image from a specific platform (marker type) was available for each year (x-axis). In this figure each dot symbolizes an image. This figure shows the distribution of 4045 satellite images by years and seasons. For Landsat imagery orthorectified top-of-the atmosphere (TOA) Reflectance values were utilized with Fmask (Function of Mask) layer in GEE. Fmask layer was used to separate Potential Cloud Pixels (PCPs) and clear-sky pixels by using rules based on cloud physical properties. Zhu & Woodcock (2012). For Sentinel-2 images Sentinel-2 MSI: MultiSpectral Instrument, Level-1C product was utilized together with its QA60 band for cloud masking. Sentinel-2 images couldn't be used in Lake Beysehir and Lake Eber because these lakes could not be covered in a single sentinel-2 image.

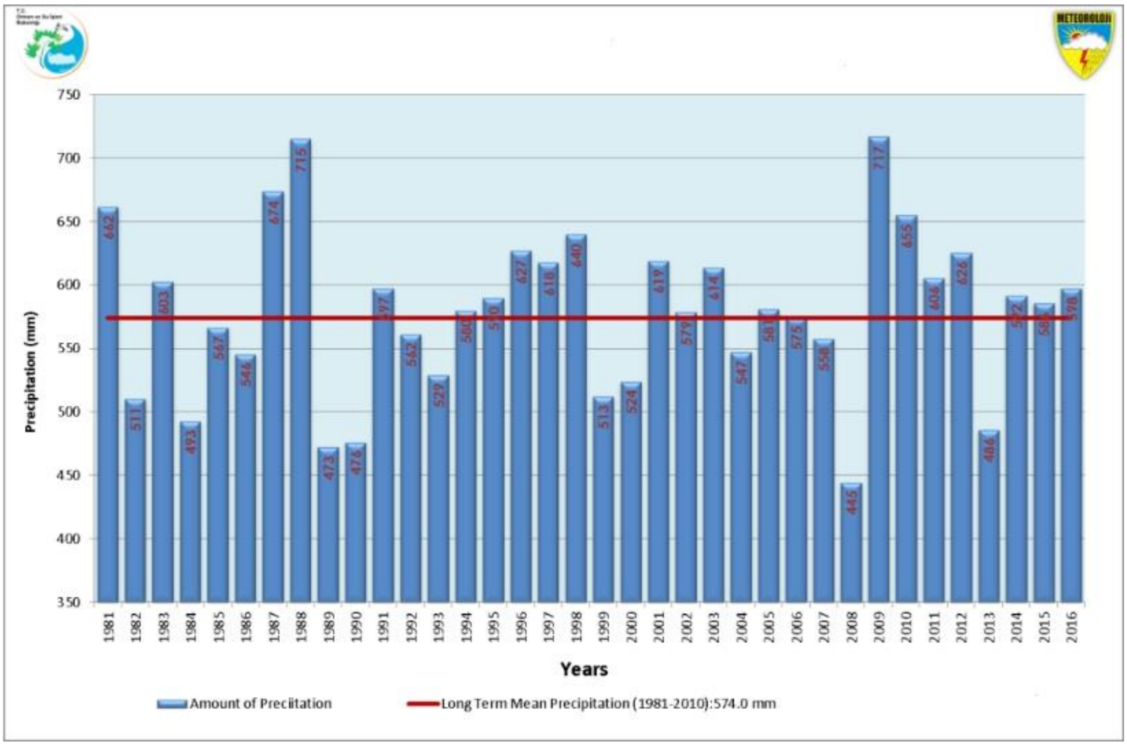

Figure 2.1. *Annual Mean Areal Precipitation for Turkey*

Table 2.1 Number of Images used for each lake

Lakes	Landsat 5	Landsat 7	Landsat 8	Sentinel 2	Total
Acigol	39	35	33	28	135
Akgol	18	8	22	51	99
Aksehir	41	31	33	47	152
Beysehir	45	31	23	NA	99
Burdur	101	91	87	232	511
Eber	43	41	37	51	172
Egirdir	48	43	36	NA	127
Gavur	35	25	33	39	132
Ilgin	124	89	130	57	400
Isikli	57	52	52	116	277
Karamik	48	39	34	112	233
Karatas	95	74	76	253	498
Kovada	55	42	48	109	254
Salda	43	42	38	120	243
Sugla	21	32	52	61	166
Yarisli	95	61	73	137	366
Total	908	736	807	1413	

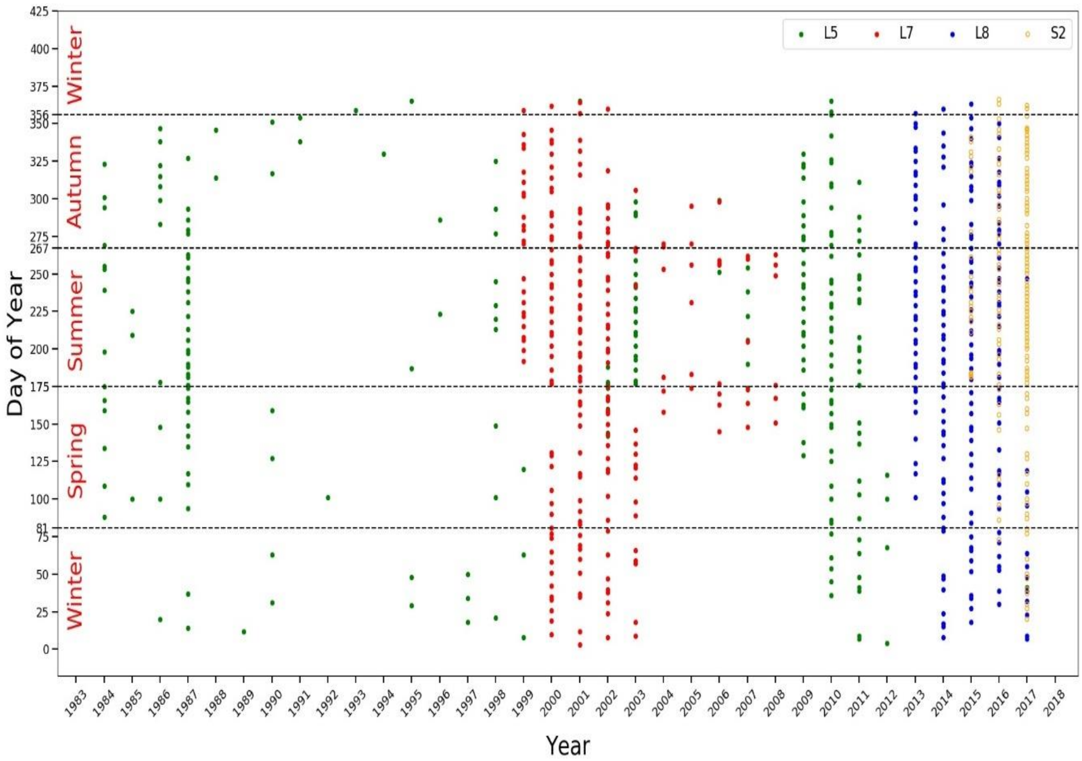

Figure 2.2. *Time distribution of Satellite Imagery utilized in this study. Time distribution of Satellite Imagery utilized in this study*

This study differs from the above studies in the Lakes Region in several aspects, first, this study covers all 16 lakes in the Lakes Region thus enabling a regional understanding of lake extents. Second, in this study all the available imagery (after quality control) for the period 1984-2018 was utilized thus dynamic behavior of the lake extents were investigated at fine temporal scales. Previous studies in the Lakes Region focused only on one or just a few lakes using only a limited number of imagery.

In this study, all available remotely sensed images of each lake between 1984 and 2018 was intended to be included in the analysis. In cases where the analyses are limited to several images, images downloaded separately can be studied in the GIS environment. However, in this study, it was unsuitable to use the image download method because it was desired to use all satellite images in the desired time period.

In this thesis, Landsat 5 TM images were used for the years 1984 through 2012. When the 10% cloud filter was applied to the image collection of this period, 908 Landsat 5 TM images which were available for 16 lakes have been identified. On the USGS website, a Landsat 5 TM image in level-1 GeoTIFF format is more than 150 megabytes (MB), five Landsat satellite images can only cover 16 lakes. If the Landsat 5 TM images covering all the study lakes between 1984 and 2012 were downloaded, 27 gigabytes of data storage space would be required. Landsat 7 ETM+ images were used for the years 1999 through 2013 and 736 images were identified in this period. A Landsat 7 ETM+ image in the level-1 GeoTIFF format is more than 250 MB, thus 36 GB of data storage space would be required if these images were downloaded.

A total of 807 Landsat 8 OLI / TIRS images were used for the period (2013-2018). A Landsat 8 OLI / TIRS image with a level-1 GeoTIFF format is more than 900 MB. Thus 142 GB of data storage space would be required if these images were downloaded. Sentinel-2 MSI images were used for the years 2015-2018 and 1413 images of this period were identified. When it is considered that six Sentinel-2 images are sufficient to cover the Region completely and the size of Sentinel-2 image in JPEG 2000 (JP2) format is more than 800 MB. Thus 184 GB of data storage space is required to download all these images. Overall, in this study, approximately 389 GB of data storage space would be needed if all the images used in the analysis were downloaded. Depending on the speed, downloading of these images requires more than 100 hours.

Moreover, the processing of these 3864 images with a personal computer would take substantial time. Considering the data storage and processing time, it would be very inefficient and ineffective to undertake this study using a personal computer. Note that analyses in this study are carried out only in a few minutes within Google Earth Engine Cloud platform without downloading any images.

2.2. Terrestrial Data

2.2.1. Meteorological Data

Stagl et al. (2014) states that critical changes in the hydrological system are mainly related with the variation in precipitation and evaporation. In this thesis precipitation and evaporation data taken from eight meteorological stations in the region operated by the Turkish State Meteorological Service were used. Seven of the station have both precipitation and evaporation data during the study time period. Lake extents were associated with the closest meteorological stations in the subsequent analysis. However, since evaporation data was not available for Station-17892, Station-17890 evaporation data was used for Lake Salda and Lake Karatas. Table 2.2 shows lakes and related meteorological stations and elevations of them and distances between them.

Table 2.2. Elevation and Distance of Lakes and Related Meteorological Stations

Lake	Elevation of Lake (m)	Related Meteorological Station	Elevation of the Meteorological Station (m)	Distance between Lake and Station (km)
Acigol	842	17238	957	30
Akgol	987	17238	957	43
Aksehir	966	17239	1002	6
Beysehir	1115	17898	1129	30
Burdur	845	17238	957	5
Eber	967	17796	1018	7
Egirdir	915	17240	997	24
Gavur	1836	17898	1129	30
Ilgin	1026	17832	1036	4
Isikli	813	17238	957	56
Karamik	1001	17796	1018	33
Karatas	1050	17892	1142	17
Kovada	908	17240	997	30
Salda	1316	17892	1142	23
Sugla	1084	17898	1129	14
Yarisli	930	17238	957	32

2.2.1.1. Precipitation

The meteorological precipitation measurement unit is expressed as the amount of water (kilogram) falling on to 1 m^2. This is equal the height of 1-millimeter water. Therefore, the amount of precipitation is also expressed in millimeters. Precipitation is measured by a rain gauge (Figure 2.3) which is situated 1 meter above the ground level. It works with a precision of 0.2 mm (Instruments and Devices Used in Meteorology, 2019).

In this thesis precipitation data from eight meteorological stations were used. According to daily precipitation data, cumulative deviations from mean precipitation versus day of year graphics were created and evaluated with lake extent graphics. Cumulative deviations were used for the advantage of easily recognizing the changes in the mean amount of precipitation (Schwarb, et al., 2011).

Figure 2.3. *Precipitation Meter (Instruments and Devices Used in Meteorology, 2019)*

2.2.1.2. Evaporation

Evaporation, which is an important element of the hydrological cycle of water in nature, is defined as the transition from a liquid to a gaseous state at temperatures below the boiling point of water. Evaporation observations are carried out on the open water surface. Round evaporation pans made of galvanized steel or stainless steel are installed in the places where the observatory areas of the park are suitable for rain, wind and sun (Figure 2.4) (Instruments and Devices Used in Meteorology, 2019).

In this thesis evaporation data from seven meteorological stations were used. For stations 17832, 17898, 17890, 17796 evaporation data was available since October 2011. According to daily evaporation data, cumulative deviations from mean evaporation versus day of year graphics were created and evaluated with lake extent graphics.

In Figure 2.5 it is seen eight meteorological stations in the region operated by the Turkish State Meteorological Service.

Figure 2.4. *Evaporation Pond (Instruments and Devices Used in Meteorology, 2019)*

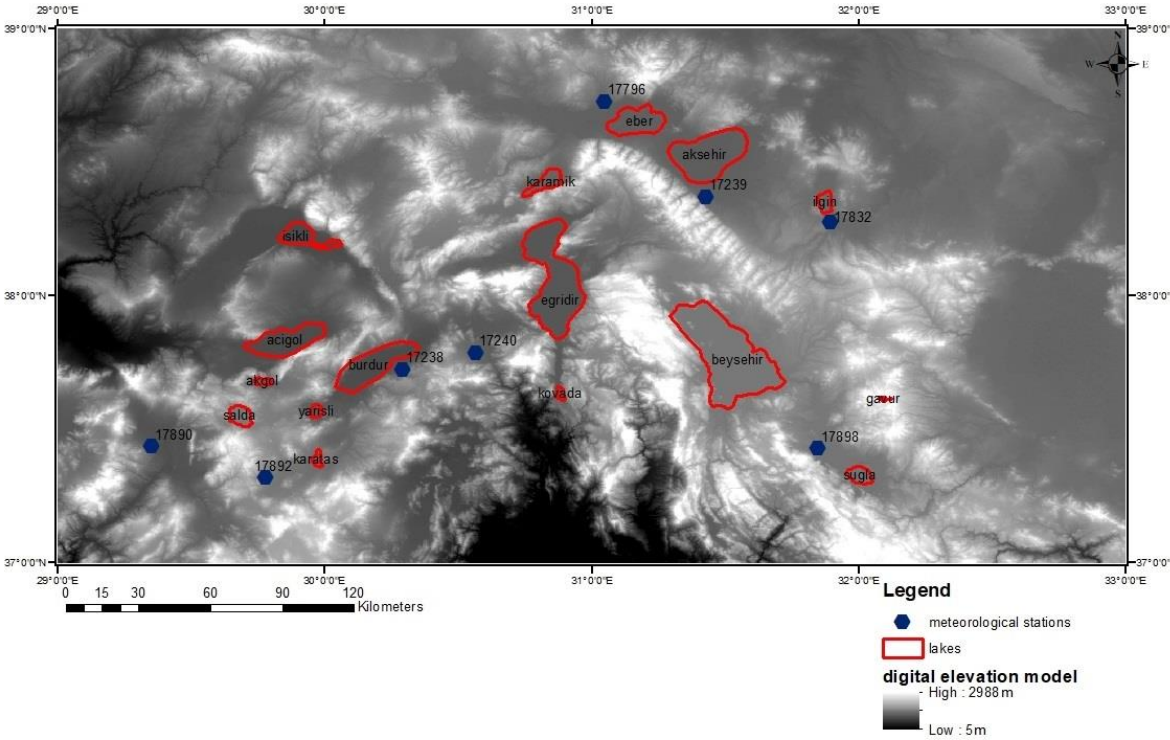

Figure 2.5. *Digital Elevation Model of the Region and Meteorological Stations*

2.2.2. Bathymetry Data

Lake bathymetry information is critical to establish link between lake water level, water surface area and lake water volume (NOAA, 2018). Bathymetric measurements are done to determine depth and shape of the lake by measuring the bottom points of the lake. Sonar devices are used to measure depth electronically (Figure 2.6) (Sapcilar & Fakioglu, 2004). In this study, bathymetric surveys available for 10 lakes were obtained from General Directorate of State Hydraulic Works (Table 2.3). In-situ lake level measurements and bathymetric surveys were used together to calculate daily variation in both surface area and the volume of the lakes. The bathymetry information thus enabled a comparison between lake water extents and lake volumes obtained by remotely sensed information and in-situ measurements for the dates when both are available.

Figure 2.6. *Echo Sounder used for depth measurement (Sapcilar & Fakioglu, 2004)*

Table 2.3. Inventory of the Bathymetric Data

Lakes	Availability and Survey Year of Bathymetric Measurements	Availability of Daily Lake Level Measurements
Acigol	-	+
Akgol	-	+
Aksehir	2017	+
Beysehir	1999	+
Burdur	2015	+
Eber	1991	+
Egirdir	1999	+
Gavur	-	+
Ilgin	2010	-
Isikli	2017	-
Karamik	-	-
Karatas	-	+
Kovada	2017	+
Salda	2015	-
Sugla	-	+
Yarisli	2017	-

2.2.3. Lake Level Measurements

In this study, changes in lake water areas were determined by using remotely sensing imageries. These area values were compared with the lake area values calculated by the lake level observations obtained through in-situ measurements. Two kind of in-situ data are needed to calculate lake area; lake level data and the bathymetric measurements. Lake level measurements were done by differential levelling using a staff gauge (Figure 2.7) (Sapcilar & Fakioglu, 2004). Daily lake level measurements are available for 11 lakes (Table 2.3) and were obtained from General Directorate of State Hydraulic Works.

Figure 2.7. *Staff gauge used in Lake level measurements (Sapcilar & Fakioglu, 2004)*

CHAPTER 3

METHODOLOGY

In this section, all the steps implemented in the thesis are explained separately. It is shown with explanations in the sections where coding was used. Figure 3.1 shows the steps and the chapters to which it belongs.

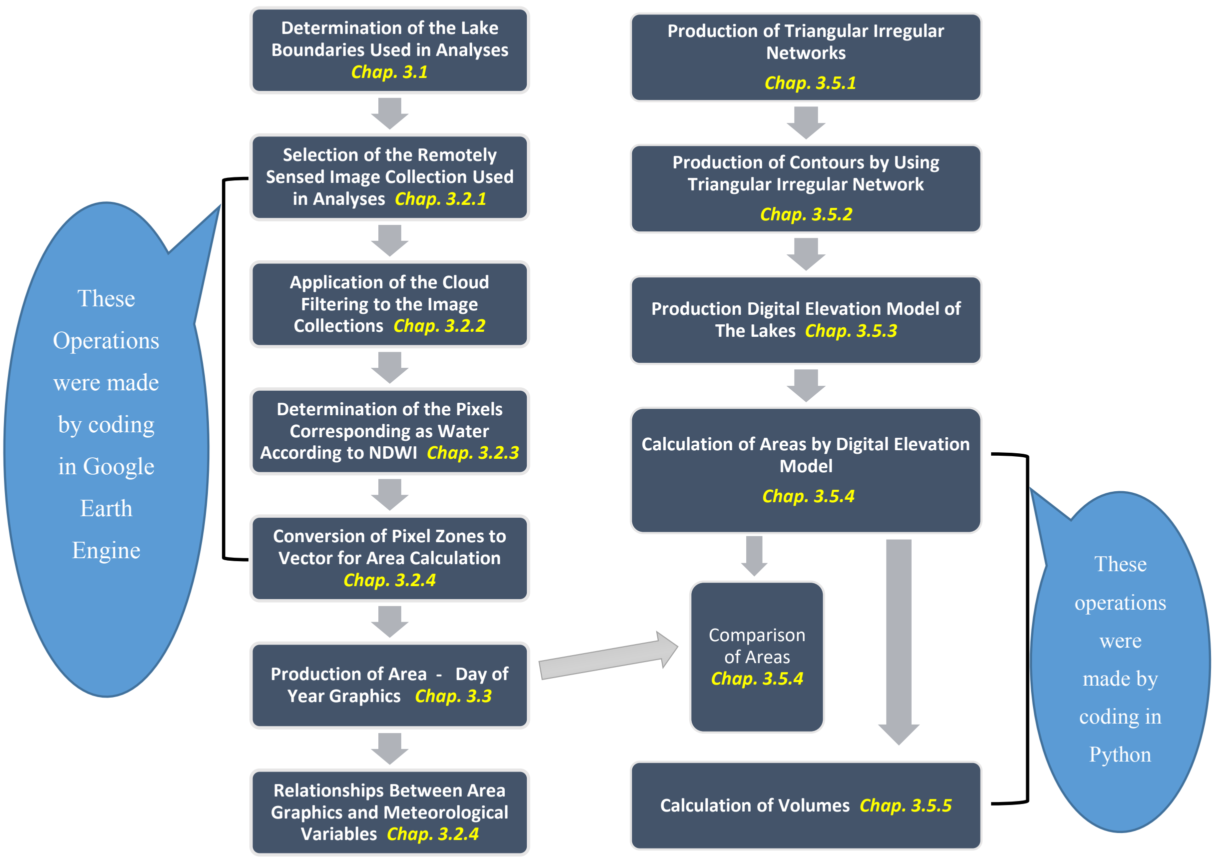

Figure 3.1. *Flowchart of the methodology*

3.1. Determination of the Analysis Boundaries for each Lake

In this study, spatio-temporal variation in water extents of the lakes in the Lakes Region was analyzed using imagery from four different satellite platforms. In order to determine the water extent changes of the lakes within these images, the analysis boundaries to be studied were determined and only changes within these boundaries were analyzed. These boundaries were determined in a way to ensure that the maximum lake extent for each lake in the study period (1984-2018) is covered within its analysis boundary. These boundaries are termed as analysis boundaries because they help to limit the analysis space from all the imagery to only around the lake. The boundaries were determined in Google Earth (Figure 3.2) and converted to shape (shp) format in the GIS environment and transferred to the Earth Engine platform.

Figure 3.2. *Determination the Boundary of Lake Burdur in Google Earth*

3.2. Determination of Water Surface Area Time Series in Google Earth Engine (GEE)

Google Earth Engine (GEE) is a cloud-based computing platform that enables to run geospatial analysis on Google's cloud infrastructure. GEE combines a multi-petabyte catalog of satellite imagery and geospatial datasets including (Landsat 4-8, Sentinel 1-2, MODIS, Aster, climate, land cover, topography etc.). A web-based Integrated Development Environment (IDE) (Figure 3.3) is used for writing and running scripts. This IDE is also used for visualization of the spatial analyses through Javascript API. GEE libraries can be used to develop codes by Javascript or Python. (Google Earth Engine, 2018). GEE makes it easy to query and parallel processing of even large collections of geospatial data with the power of cloud-computing platform (Gorelick, 2017). All analysis described in Sections 3.2.1, 3.2.2, 3.2.3, 3.2.4 were implemented through writing scripts in IDE of the GEE platform.

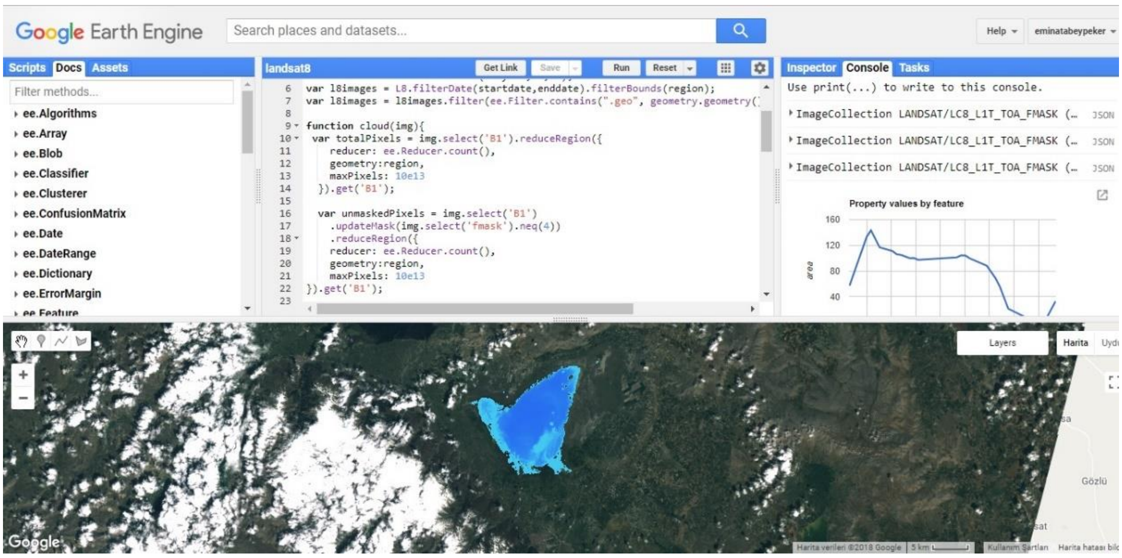

Figure 3.3. *A view of Google Earth Engine with Code Editor*

3.2.1. Selection of the Remotely Sensed Image Collection Used in Analyses

After determining the study lakes and their analysis boundaries all the remotely sensed imagery between 1984 and 2018 which include these boundaries were queried in GEE database. Separate folders for Landsat 5 TM, Landsat 7 ETM+, Landsat 8 OLI/TIRS and Sentinel 2 MIS images were created and individual codes were written for all these satellites. In these queries, the date range of 1984-2018 was filtered and image collection was created according to this filter. These image collections form the basis for the analysis performed in this study.

A sample GEE code that enable the selection of an image collection according to date filtering is shown in Figure 3.4.

```
var L8 = ee.ImageCollection("LANDSAT/LE8_L1T_TOA_FMASK"),

var geometry = ee.FeatureCollection("users/eminatabeypeker/burdur");

var region=geometry

var startyear = 2013;

var endyear = 2018;

var startdate = ee.Date.fromYMD(startyear,1,1);
var enddate = ee.Date.fromYMD(endyear,12,31);

var l8images = L8.filterDate(startdate,enddate).filterBounds(region);

var l8images = l8images.filter(ee.Filter.contains(".geo", geometry.geometry()));
```

Selection of the satellite

Importation of the lake boundary in shp format from local computer

Date filtering

Detection the images that including the entire lake boundaries, not just intersecting with lake boundaries.

Figure 3.4. *A sample GEE code that enables the selection of the an image collection according to date filtering*

3.2.2. Application of the Cloud Filtering to the Image Collections

After obtaining image collections according to date filtering, it was desired to calculate lake areas in these images, but firstly cloud filtering should be applied to the images because clouds prevent the pixels from being determined as water. Images that have cloud ratio below 10% were selected for the analysis while the rest were excluded. Cloud ratio information is present in the metadata of each satellite image. However, this is the data of the whole frame, whereas in this study, only the analysis boundaries of the lakes were subjected to analysis. Hence, only the cloud ratio within the analysis boundary was required. Cloud filtering was applied only to the desired areas by a new parameter produced with the codes written in GEE. After this process, image collections with desired cloudiness in the intended time period (1984-2018) were obtained. A sample GEE code that enable the partial cloud filtering is shown in Figure 3.5.

```
function cloud(img){

 var totalPixels =
img.select('B1').reduceRegion({
   reducer: ee.Reducer.count(),
   geometry:region,
   maxPixels: 10e13
  }).get('B1');
```

Detection the number of the total pixels in the study region

```
  var unmaskedPixels = img.select('B1')
    .updateMask(img.select('pixel_qa').neq(5))
    .reduceRegion({
    reducer: ee.Reducer.count(),
    geometry:region,
    maxPixels: 10e13
 }).get('B1');
```

Detection the number of the cloud-free pixels in the study region by metadata of the images

```
totalPixels = ee.Number(totalPixels);
unmaskedPixels = ee.Number(unmaskedPixels);
var cld = totalPixels.subtract(unmaskedPixels).divide(totalPixels).multiply(100);
return img.set('cloudness_ratio', cld);}
```

Production of a parameter called "cloudness_ratio" that have information on cloudness ration for just the study region

```
var cloudness = l8images.map(cloud).filterMetadata("cloudness_ratio","less_than",10);
```

Creation of Image collecion which contains images that have less than 10% cloudness ration in the study region

Figure 3.5. *GEE codes that enable the partial cloud filtering*

3.2.3. Detection of Water Pixels

Up to this stage of the thesis, image collections of Landsat 5 TM, Landsat 7 ETM +, Landsat 8 OLI / TIRS and Sentinel-2 satellites with a cloudiness of less than 10% within the analysis boundaries of 16 lakes were obtained between 1984 and 2018. There are more than 4000 images in these collections. One of the most important parts of this study is to be able to detect the water pixels within the analysis boundaries and to show its temporal change. For detection of the water in the images, NDWI was selected among the indices. To determine the NDWI threshold in identifying water and non-water pixels, randomly selected satellite image for each lake was manually digitized and the water surface areas were calculated by Arcgis Software version 10.1. For the same satellite images series of NDWI thresholds varying between 0.1 and 0.5 were set and corresponding water surface areas for each threshold were calculated in

GEE. The accuracy of the water surface areas calculated by NDWI in GEE for each threshold were then compared by those by manually digitized water surface area values. This comparison showed that the most accurate values were obtained by an NDWI threshold of 0.1 (Table 3.1). Note that Lake Karamik is a wetland and the presence of vegetation in the lake has a negative impact on water surface area determination using NDWI.

Table 3.1. Accuracy of the various NDWI threshold values

		Areas calculated in GEE according to NDWI					Area (km²) calculated by digitizing manually
	NDWI Thresholds	NDWI>0.5	NDWI>0.4	NDWI>0.3	NDWI>0.2	NDWI>0.1	
Lake Aksehir 05.03.2017 Landsat 8 OLI/TIRS	Area (km²)	1.818	7.424	13.978	19.147	25.015	24.421
	Accuracy (%)	7.4	30.4	57.2	78.4	97.6	
Lake Eber 03.04.2016 Landsat 8 OLI/TIRS	Area (km²)	4.119	25.257	45.558	66.226	85.604	107.055
	Accuracy (%)	3.8	23.6	42.6	61.9	80.0	
Lake Ilgin 15.04.2017 Landsat 8 OLI/TIRS	Area (km²)	22.440	22.695	22.890	23.038	23.192	23.326
	Accuracy (%)	96.2	97.3	98.1	98.8	99.4	
Lake Beysehir 03.04.2016 Landsat 8 OLI/TIRS	Area (km²)	633.901	636.295	638.563	641.385	645.402	652.829
	Accuracy (%)	97.1	97.5	97.8	98.2	98.9	
Lake Egirdir 05.03.2017 Landsat 8 OLI/TIRS	Area (km²)	453.518	454.396	455.298	456.450	457.074	470.097
	Accuracy (%)	96.5	96.7	96.9	97.1	97.2	
Lake Sugla 15.04.2017 Landsat 8 OLI/TIRS	Area (km²)	36.644	36.801	36.917	37.017	37.147	37.221
	Accuracy (%)	98.4	98.9	99.2	99.5	99.8	
Lake Karamik 19.04.2016 Landsat 8 OLI/TIRS	Area (km²)	0.000	0.881	5.946	9.540	14.520	35.371
	Accuracy (%)	0.0	2.5	16.8	27.0	41.1	
Lake Kovada 6.04.2017 Landsat 8 OLI/TIRS	Area (km²)	0.002	4.819	6.789	7.372	7.628	7.912
	Accuracy (%)	0.0	60.9	85.8	93.2	96.4	
Lake Gavur 30.04.1999 Landsat 5 TM	Area (km²)	0.005	0.188	1.396	2.179	2.306	2.328
	Accuracy (%)	0.2	8.1	60.0	93.6	99.1	
Lake Burdur 29.04.2017 Landsat 8 OLI/TIRS	Area (km²)	127.962	129.076	129.529	129.920	130.307	132.106
	Accuracy (%)	96.9	97.7	98.0	98.3	98.6	
Lake Acigol 04.11.2016 Landsat 8 OLI/TIRS	Area (km²)	28.292	30.216	31.739	34.588	36.430	38.632
	Accuracy (%)	73.2	78.2	82.2	89.5	94.3	
Lake Isikli 28.03.2017 Landsat 8 OLI/TIRS	Area (km²)	27.665	46.313	49.170	50.697	52.153	55.562
	Accuracy (%)	49.8	83.4	88.5	91.2	93.9	
Lake Salda 29.04.2017 Landsat 8 OLI/TIRS	Area (km²)	32.599	43.060	43.546	43.792	43.961	44.164
	Accuracy (%)	73.8	97.5	98.6	99.2	99.5	
Lake Yarisli 29.04.2017 Landsat 8 OLI/TIRS	Area (km²)	13.953	14.082	14.178	14.281	14.371	14.548
	Accuracy (%)	95.9	96.8	97.5	98.2	98.8	
Lake Karatas 29.04.2017 Landsat 8 OLI/TIRS	Area (km²)	7.057	7.240	7.386	7.547	7.728	8.057
	Accuracy (%)	87.6	89.9	91.7	93.7	95.9	
Lake Akgol 26.04.2016 Landsat 8 OLI/TIRS	Area (km²)	3.356	3.356	5.234	6.154	7.093	7.426
	Accuracy (%)	45.2	45.2	70.5	82.9	95.5	

After determination of the NDWI threshold as 0.1, a series of codes were written in GEE API to construct, for each lake, time series of lake water surface areas from 3864 images in the image collections. These steps are explained in the following sections. Figure 3.6 shows the GEE code to determine the water pixels using NDWI thresholding.

```
var l8_ndwi = cloudness.select(["B3","B5"]);
```

Selection of the bands (Green, NIR) used for calculating NDWI

```
function L8NDWI(img)  {
  var ndwi = img.normalizedDifference(['B3', 'B5']).rename('NDWI').clip(region)
  ndwi = ndwi.updateMask(ndwi.gt(0.1))
  return img.addBands(ndwi) }
```

Creation of a function to be able to calculate NDWI that is greater than 0.1 by green and NIR bands in the lake boundary

```
var l8ndwi = l8_ndwi.map(L8NDWI).select('NDWI')
```

Application of the function to the image collection

Figure 3.6. *GEE code to determine the water pixels using NDWI thresholding*

3.2.4. Conversion of Pixel Zones to Vector for Area Calculation

After determination of water pixels within the analysis boundaries, it was necessary to calculate the area corresponding to these water pixel zones. For calculation of the area values, it was necessary to convert the pixel zones to vector. A GEE code was written to convert the pixel zones to vector and to calculate the area of these vectors.

GEE codes that enables these operations are shown in Figure 3.7.

```
function vectorArea(img){
  var zones = img.gt(0.1);

  var vectors = zones.addBands(img).reduceToVectors({
    geometry: region,
    geometryType: 'polygon',
    eightConnected: false,
    crs: img.projection(),
    labelProperty: 'zone',
    reducer: ee.Reducer.mean()   });
   var selected_zones = vectors.filter(ee.Filter.eq("zone", 1))
   var area = selected_zones.geometry().area(1).divide(1000 *
1000);

var date=ee.Date(img.get('system:time_start'));
   return img.set('area', area).set('date', date); }

var collArea = l8ndwi.map(vectorArea);


print(ui.Chart.feature.byFeature(collArea, 'date', 'area'))
```

Creation of a function which converts the pixel zones to vectors and calculates the area of these vectors

Application of the function to the image collection and creation of the area values of the vectors

Generation of charts showing area values according to dates

Figure 3.7. *The code to convert the pixel zones to vector and to calculate the area of these vectors*

3.3. Displaying Water Surface Area Time Series for each Lake

There is a function in GEE API that enables construction of time series chart from image collections. However, this function displays only the dates with imagery on the x axis and hence the time gaps between the imagery dates cannot be visualized properly. To show the complete days, with or without imagery, between 1984 and 2018, bar charts in Microsoft Excel was used. For this task, water surface area time series were exported from GEE and then imported to Microsoft Excel. The dates without imagery were then added to the time series. For example, Figure 3.8 shows the daily water surface area variation in Lake Burdur. Note that the bars in this chart shows the water surface area calculated within GEE platform for the days for which an image with less than 10% of cloud cover is present in the collection. The days without a bar indicate that no image or no cloud-free image is present at that day. The bars are color coded to represent the satellite platform.

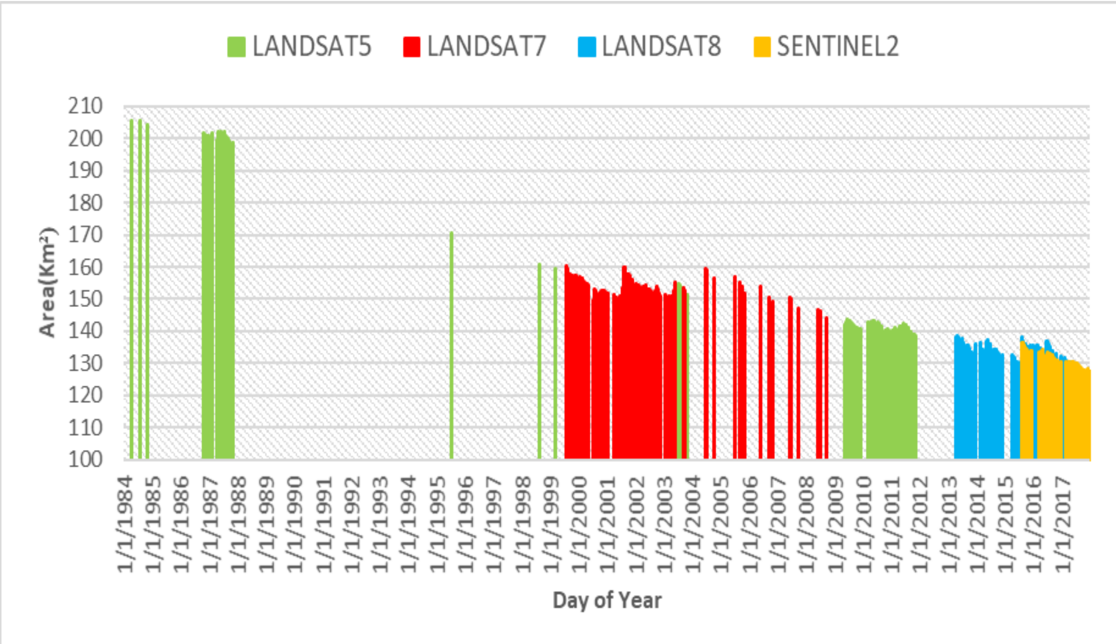

Figure 3.8. *Daily water surface area time series for Lake Burdur (1984-2018)*

3.4. Analysis of Relationships between Lake Water Extents and Meteorological Variables

Previous sections detail the calculation of water extent time series for 16 lakes in the Lakes Region for the period of 1984-2018 using GEE platform. To investigate possible links between lake water extents and meteorological variables, daily precipitation and evaporation time series were also plotted on water extent time series as a secondary y-axis (Figure 3.9 and 3.10). To better understand wet and dry periods, daily cumulative deviation from mean precipitation/evaporation values were used in these charts. For example, upward (downward) trends in cumulative deviation from mean precipitation values indicate wet (dry) periods compared to mean precipitation, whereas increasing (decreasing) trends in cumulative deviation from mean evaporation values indicate periods with high (low) evaporation compared to the mean evaporation. If there is no other factor, lake extents are expected to positively respond to trends in precipitation and negatively respond to trends in evaporation.

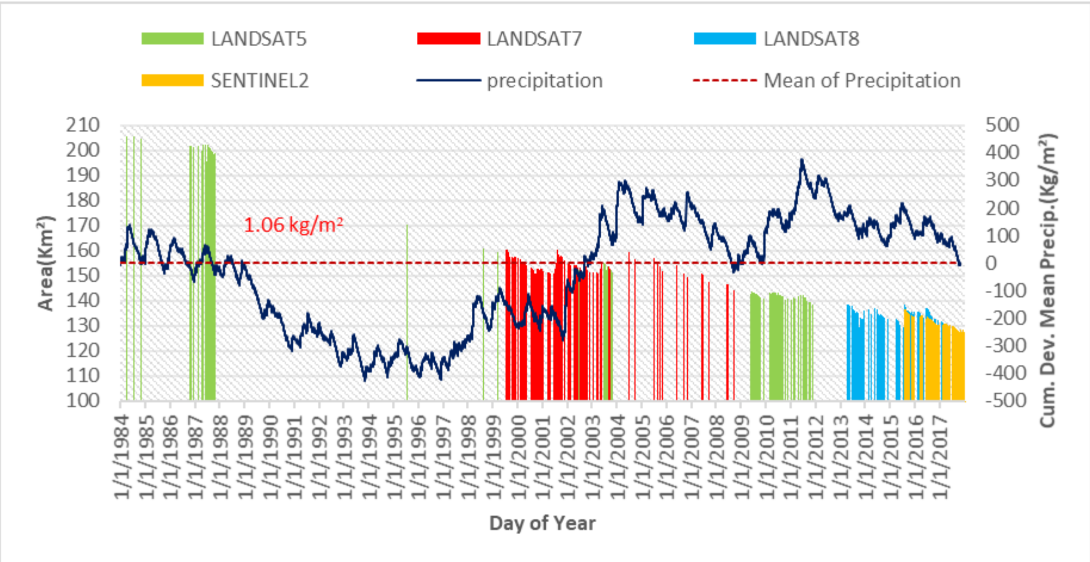

Figure 3.9. *Time series of lake water extent and cumulative deviation from mean precipitation for Lake Burdur*

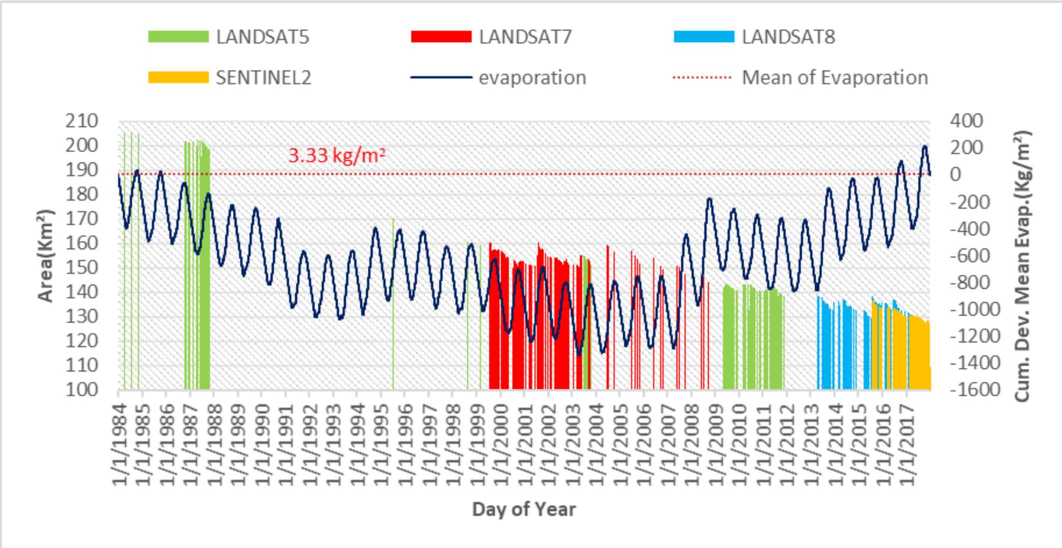

Figure 3.10. *Time series of lake water extent and cumulative deviation from mean evaporation for Lake Burdur*

3.5. Determination of Lake Water Extent using Bathymetry and In-Situ Water Level Measurements

Availability of in-situ lake level measurements together with Lake bathymetry enables determination of lake water extent. Thus, comparison of the lake water extents from in-situ measurements and remote sensing techniques can be made to investigate the degree of agreement between the two methods. Table 2.3. in Chapter 2 lists the lakes for which bathymetry data and lake level measurements are available. It can be seen from this table that both datasets are available for six lakes, namely, Lake Aksehir, Lake Beysehir, Lake Burdur, Lake Egirdir, Lake Kovada and Lake Eber.

However, there was a discrepancy between lake level measurements and bathymetric survey for Lake Eber which hindered the calculation of water extent. According to bathymetric survey of Lake Eber, highest elevation value is 966.1 meters but as seen in Figure 3.11 according to lake level measurements elevation values already exceeds 967 meters. The reason of this incompatibility is possibly the date of the bathymetric

After determination of the NDWI threshold as 0.1, a series of codes were written in GEE API to construct, for each lake, time series of lake water surface areas from 3864 images in the image collections. These steps are explained in the following sections. Figure 3.6 shows the GEE code to determine the water pixels using NDWI thresholding.

```
var l8_ndwi = cloudness.select(["B3","B5"]);

function L8NDWI(img)  {
  var ndwi = img.normalizedDifference(['B3', 'B5']).rename('NDWI').clip(region)
  ndwi = ndwi.updateMask(ndwi.gt(0.1))
  return img.addBands(ndwi) }

var l8ndwi = l8_ndwi.map(L8NDWI).select('NDWI')
```

Selection of the bands (Green, NIR) used for calculating NDWI

Creation of a function to be able to calculate NDWI that is greater than 0.1 by green and NIR bands in the lake boundary

Application of the function to the image collection

Figure 3.6. *GEE code to determine the water pixels using NDWI thresholding*

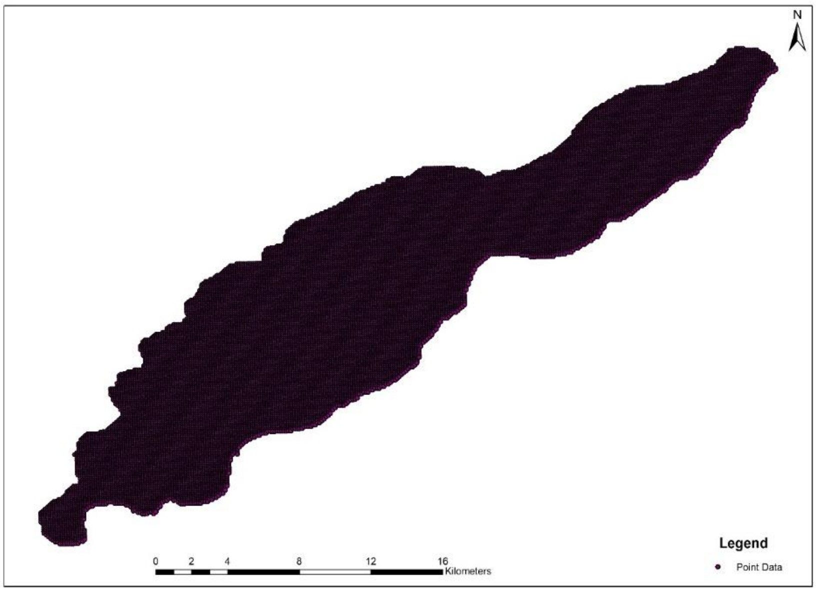

Figure 3.12. *Bathymetric Survey Points for Lake Burdur*

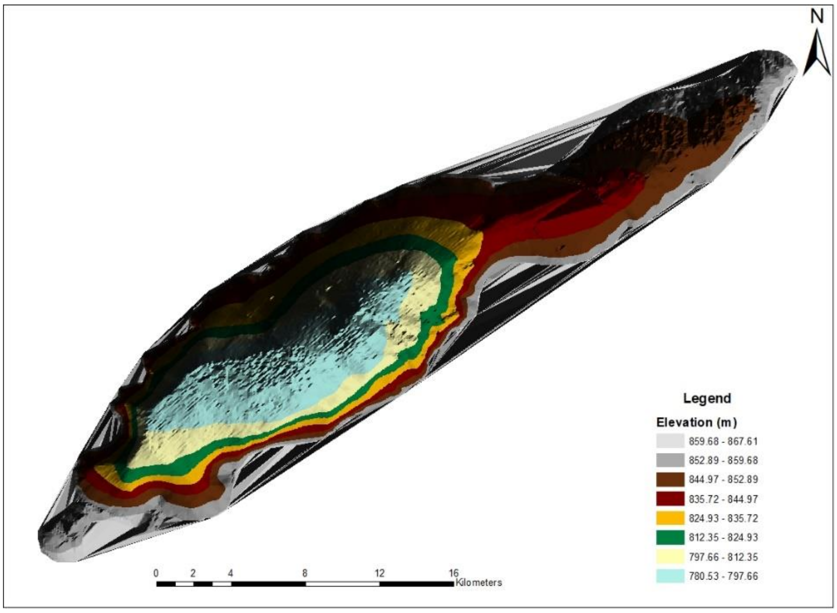

Figure 3.13. *Triangular Irregular Network (TIN) for Lake Burdur*

3.5.2. Production of Contours by Using Triangular Irregular Network

Contours are lines representing the equal elevation data. Contours were created from TIN using ArcGIS Software version 10.1 and 3D Analyst tools (Figure 3.14) and the digital elevation model (DEM) was created.

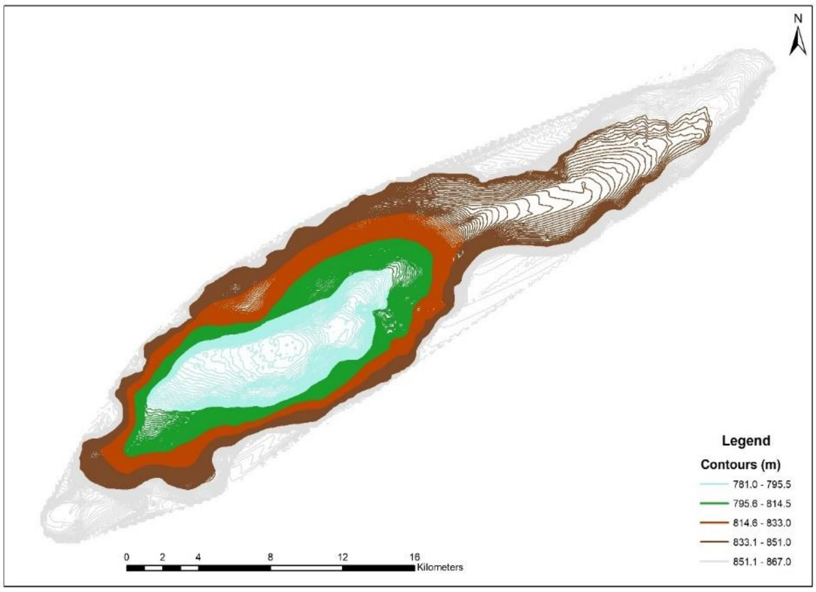

Figure 3.14. *Elevation Contours for Lake Burdur*

3.5.3. Production of Digital Elevation Model of the Lakes

Digital Elevation Model (DEM) is the digital representation of the bare surface and it is used to determine elevation at any point. DEM for each lake was constructed from the contour data by natural neighbor interpolation (Figure 3.15). By the production of the DEM, the lake area and volume corresponding to any elevation can be constructed.

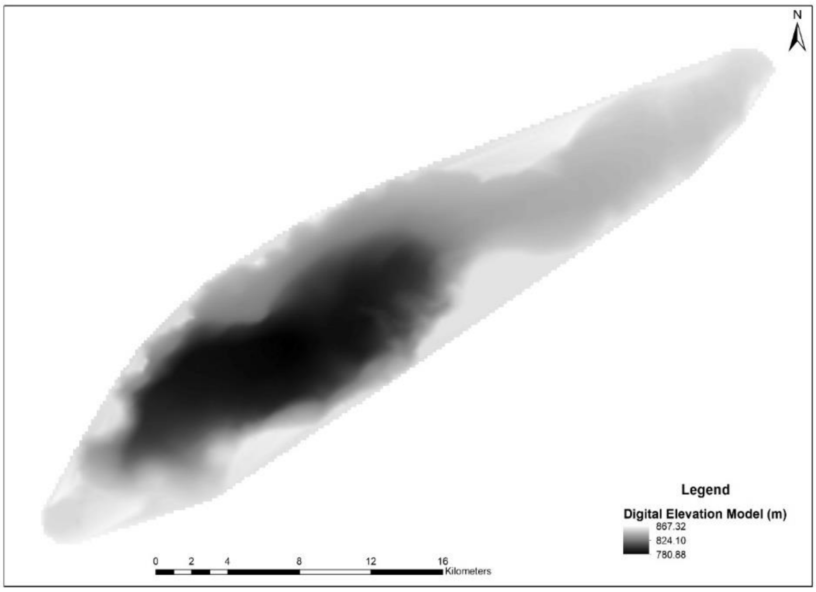

Figure 3.15. *Digital Elevation Model of Lake Burdur*

3.5.4. Calculation of Areas by Digital Elevation Model and Comparisons with Areas Calculated by Satellite Images

Lake areas calculated by satellite images give information about the lake area at the time the image was taken. Since temporal resolution (repeat coverage) is 16 days for Landsat TM, ETM+, OLI/TIRS and 5 days for Sentinel-2 and some of days were cloudy, there couldn't be achieved available images for every day.

Table 3.2 shows date ranges during which the lake level measurement data taken from General Directorate of State Hydraulic Works were available. Lake water extents for five lakes were calculated for the periods listed in Table 3.2 using in-situ lake levels together with elevation/area functions. Comparison of lake water extent obtained from remote sensing and in-situ measurements can be made only for those days both data are available. Number of overlapping days between satellite images and level measurements that allow area comparisons are 38 for Lake Aksehir, 60 for Lake Beysehir, 298 for Lake Burdur, 124 for Lake Egirdir and 178 for Lake Kovada. Results of these comparisons are discussed in Chapter 4.

Table 3.2. Available Lake Level Measurements

Lakes	Date Range for Available Lake Level Measurements
Aksehir	1984-2005
Beysehir	1984-2016
Burdur	2000-2017
Egirdir	1984-2017
Kovada	1984-2017

Manual calculate of the lake area repeatedly for different water levels in ArcgGIS is a time consuming process. Therefore Python programming functionality within ArcGIS was used and a code was written that takes water level time series as input and outputs the lake water area time series (Figure 3.16).

```
import arcpy, os

arcpy.CheckExtension("3D")
raster = r"C:\Users\...\burdur_DEM"
contour_list = r"C:\Users\...\level.txt"
outputCsv = r"C:\Users\...\areas.csv"
```

Show DEM and lake level list and output location in local computer.

```
with open(contour_list) as f:
   levels = f.read().split("\n")
```

Asset water levels to a variable.

```
if arcpy.Exists(r"in_memory\conts"):

   arcpy.Delete_management(r"in_memory\conts")
if arcpy.Exists(r"in_memory\diss"):
   arcpy.Delete_management(r"in_memory\diss")
```

Dublication control in temporary working location

```
contours = arcpy.ContourList_3d(raster, r"in_memory\conts", levels)
```

Production the contour line for the water level

```
arcpy.AddField_management(contours,"area","DOUBLE")
```

Creation of the field for area

```
with arcpy.da.UpdateCursor(contours, ["shape@","oid@","area"]) as n:
   for i in n:
      for j in i[0]:
         pol = arcpy.Polygon(j)

         if pol.area:
            i[2] = pol.area/1000000
      n.updateRow(i)
```

Asset of the calculated area value to the area field in kilometer

```
diss = arcpy.Dissolve_management(contours, r"in_memory\diss",
 'Contour', 'area SUM', 'MULTI_PART', 'DISSOLVE_LINES')
```

Dissolution of the same elevation contours

```
with open(hedefCsv,"w") as m:
  with arcpy.da.SearchCursor(diss,["Contour","SUM_area"]) as m:
    text = ""

    for i in m:
      text += str(i[0]) + ";" + str(i[1]) + "\n"
  m.write(text)
```

Asset the contour and area values to the output

Figure 3.16. *Python codes that enable the area calculation by digital elevation model and lake level measurement.*

3.5.5. Calculation of Volumes

Volume of lakes provide critical information for lake water balance analysis and water resources management (Sobek, Nisell, & Folster, 2011). In this study volumes of the lakes were calculated using digital elevation model for certain elevation values, similar to the area calculation. Similar to area calculation, manual volume calculation for each elevation value is inefficient in Arcgis. For this reason Python programing language was used for volume calculations (Figure 3.17). Elevation-Area-Volume relationship for Lake Burdur is given in Figure 3.18.

```
import re, arcpy


arcpy.CheckOutExtension("3D")

inputcsv=r"C:\Users\...\elevations.csv"
outputcsv=r"C:\Users\...\burdur_volumes.csv"
raster = r"C:\Users\...\burdur_DEM"


with open(inputcsv) as f:
   head=f.readline()
   data = f.readlines()


text = ""

for i in data:
   row = i.strip().split(";")

   date = row[0]
   h = row[1].replace(",",".")
   if h:
      a=arcpy.SurfaceVolume_3d(raster, '#', 'BELOW', float(h), '1', '0')
      mes = a.getMessages()
      text += date+";"+re.findall(".*Volume=(.+?)\n.*",mes)[0]+"\n"

with open(outputcsv,"w") as m:
   m.write(text)
```

Show DEM and lake level list and output location in local computer.

Asset water levels to a variable.

Calculation the volume values according to DEM and elevations

Figure 3.17. *Python code for calculating volume from digital elevation model for selected elevations*

The functions relating elevation to area and elevation to volume was constructed for each lake using Arcgis Software version 10.1 and 3D Analyst tools (Figure 3.18). These functions then can be utilized together with in-situ lake level measurements to calculate water surface area and water volume corresponding to each in-situ lake level measurement.

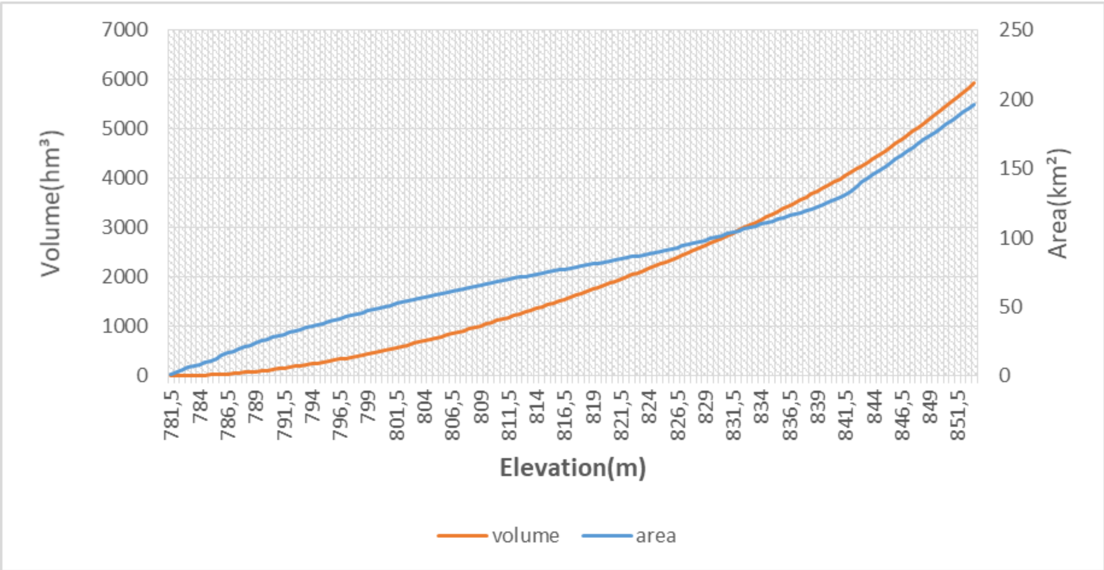

Figure 3.18. *Variation of area and volume values according to elevation*

CHAPTER 4

RESULTS

4.1. Temporal Changes in Lake Water Extent and Relations with Meteorological Variables

4.1.1. Lake Aksehir

Figure 4.1 shows the temporal variation in Lake Aksehir water extent for the 1984-2017 period. It can be seen that the largest water extent occurred in spring 1984 with a value of 330 km², and the water extent was reduced to 300 km² in the summer of 1984. No imagery was available for 1985-1986 period. In 1987, water extent has decreased from 300 km² to 275 km² towards the end of the year. After a gap in imagery between 1987 and 1998, water extent of the lake was calculated as 220 km² in the summer of 1998 which then decreased to 210 km² in 1999, and continued decreasing until the end of 2001. As of 2002, the area has increased again and reached to 186 km² in the summer of 2004. The lake extent, which is marked by sharp decline starting from 2004, almost completely dried (0.005 km²) in the autumn of 2008. Note that the water extent values for the 2004-2008 period was calculated by downloading the Landsat 7 images because an image gap filling algorithm was not available in GEE to use for Scan Line Corrector (SLC) failure of the sensor causing data gaps.

A management plan was prepared in 2008 to replenish the existing water resources in Lake Aksehir and Lake Eber (Lake Aksehir and Lake Eber Wetland Management Plan (2008-2012), 2008). After this date, the lake area has increased, partly due to wet conditions, and in the spring of 2009, reached to 125 km². The lake area, which started to show a seasonal change between the spring of 2009 and autumn of 2011, reached 120 km² in the spring and decreased to 70 km² in the autumn in this period. In 2013, the water extent was determined as 100 km² in the spring and decreased to 45 km² in autumn. In 2014, the lake almost completely dried, with water extent values as low as 0.4 km² in the spring and 0,005 km² in the autumn. The lake extent, increased to 50 km² in January of 2015, and to 130 km² in spring 2015 and started to decrease down to 100 km² by the end of the year. With a steady decrease in 2016, the lake extent decreased from 100 km² in spring towards 0.2 km² at the end of the year. In the spring of 2017, the lake extent increased to 80 km², and dried almost completely at the end of the year with an extent of 0.2 km².

In summary, Lake Aksehir water extent has been steadily declining since 1984 almost completely dried in 2008, 2014, 2016 and 2017 based on available imagery. By the year 2017, Lake Aksehir lost 84% of the water extent as compared to the year 1984.

Figure 4.2 shows cumulative deviation from mean daily precipitation together with the water extent change of Lake Aksehir to easily recognize the change in precipitation and its possible effect on lake extent. It is seen that, there has been a decrease in the lake area despite the increase in the precipitation between 1984 and 2000. Decreasing in the lake area during 2001 shows a similarity with decreasing in precipitation for the same year. In 2004, the highest precipitation values were reached, then the precipitation started decreasing and reached the lowest level in 2014 since 1987. In 2014, the values of the area decreased and fell below 1 km² following the decrease in precipitation. However, the increase in the precipitation values between the years of 2008 and 2011 is not followed by the area values. The value of area which started to rise as of 2015 started to decrease in 2016 and reached below 1 km² at the end of the year. This is in parallel with the precipitation fluctuation in the same period. The same parallelism is also valid for 2016-2017 period.

As seen in the Figure 4.3, the evaporation values decreased regularly and reached their lowest values in the early 2000s. After that date, the evaporation values that have increased regularly reached the highest level in 2017. As a summary of 1984-2018, it is seen that precipitation and evaporation is inversely proportional before and after the break in the beginning of 2000s.

According to (Erdem, 2007), drying of Lake Aksehir and Lake Eber is due to anthropogenic effects such as keeping the rivers that feed the wetland in dam or changing their direction and excessive use of groundwater. Similarly Catal and Dengiz (2015) argued that the level of lake has been continuously decreased due to reduction of precipitation, increase in evaporation, discontinuation of water supply to the lake by dams and ponds, unconscious increase in agricultural irrigation, uncontrolled groundwater wells, establishment of factories and organized industrial zones, thermal hotels, increase in population and hence increase in domestic water consumption. In this thesis, the decrease in long-term precipitation values and increase in long term evaporation values especially starting from early 2000s were found to be an important factor in the decrease in Lake Aksehir water extent.

Images in Figure 4.4 show the water extent of Lake Aksehir for three different years, visually depicting the significant decrease in water extent.

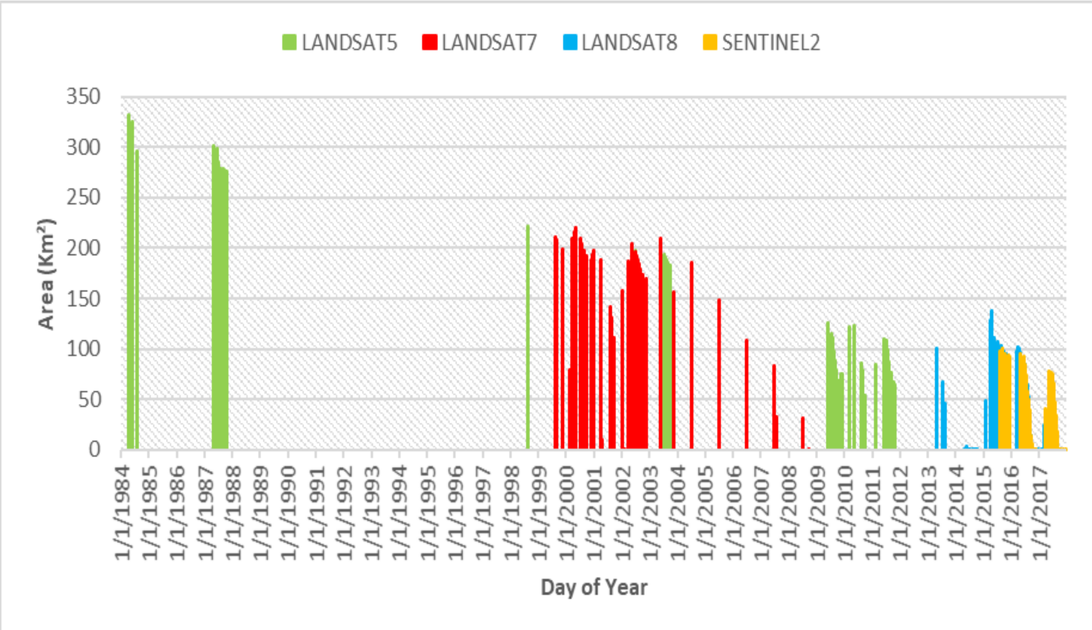

Figure 4.1. *Water Extent Change of Lake Aksehir*

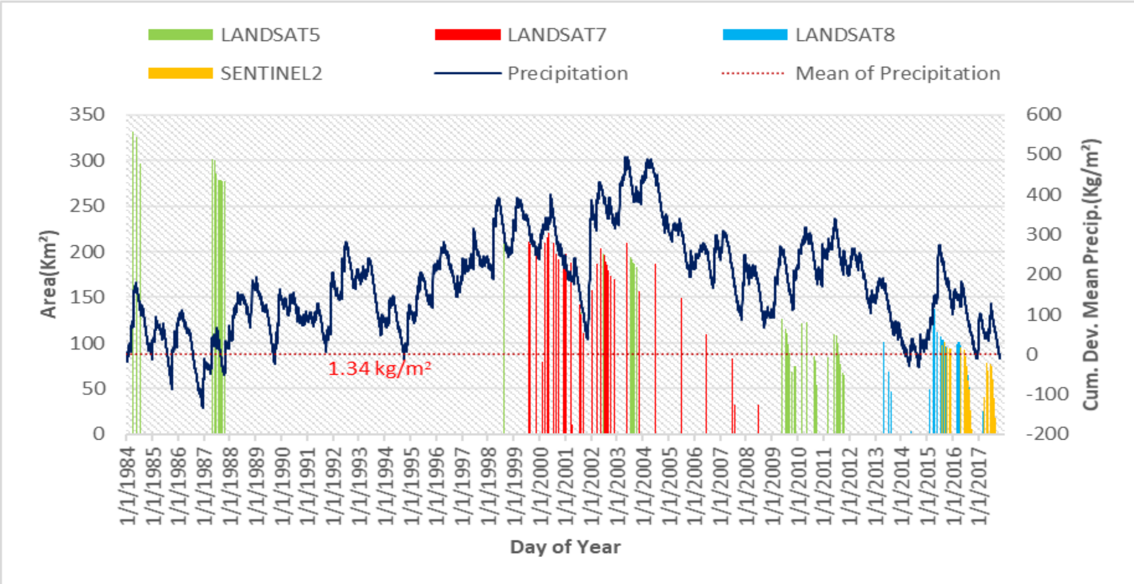

Figure 4.2. *Water Extent Change of Lake Aksehir and Cumulative Deviation from Mean Daily Precipitation*

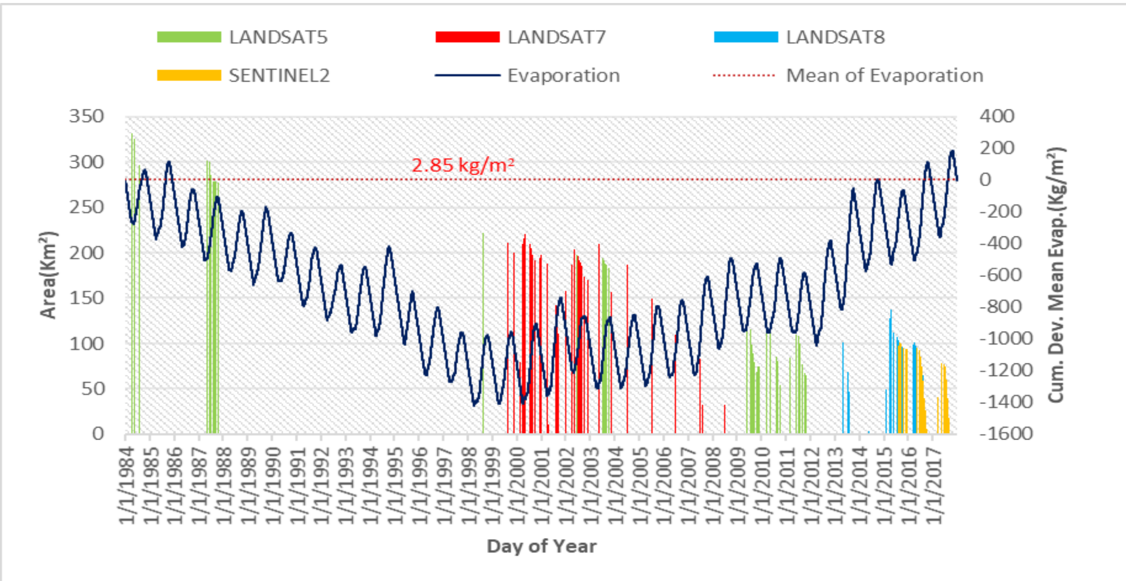

Figure 4.3. *Water Extent Change of Lake Aksehir and Cumulative Deviation from Mean Daily Evaporation*

Figure 4.4. *Water Extent of Lake Aksehir; (a) 19.8.1999 Area: 209 km² (Landsat 7), (b) 09.08.2016 Area: 52 km² (Landsat 8), (c) 20.08.2017 Area: 7 km² (Sentinel 2)*

4.1.2. Lake Eber

The lake, which mostly consists of reeds, is also a marsh (Ozturk, 2005). This situation presents difficulty in using remote sensing to delineate water extent of Lake Eber. As seen in Figure 4.5 the lake area, which was 96 km² in spring 1984, fell to 20 km² in the summer. In the spring of 1987, the area was 70 km² and in the summer of the same year it decreased to 5 km². A decrease in lake area was observed from 1984 to 1987. Due to lack of imagery, area values could not be calculated between 1987 and 1999 except 4 km² in 1998. The area value which was 7 km² in the summer of 1999 completed this year with 28 km², and the area value which increased in 2000 reached to the highest level with 100 km² in spring. In accordance with seasonal changing, area value in 2000 started decreasing in summer and autumn and finished this year with 18 km². The area value, which was 30 km² in the spring of 2001, fell below 1 km² at the end of this year. The area value, which started to increase again at the beginning of 2002, was 66 km² in the spring of this year and completed the year with 22 km². The area value which was 85 km² in the spring of 2003 started decreasing since and fell below 1 km² in 2008. The area values of this period were calculated by downloading and digitizing Landsat 7 images. "Aksehir-Eber Lakes Wetland Management Plan 2008 – 2012" was prepared in 2008 to feed existing water resources (Lake Aksehir and Lake Eber Wetland Management Plan (2008-2012), 2008) and as of 2009, the value of the area has increased again to 6 km² in the spring of this year and 56 km² in the spring of 2010. In the spring of 2011, the area value which was 17 km² decreased to 7 km² in autumn. No imagery was available in 2012 for Lake Eber. Although the value of the area was 50 km² in the spring of 2013, this value has decreased to 1 km² at the end of the year. The fluctuation of the area between spring and autumn is 37 km² to 7 km² for 2014 and 82 km² to 40 km² for 2015, 85 km² to 30 km² for 2016 and 50 km² to 10 km² for 2017. At the end of 2017, the area was determined as 30 km². In summary, the variation in lake extent follows seasonal pattern with increase in the spring and decrease in the autumn.

In the lake which reached the highest area values in spring season, the values decreased since 2015 and with respect to maximum values in 2000, it is determined that the water extent decreased by 45 % as of 2017. Note also the marsh conditions depicted in the images.

As seen in Figure 4.6 decrease in precipitation from 1984 to 1987 is compatible with decrease in area for the same period. Precipitation values which increased from 1999 to 2000, decreased in 2001 and increased again in 2002 and 2003 is followed by similar changes in the lake area values in the same period. The change in area values which falls below 1 km² in 2008 following significant decrease in precipitation in the same period. Increase in precipitation in 2009 and 2010 was consistent with the increase in the area for same years however despite the increase in precipitation in 2011, the area decreased. Precipitation variation characterized by a decrease from 2013 to 2014 and an increase until spring 2015, are consistent with areal changes for same period. However, in 2015, although the precipitation values reached the maximum value, the same increase was not observed in the area values. Decrease in area from 2016 to 2017 is similar with decrease in precipitation.

Figure 4.7 shows the cumulative deviation from mean evaporation from 1984 to 1987 together with the lake extent. In the long term, evaporation values are characterized by two periods with increasing trend (1984-1990 and 2006-2011) and a period with decreasing trend (1991-2005). It is however difficult to infer any relationship from this figure between lake extent and evaporation in long time scales. Focusing on the seasonal fluctuations in evaporation, it can be seen that the high values of lake area coincide consistently with the seasonal low values of evaporation (winter); see for example the years 1984, 1987, 2000, 2003 and 2010. Evaporation values for the station 17796 that's related with Lake Eber is only available until October 2011.

Figure 4.8 shows the water extent change of the lake with images belonging to 3 different years.

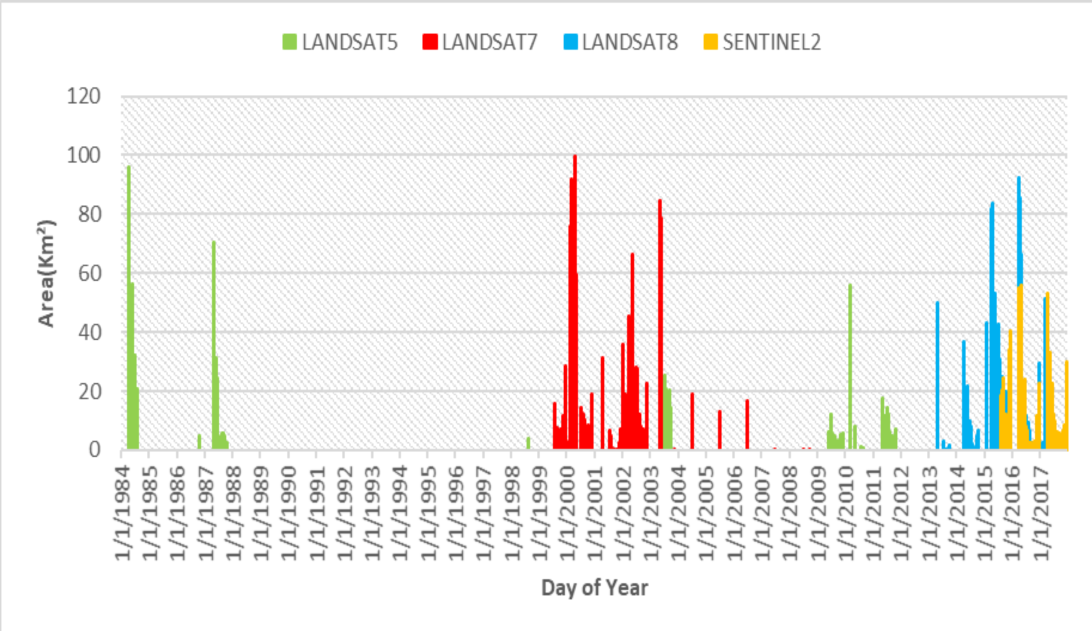

Figure 4.5. *Water Extent Change of Lake Eber*

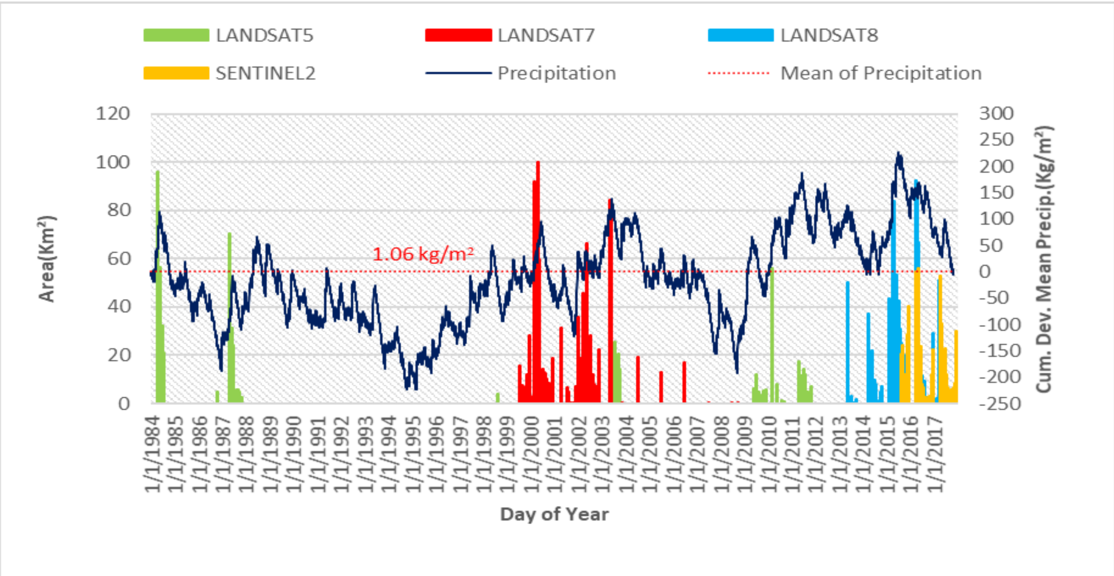

Figure 4.6. *Water Extent Change of Lake Aksehir and Cumulatie Deviation from Mean Daily Precipitation*

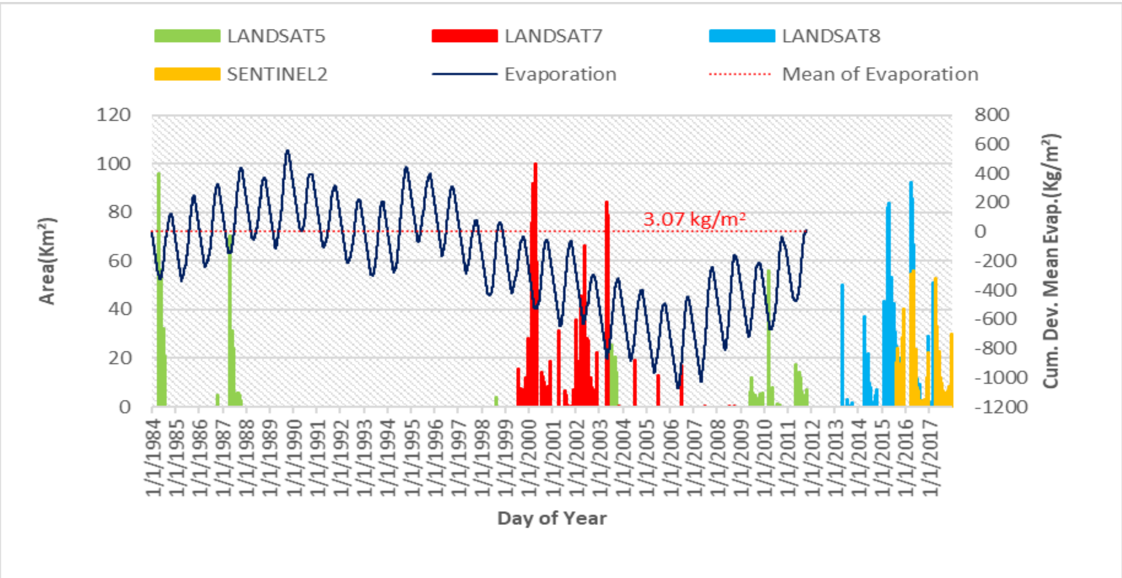

Figure 4.7. *Water Extent Change of Lake Eber and Cumulative Deviation from Mean Daily Evaporation*

Figure 4.8. *Water Extent of Lake Eber; (a) 15.4.2000 Area: 100 km² (Landsat 7), (b) 19.4.2016 Area: 40 km² (Landsat 8), (c) 27.4.2017 Area: 33 km² (Sentinel 2)*

4.1.3. Lake Ilgin

As seen in Figure 4.9 the area of the lake, which was determined 26 km² during the 1984, decreased to 20 km² in the summer of 1985. It was 25 km² in the spring of 1986, but decreased to 15 km² at the end of 1986. The area value, which was 23 km² in spring in 1987, decreased by the summer and reached to 15 km² in the autumn and showed a seasonal change. In 1990, with data only in the spring period, area was determined as 24 km². Between the years 1990-1998, there is no area value due to lacking of available images in this period. The area value, which was 25 km² in spring of 1998, again showed seasonal change and fell to 18 km² until autumn. The fluctuation of the same period was between 26 km² and 20 km² in 1999, 25 km² to 16 km² for 2000, 18 km² to 12 km² for 2001 and 26 km² to 22 km² for 2002 and 2003. In the summer of 2004, the area value was determined as 24 km² by the downloaded Landsat 7 image. For 2005, 2006, 2007 and 2008, the area values of summer months are around 15 km². In this period area values produced by downloading and digitizing Landsat 7 images are consistent with the area values produced by NDWI with Landsat 5 images. The area value, which was 22 km² in spring in 2009, dropped in summer and reached 17 km² at the end of the year. Very similar fluctuations in lake area value are valid for 2010 and 2011. In 2012, the lake has no area value. The area value which was 26 km² in the spring of 2013 decreased to 18 km² by the end of the year. Similar fluctuation was between 20 km² to 15 km² for 2014, 25 km² to 20 km² for 2015, 25 km² to 15 km² for 2016 and 23 km² to 10 km² for 2017.

In the lake which reached the highest area values in spring, the values decreased since 2015 and with respect to maximum values in 2003, it is determined that the water extent decreased by 19 % as of 2017. In the summer of 2017, even if the area values have fallen, the spring average is over 20 km².

Figure 4.10 shows the relationship between precipitation and lake extent. It can be seen from this figure that the spring periods with high precipitation values are followed by high lake area values. The agreement between the decrease in the area values and the decrease in the precipitation values in autumn is also seen clearly. Besides the seasonal changes, the long term decrease in precipitation between 2003 and 2009 is reflected with similar decrease in lake area values for the same period. Same situation is also observed after 2015; decrease in precipitation is followed by a decrease in area values. The results indicate that Lake Ilgin water extent is highly driven by the seasonal changes in precipitation.

It is also understood from the evaporation graph (Figure 4.11) that the area changes seasonally in the lake. The periods which the evaporation reached the lowest values during the year are the periods in which the area values increase. Evaporation values for the station 17832 that's related with Lake Ilgin is only available until October 2011.

Figure 4.12 shows the areal changes of the lake with images of 3 different years.

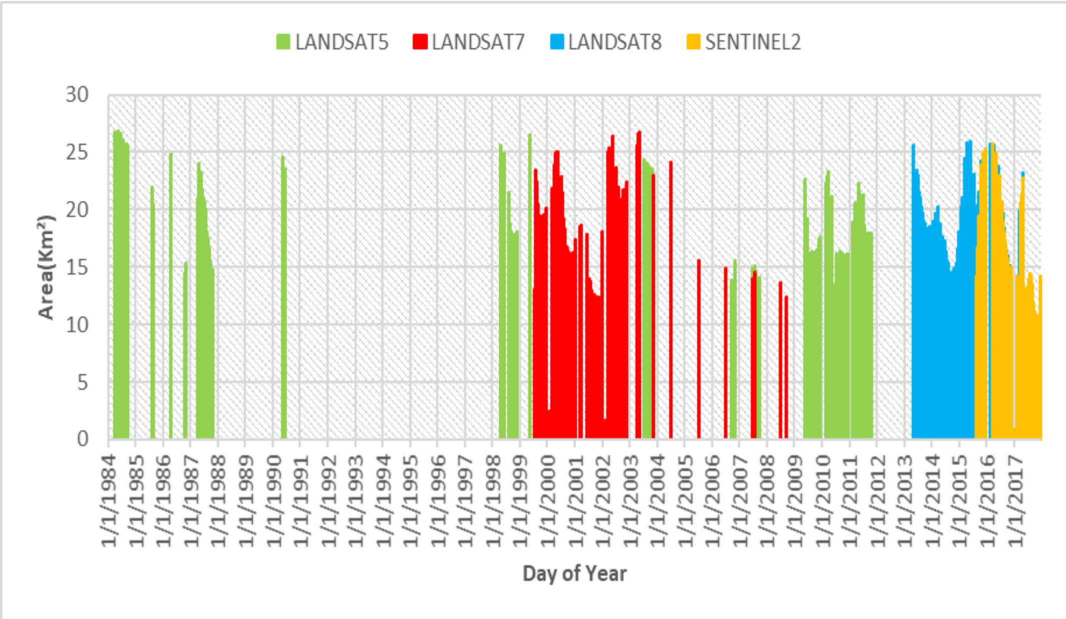

Figure 4.9. *Water Extent Change of Lake Ilgin*

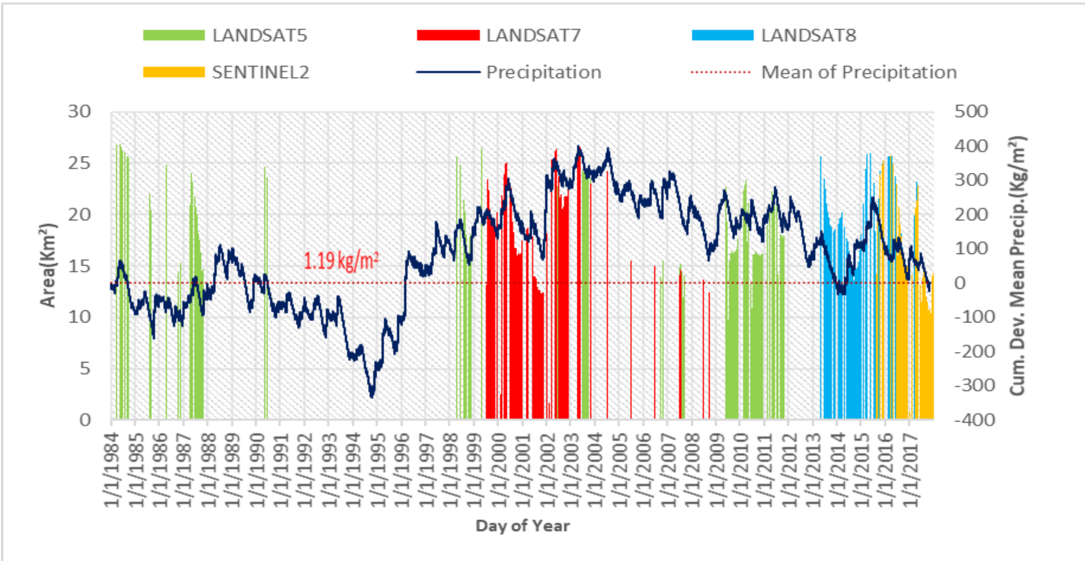

Figure 4.10. *Water Extent Change of Lake Ilgin and Cumulatie Deviation from Mean Daily Precipitation*

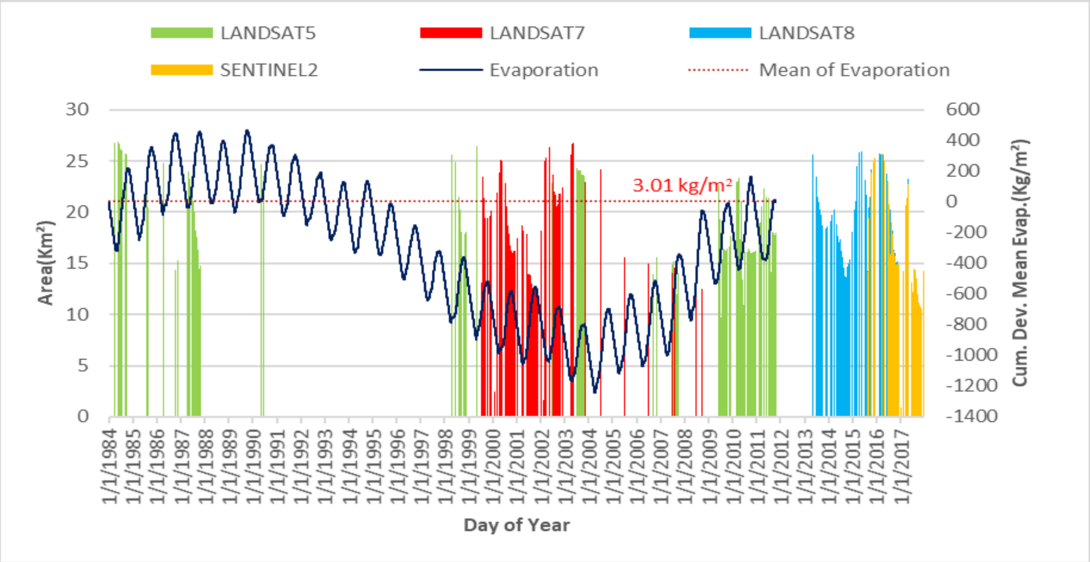

Figure 4.11. *Water Extent Change of Lake Ilgin and Cumulatie Deviation from Mean Daily Evaporation*

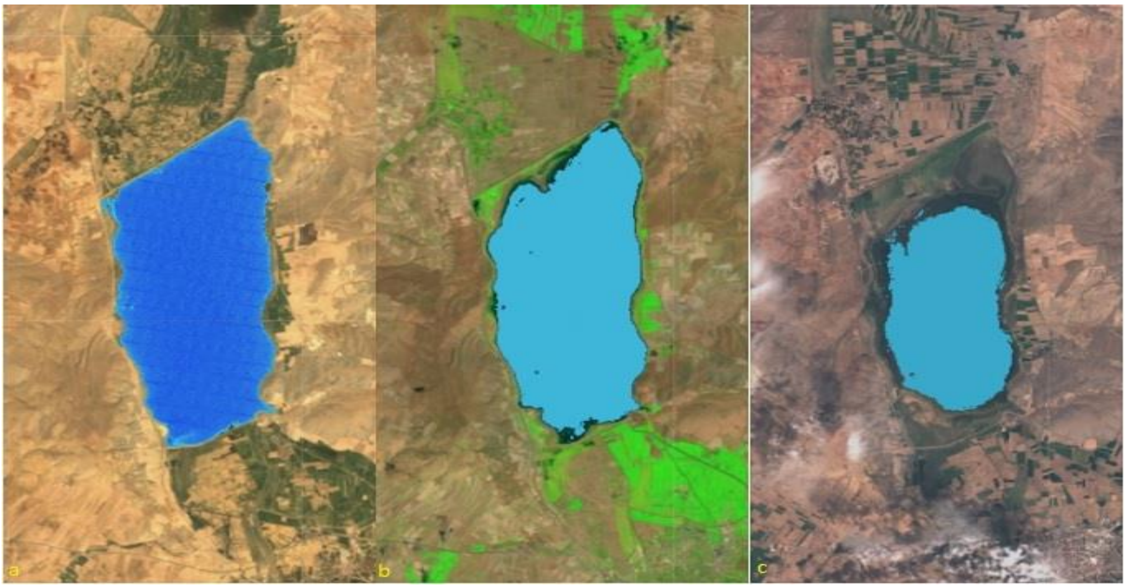

Figure 4.12. *Water Extent of Lake Ilgin ; (a) 10.8.1984 (Landsat 5), Area : 25.9 km² (b) 03.08.1999 Area : 22.5 km² (Landsat 7), (c) 20.08.2017 Area : 13 km² (Sentinel 2)*

4.1.4. Lake Beysehir

As seen in Figure 4.13 the lake area, which was 658 km² in spring 1984, was 655 km² in autumn. The change between spring and autumn in 1986 was 661 km² and 647 km² and 658 km² and 644 km² in 1987. No imagery was available between 1987 and 1998. The lake area, which was identified as 616 km² in the summer of 1998, fell from 646 km² to 633 km² in 1999 from spring to the end of the year, and from 637 km² to 622 km² in 2000 for same period in the year. The value of the area fell 637 km² to 622 km² from spring to autumn in 2010 and 625 km² to 606 km² in 2001. In the lake which has rarely satellite image in winter like other lakes, the area value increased in spring and decreased in autumn and showed a seasonal change, however with a general tendency to decrease until the end of 2001. The area value that increased again in 2002 was determined 634 km² in spring and fell to 627 km² until autumn. The areal change for same period is 635 km² to 625 km² in 2003. The lake area which was 641 km² in summer of 2004 was determined 632 km² and 619 km² in summer and autumn of 2005. In 2006 area of lake was 639 km² and 614 km² in summer and autumn. The lake area which was 643 km² in summer of 2007 was determined 643 km² and 632 km² in summer and autumn of 2008. All 8 area values between 2004 and 2009 was calculated by downloaded and digitized Landsat 7 images. From the summer of 2009 until the end of the year the area value was around 625 km². Variation of area between spring and autumn were determined between 649 km² and 628 km² for 2010 and 640 km² and 630 km² for 2011. In the lake, which has no imagery for 2012, 670 km² has been identified by reaching the highest value in the spring of 2013 and this value has decreased to 635 km² in the autumn of the same year. In 2014 there wasn't any imagery for spring and during summer and autumn area was around 630 km². The change of area in the lake from spring to autumn was determined between 651 km² and 633 km² in 2015 and between 648 km² and 617 km² in 2016. There wasn't any area value for 2017 in the lake.

In the lake it was reached the highest area values in spring. Area values started to decrease after 2013. With respect to maximum values in 2013, it is determined that the water extent decreased by 5 % as of 2017.

As seen in Figure 4.14, although there was a sharp decline in precipitation values from 1984 to 1987, area values did not decrease similarly. The decrease in the area values from 1999 to the end of 2001 and the increase in 2002 and 2003 are proportional to the change in precipitation in the same periods. Although the decrease in the area between 2004 and 2006 was also proportional to the decrease in the precipitation values, the precipitation values continued to decline in 2007 and 2008 despite the area values slightly increase in this period. The increase in precipitation values between 2009 and 2014 shows a similar increase in the area values. The decrease in area and precipitation values after 2015 is parallel. Note that the lake extent may not proportionally reflect the decrease in lake kevels for the lakes with steeply sloped bathymetry. This situation is valid for Lake Beysehir and will be further discussed in Section 4.2.

Figure 4.15, shows cumulative deviation from mean evaporation values together with lake levels. The evaporation values two significant periods –an increasing trend between 1984 and 1994, followed by a decreasing trend between 1995 and 2011. Note that no evaporation data is available after October 2011. A clear relationship between evaporation and lake area could not be inferred from the available data. Note that for the 2004 - 2009 period, the area values were calculated by downloaded Landsat 7 imagery and these images belong to the summer months corresponding to high evaporation values.

Figure 4.16 shows the areal changes of the lake with images of 3 different years.

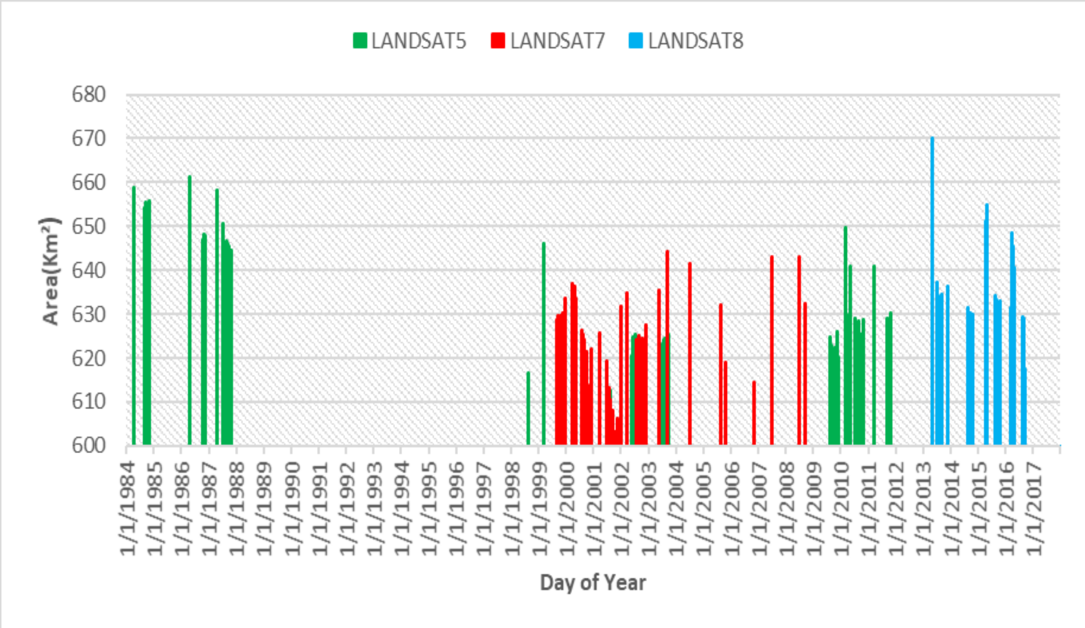

Figure 4.13. *Water Extent Change of Lake Beysehir*

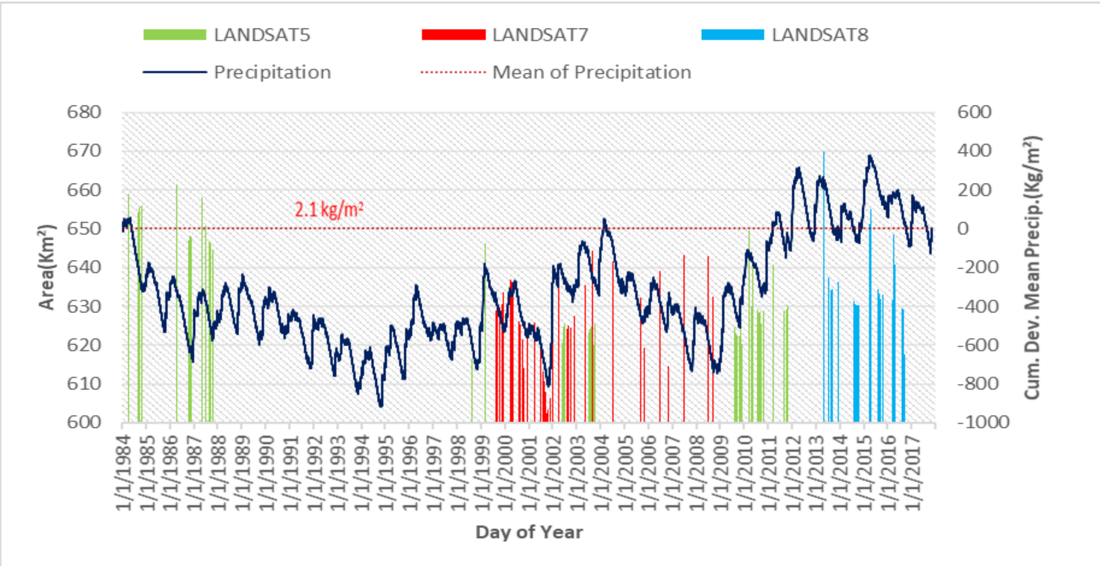

Figure 4.14. *Water Extent Change of Lake Beysehir and Cumulatie Deviation from Mean Daily Precipitation*

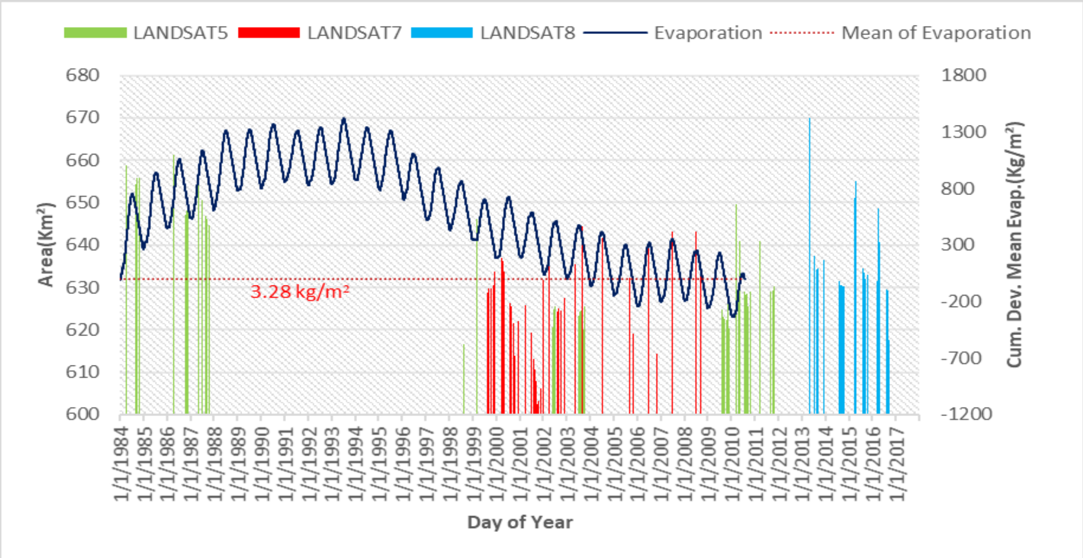

Figure 4.15. *Water Extent Change of Lake Beysehir and Cumulative Deviation from Mean Daily Evaporation*

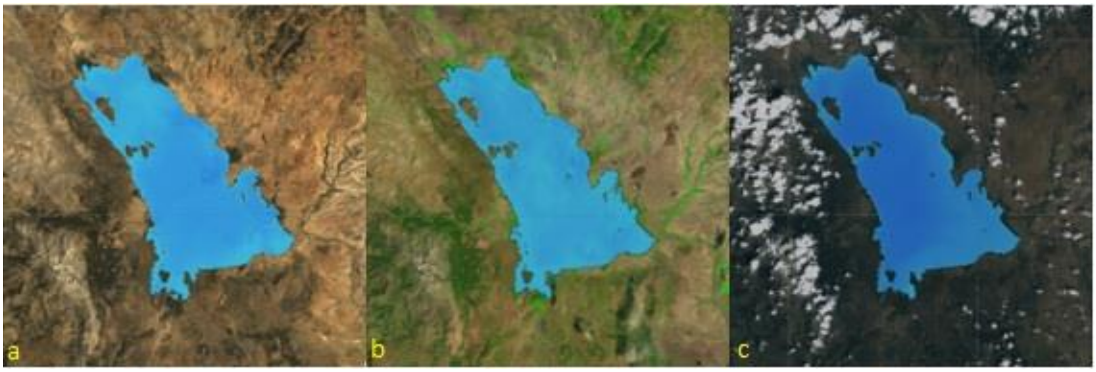

Figure 4.16. *Water Extent of Lake Beysehir; (a) 23.8.1986 Area: 646 km² (Landsat 5), (b) 19.8.1999 Area: 629 km² (Landsat 7), (c) 23.8.2015 Area: 633 km² (Landsat 8)*

4.1.5. Lake Egirdir

Figure 4.17 shows the time series of the Egirdir Lake extent for the dates on which imagery was available. In the study time period, the largest lake extent was observed in the autumn of 1984 with a value of 469 km². In the autumn of 1986, the lake extent was very similar with a value of 466 km². The lake area which was again 469 km² in the spring of 1987, decrease to a value of 461 km² in autumn. No imagery was then available until 1998. The area was determined as 454 km² in summer of 1998. In the spring of 1999, the lake area, which was 462 km², decreased to 438 km² in summer and reached 460 km² at the end of the year. The area value which was 467 km² at the beginning of 2000 decreased to 455 km² in summer and ended the year at this level. At the beginning of 2001, the area value was 462 km², and then decreased to 454 km² in summer and ended the year at these levels. For 2002, area was determined as 461 km² at the beginning of the year then decreased to 454 km² in summer and ended the year at 457 km². In the spring of 2003, the area value of 460 km² was 455 km² in summer and 454 km² in autumn.

According to the downloaded Landsat 7 images from 2004 to 2008, the lake area was 456 km² in the summer of 2004, 455 km² in the summer of 2005, 449 km² in the autumn of 2005, 455 km² in the summer of 2006, 445 km² in the autumn of 2006, 455 km² in the autumn of 2007, 453 km² in the summer of 2007 and 450 km² in the autumn of 2008. In the spring of 2009, the value of 453 km² fell to 451 km² and reached 454 km² at the end of the year. In 2010, the area value of 457 km² in spring was determined as 453 km² in summer. In the spring of 2011, the area value of 457 km² was reduced to 453 km² in summer and remained at this level until the autumn. There was no area value for 2012. In the spring of 2013, the area value which was 458 km², decreased to 432 km² in summer and increased again to 459 km² at the end of the year. At the beginning of 2014, the area value of 459 km² was reduced to 452 km² in summer and remained at this level until the autumn. In the spring of 2015, the area value which was 459 km² was reduced to 453 km² in summer, but at the end of the year it increased again to 459 km². In spring of 2016, the area value of 458 km² was reduced to 452 km² in summer and remained at this level until the autumn. In the spring of 2017, the lake area was determined 457 km².

The area of the lake reached the highest level in 1984 and 1987 exceeding 465 km². This value was approached again in 2000, however after early 2000s lake area did not exceed 458 km². The lake area increased in the spring and fell in the autumn and showed a seasonal change. The results show that the variation in Egirdir lake extent is only 10-15km^2, which is 2-3% of the maximum extent.

It can be seen in Figure 4.18 that the precipitation conditions get drier and drier for the period 1984-1997. Wet years of 1998 and 1999 are followed by a dry period until 2001. Lake extent approached to its highest observed values at the end of 1999, however the maximum lake extent values decreased and stabilized around 458km^2 with a general trend following wet/dry precipitation pattern.

Evaporation trend shown in Figure 4.19 indicates that 1984-1992 and 2009-2017 periods are marked by decreasing evaporation, whereas 1993-2008 period is marked by increasing evaporation pattern. No significant relationship was found between the change in area values and evaporation pattern in Lake Egirdir.

Figure 4.20 shows the areal changes of the lake with images of 3 different years.

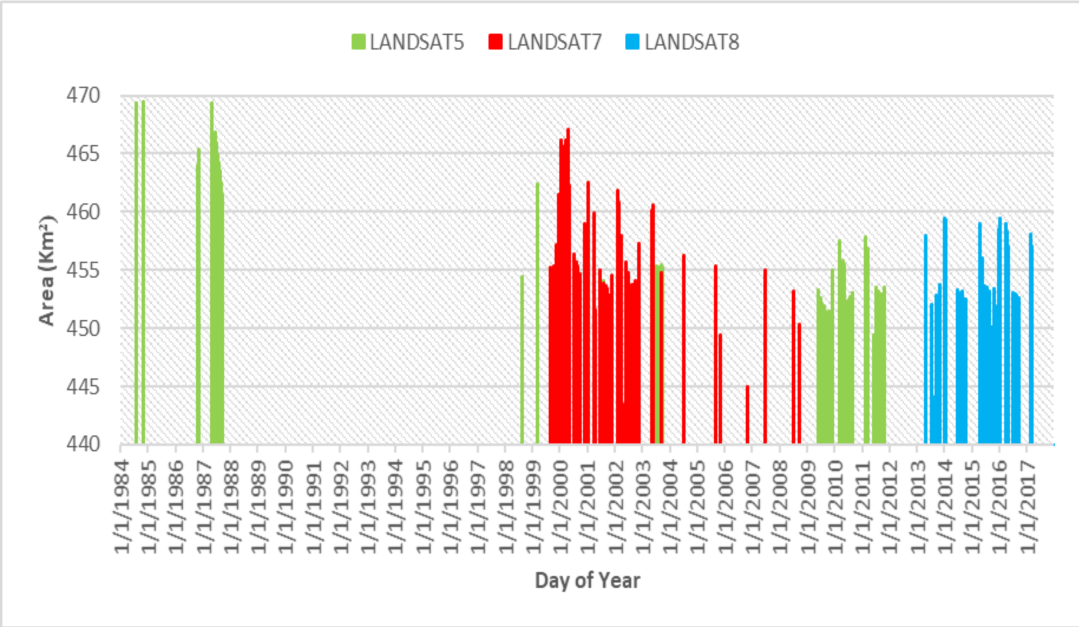

Figure 4.17. *Water Extent Change of Lake Egirdir*

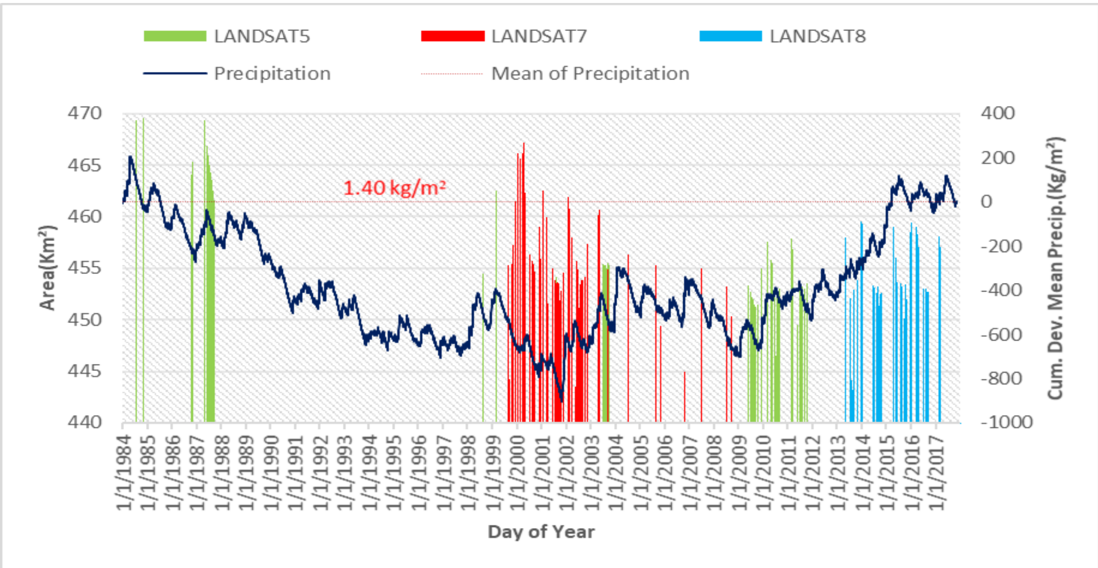

Figure 4.18. *Water Extent Change of Lake Egirdir and Cumulatie Deviation from Mean Daily Precipitation*

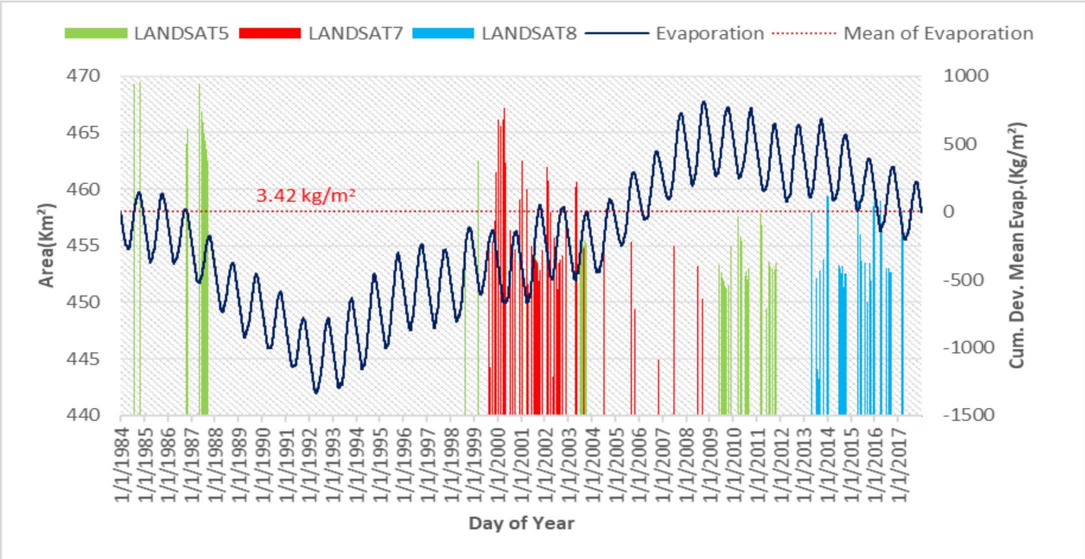

Figure 4.19. *Water Extent Change of Lake Egirdir and Cumulative Deviation from Mean Daily Evaporation*

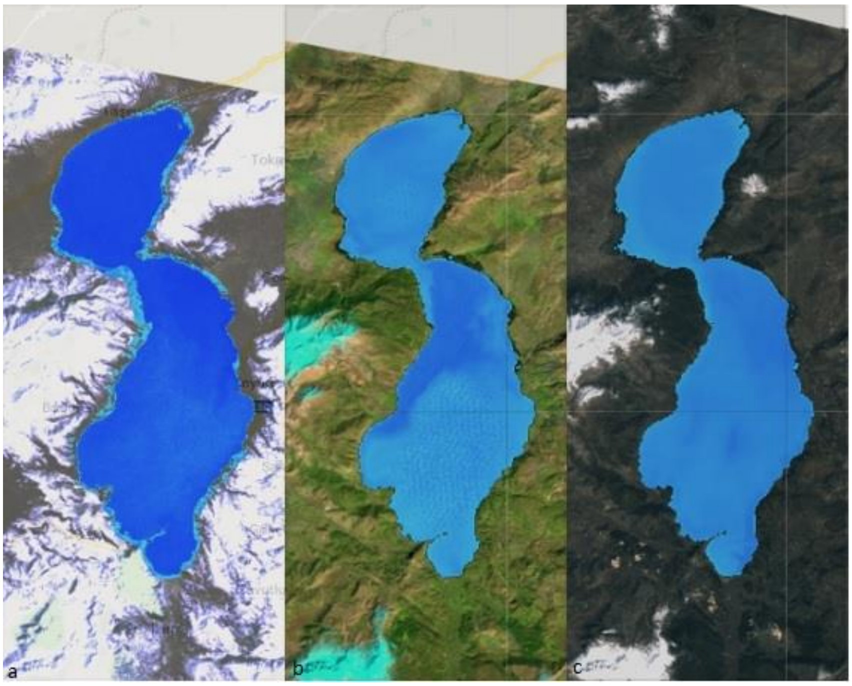

Figure 4.20. *Water Extent of Lake Egirdir; (a) 19.3.1987 Area: 470 km² (Landsat 5), (b) 17.3.2001 Area: 460 km² (Landsat 7), (c) 18.3.2016 Area: 460 km² (Landsat 8)*

4.1.6. Lake Sugla

As seen in Figure 4.21 although the lake area was 86 times determined with satellite images between the years 1984-2003, a limited number of area values could be distinguished in the figure. This is due to the fact that the lake area was determined as 0 km² for 36 times as and less than 0.01 km² for 48 times. The area was determined 0 km² in 1985 and 37 km² in January 1986. Until it was determined 12 km² in December 1988, area values were around 1 km² and below. The area value, which was 27 km² in January 1990, decreased to 16 km² at the end of the same year. The lake area which was 7 km² at the end of 1991 was 11 km² in the spring of 1992. The lake area which was 15 km² in the autumn of 1994 increased to 40 km² at the beginning of 1995 and reached the highest level. Until the end of 2001, the lake area, which was generally below 1 km², was identified at 38 km² at the end of 2001. The area of the lake, which was determined 15 km² in spring 2002, was around 2-3 km² until February 2003. In 2003 a dam was built in the lake that significantly increased the lake area (The General Directorate of State Hydraulic Works, 2014). The lake area, which was 32 km² in the autumn of 2005, was found 35 km² in the summer and autumn of 2006. The lake area, which was 25 km² in autumn 2007, was found 33 km² in the autumn of 2008. The area of the lake, which was fixed to around 37 km² for the period 2013-2017, was detected at less than 5 km² only at the beginning of 2017. It can be said that the dam constructed in 2003 had a significant effect on the lake area. Since there are no images of the lake for the period 2009-2013 no comments can be made about this period. In the Figure 4.21 it is intended to emphasize the dates that the area was determined as 0 km² by the dotes as black. In this way it is shown that there couldn't determine water. It should not be understood that there were no images on these dates.

As can be seen in the Figure 4.22, precipitation values decreased from 1984 to 1995. After that, except for the decrease in 2001-2002 period, it has been in an upward trend until 2004. Precipitation values tend to decrease until 2009 and tend to increase until 2015 except for a dry period in 2014. 2015-2017 period is characterized by drier conditions. Although a relationship between lake extent and precipitation can be deduced from the figure for the 1984-1995 period, no relationship can be deduced after 1995. Note that dam construction significantly Increase lake levels in spite of significant variation in precipitation

As seen in Figure 4.23, evaporation values were increased from 1985 to 1995 and started to decrease until October 2011. The evaporation data for the period before 1985 and after 2011 are not available in the meteorological station (17898) associated with this lake.

The relationship between area and meteorological data could not be observed due to the high number of low area values and the stabilization of the area values after the dam construction. However, in 1986, 1990, 1995 and 2001, the area values which were relatively high (more than 15 km²) were reached not in spring periods but in December-January periods. As seen in the Figure 4.22 and 4.23, these periods were the periods when precipitation is on the rise and evaporation is in decline.

Figure 4.24 shows the areal changes of the lake with images of 3 different years.

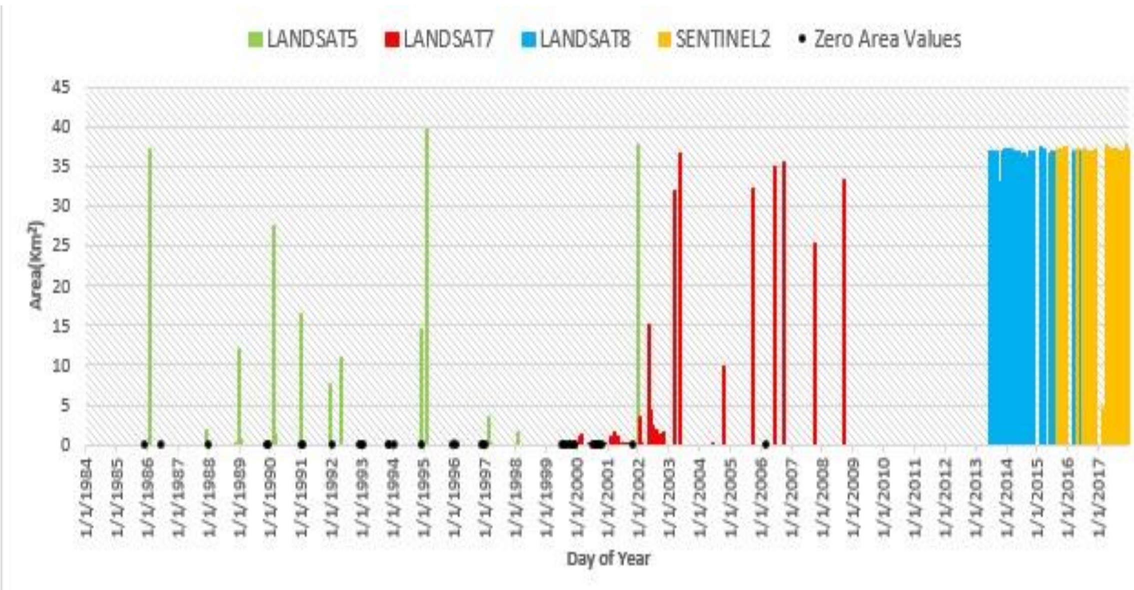

Figure 4.21. *Water Extent Change of Lake Sugla*

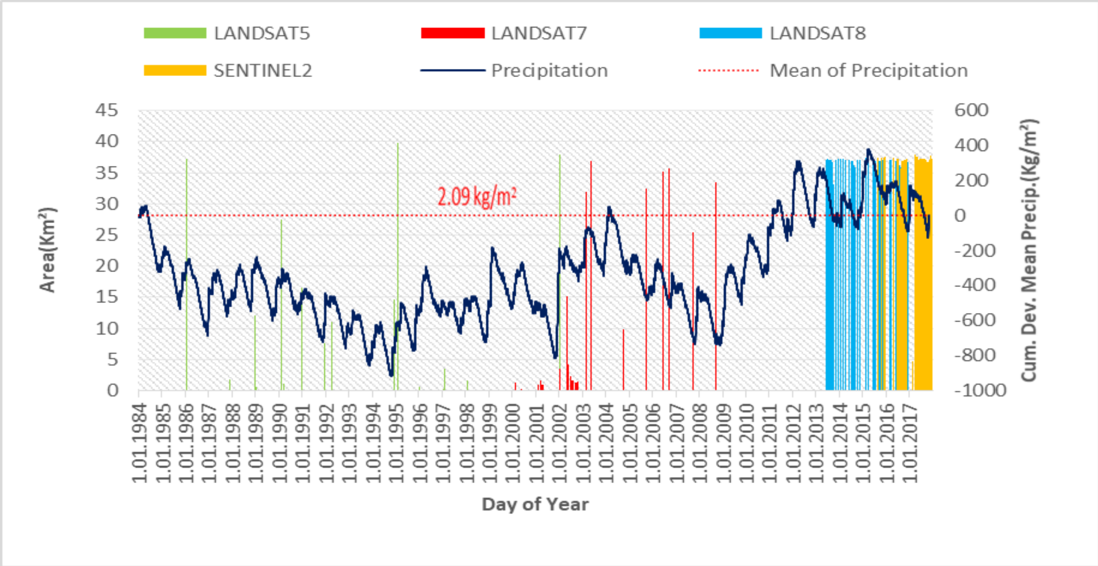

Figure 4.22. *Water Extent Change of Lake Sugla and Cumulative Deviation from Mean Daily Precipitation*

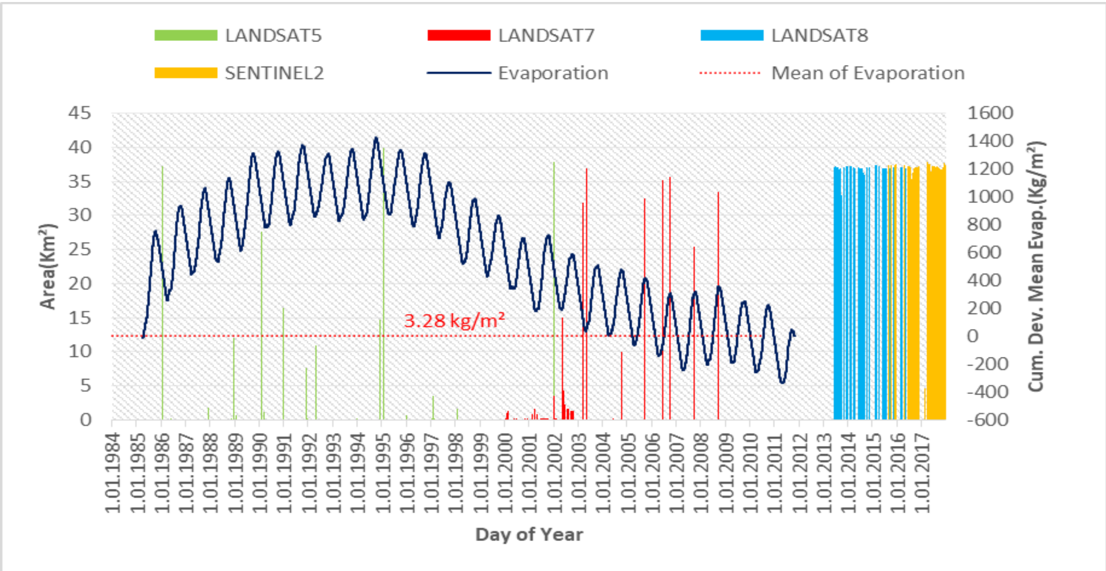

Figure 4.23. *Water Extent Change of Lake Egirdir and Cumulative Deviation from Mean Daily Evaporation*

Figure 4.24. *Water Extent of Lake Sugla; (a) 27.7.1999 Area 0 km² (Landsat 7) (b) 30.4.2002 Area: 15 km² (Landsat 7), (c) 27.4.2017 Area: 37, 5 km² (Sentinel 2)*

4.1.7. Lake Karamik

Reeds and marshes account for more than 90% of Lake Karamik (Hasbek & Ari, 2018). This situation exerts difficulty in satellite remote sensing detection of lake extent. As seen in Figure 4.25 the lake area, which was 5.6 km² in the spring of 1984, was 3.8 km² in the summer of the same year. The only value for 1986 is 5.3 km² of autumn. The lake area which was 10 km² at the beginning of 1987 increased to 18 km² in spring. The value of the lake area which change between 3 km² and 9 km² in summer has decreased to 2 km² in autumn. The area value which was 2.3 km² in the summer of 1998, determined 2.2 km² in the summer of 1999 and remained at this level until the end of the year and increased to 10 km² at the end of the year. The lake area that reached the highest level by 27 km² in spring of 2000, decreased in summer to values around 1 km². Lake area which change seasonally determined 14 km² in spring of 2001 then it decreased in summer and got values around 1 km² then it increased till the end of the year and determined as 9 km². The spring, summer and year-end values for 2002 were 10 km², 1 km² and 4 km² respectively. In the spring of 2003, the area value, which was 8.5 km², decreased to about 1 km² in summer and was around 0.1 km² at the end of the year. The area of the lake, which was around 1 km² from 2004 until the end of 2009, increased to 6 km² at the end of 2009. The area value which was 13 km² in the spring of 2010 has fallen by the end of summer and has been determined as 2 km². The area value which was 25 km² in the spring of 2011 fell down to the end of summer and determined 2 km². In the lake which has no area value in 2012, area was determined 25 km² in spring 2013. In the summer of 2013, the area value, which is 3 km², was determined as 5 km² in the autumn. In the spring of 2014, the area value, which was 16 km², fell to 4 km² in summer and remained at this value in the autumn. The area value, which was 18 km² at the beginning of 2015, decreased to 5 km² in summer and increased to 12 km² at the end of the year. The lake area which showed seasonal change in 2016 took values 23 km², 4 km² and 10 km² in spring, summer and year-end respectively. In 2017, these values were 20 km², 4 km² and 10 km² respectively for same period with 2016. The rise of the lake area in the spring, the fall in the summer and rising again towards the end of the year is a sign of seasonal change.

Figure 4.26 shows the close relationship between precipitation and lake levels at long time scales and at seasonal scale; dry periods are marked by decrease in lake levels and in the spring (summer) periods where the precipitation values are high (low) area values are also high (low).

Figure 4.27 shows clearly the seasonal correspondence in evaporation and lake area. Low evaporation season of 1987, 2000, 2001, 2002, 2003, 2010 and 2011 are marked by high lake areas.

Figure 4.28 shows the areal changes of the lake with images of 2 different years. Note that reeds and marshes within the lake results in patchy NDWI values.

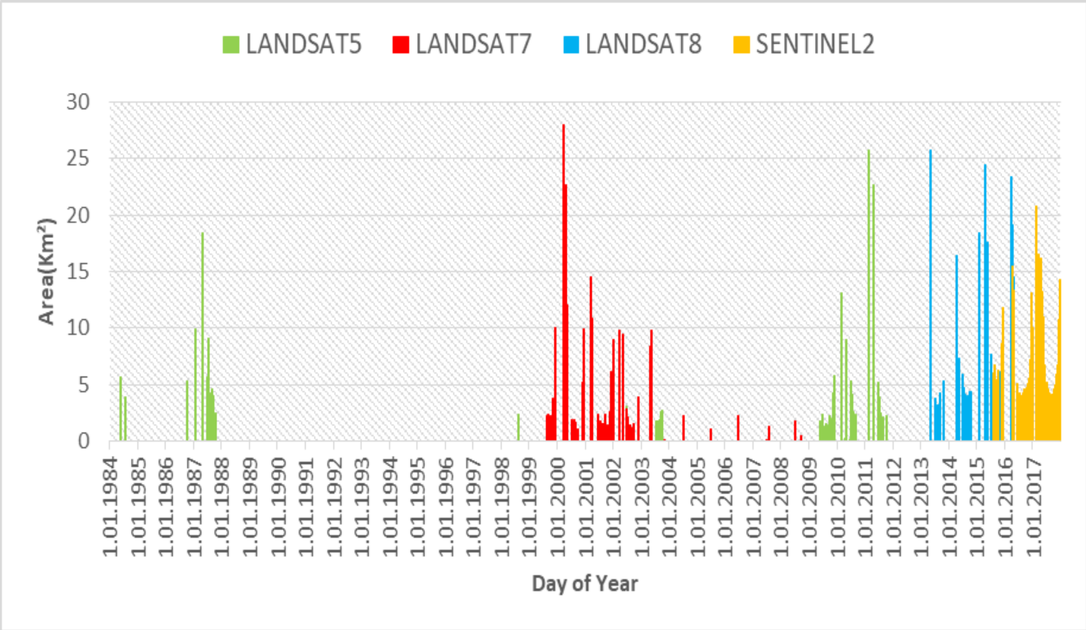

Figure 4.25. *Water Extent Change of Lake Karamik*

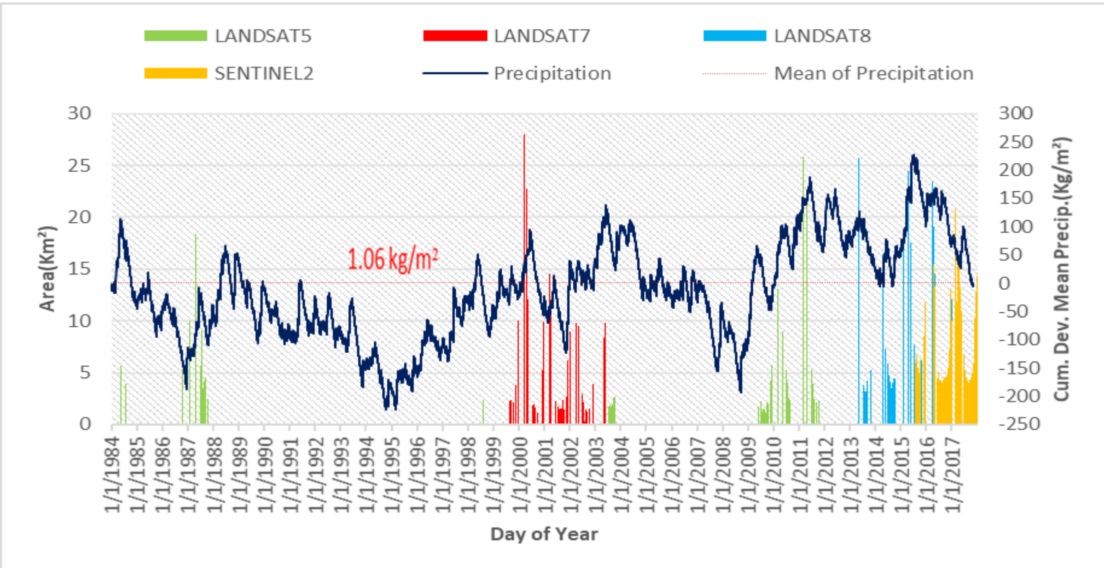

Figure 4.26. *Water Extent Change of Lake Karamik and Cumulative Deviation from Mean Daily Precipitation*

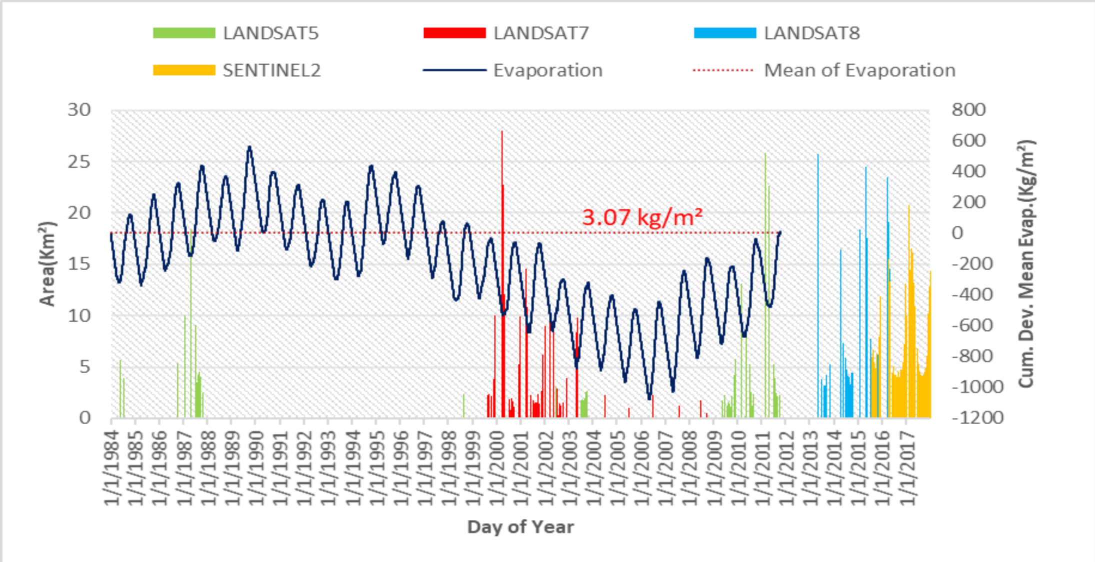

Figure 4.27. *Water Extent Change of Lake Karamik and Cumulative Deviation from Mean Daily Evaporation*

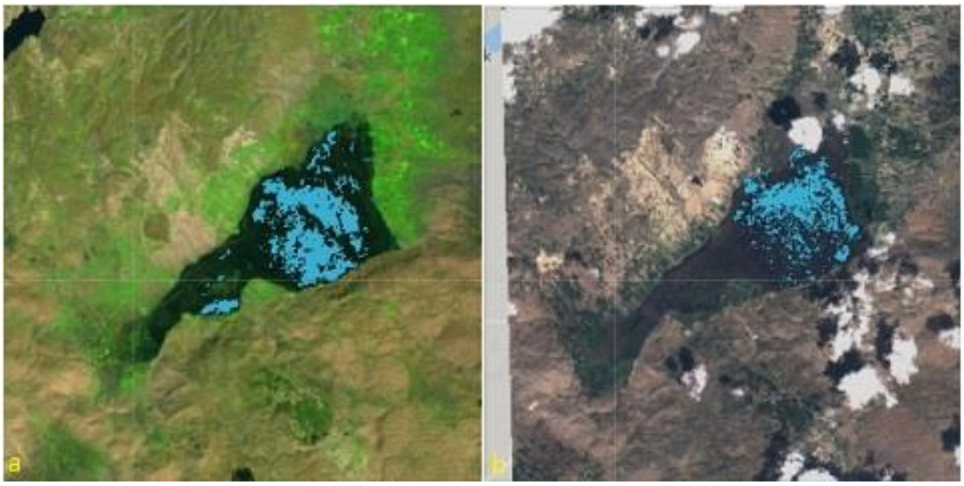

Figure 4.28. *Water Extent of Lake Karamik; (a) 01.5.2000 Area: 12 km² (Landsat 7), (b) 10.5.2017 Area: 9 km² (Sentinel 2)*

4.1.8. Lake Kovada

As seen in Figure 4.29 in the spring and summer of 1984, the lake area was 8.1 km^2 and it was 8.3 km^2 in the autumn. The only value for 1986 was 7.1 km^2 in autumn. In 1987 the lake area which was determined 7.4 km^2 in the spring decreased to 6.9 km^2 in the summer and the area value increased again to 8.2 km^2 in the autumn. In the lake which has no area value for 1987 to 1998, the area was determined 7.5 km^2 in summer of 1998. The lake area, which was 8.2 km^2 in the spring of 1999, fell to 7.5 km^2 in summer and increased to 7.8 km^2 at the end of the year. In 2000, the seasonally changing area value was determined as 8 km^2 in spring and decreased to 7.4 km^2 in the summer and increased to 7.7 km^2 in autumn. In 2001 the changing area values for the spring, summer and year-end were 7.8 km^2, 7.5 km^2 and 7.7 km^2. The area value which was 8.3 km^2 at the beginning of 2002, decreased to 7.7 km^2 in spring. It was 7.5 km^2 in summer and 7.8 km^2 at the end of the year. At the beginning of 2003, the area value which was 8.1 km^2 decreased until summer and determined 7.6 km^2. In the autumn, the area value increased to 7.8 km^2. Area values calculated with downloaded Landsat 7 images between 2004 and 2009 have been around 7.5 km^2. The area value which was determined 7.6 km^2 in spring of 2009 has fallen to 7.3 km^2 in summer then it increased until the end of the year and reached to 7.8 km^2. The area value which was 8.1 km^2 in the spring of 2010 has fallen to 6.5 km^2 in the summer and has reached to 8 km^2 at the end of the year. The area values reached the highest values at the beginning of the year and decreased in summer then it increased at the end of the year again. These cycles for area values continued also for 2011 and get values as 7.9 km^2, 6.2 km^2, 7.7 km^2 respectively. In the lake which has no area value in 2012, the area was determined 7.8 km^2 in spring of 2013. The area value which decreased to 7 km^2 in summer increased to 7.7 km^2 till the end of the year. The changes in the area between the beginning of the year, summer and the end of the year were 8 km^2, 7.2 km^2 and 7.7 km^2 respectively for 2014. In the spring of 2015, the area value, which was 7.9 km^2, fell to 7.3 km^2 in the summer and increased again to 7.8 km^2 at the end of the year. In the spring of 2016, the area value, which was 7.9 km^2, fell to 6.5 km^2

in summer, but increased to 7.9 km^2 at the end of the year. The area value, which was 7.9 km^2 at the beginning of 2017, fell to 6.5 km^2 in the summer, but at the end of the year it increased again to 7.9 km^2. The highest values in the lake area were seen in the December-January period. These values were decreased in summer and increased till the end of the year again. These periodic values are indicative of a seasonal variation in the area.

As seen in Figure 4.30 if the precipitation values are evaluated in the long term, it is seen that precipitation values decreased from 1984 to 2002 and then increased until 2017 except for the decrease in 2005-2009 period. Since there was no significant change in the area values in the long term, there was no relationship between the area change and precipitation. At the seasonal scale, although the precipitation values got the highest values in spring, lake area did not present this behavior.

As seen in Figure 4.31 if the evaporation values are evaluated in the long term, it is seen that evaporation values decreased from 1984 to 1992 and then increased until 2011 then decreased again until 2017. Since there was no significant change in the area values in the long term, there was no relationship between the area change and evaporation. No relationship between lake area and evaporation were found at the seasonal scale as well.

Figure 4.32 shows the areal changes of the lake with images of 3 different years.

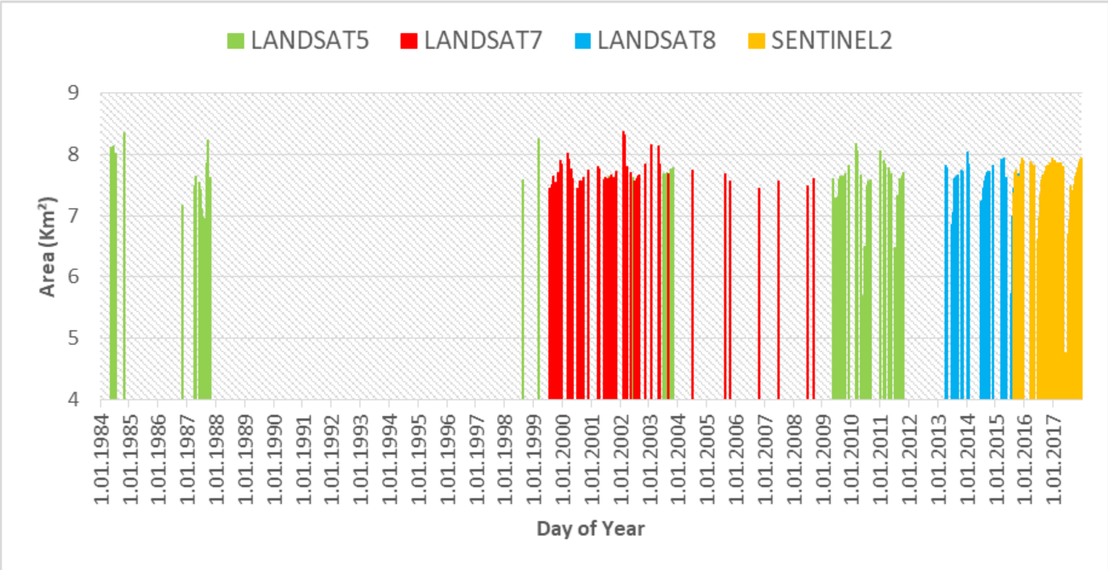

Figure 4.29. *Water Extent Change of Lake Kovada*

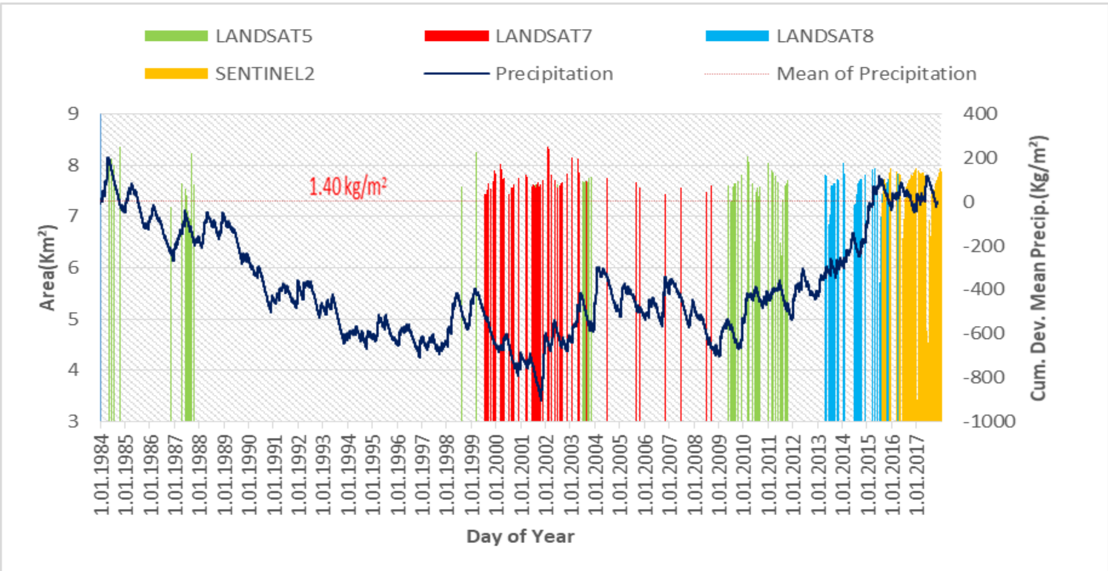

Figure 4.30. *Water Extent Change of Lake Kovada and Cumulative Deviation from Mean Daily Precipitation*

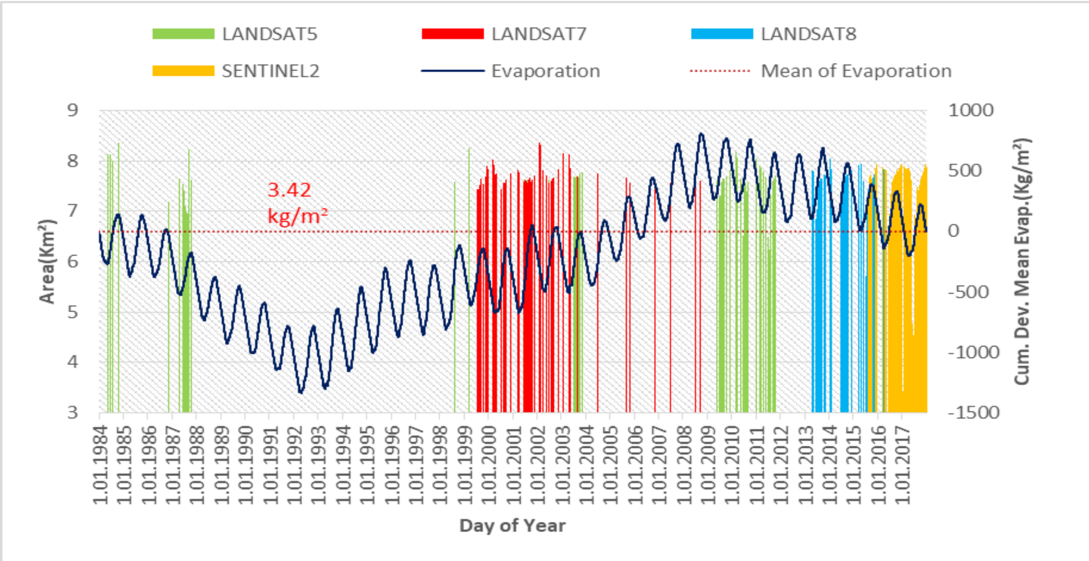

Figure 4.31. *Water Extent Change of Lake Kovada and Cumulative Deviation from Mean Daily Evaporation*

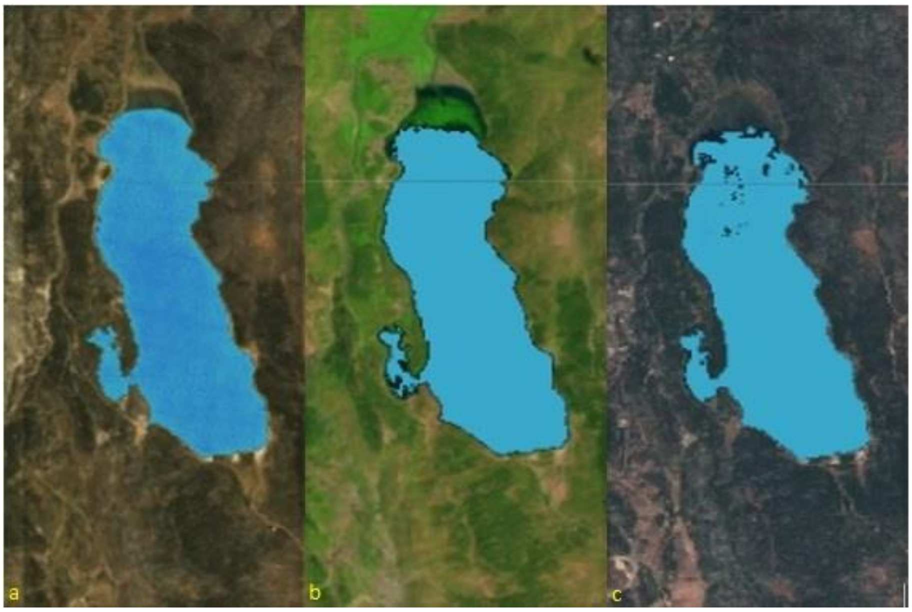

Figure 4.32. *Water Extent of Lake Kovada; (a) 14.6.1984 Area: 8 km² (Landsat 5) , (b) 03.08.1999 Area: 7,4 km² (Landsat 7), (c) 31.7.2017 Area: 7,5 km² (Sentinel 2)*

4.1.9. Lake Gavur

Note that Lake Gavur is the smallest lake included in this study with maximum area value around 3 km^2. As seen in Figure 4.33 the area of the lake was found to be greater than 1 km^2 between 1984 and 2018 only 12 times. There are 189 area values belonging to the lake in this date range. 164 of them are smaller than 0.1 km^2. The lake area which was 0.7 km^2 in the spring of 1985 was 2.3 km^2 in the spring of 1987 and it was 1.4 km^2 in the spring of 1990. The lake area which was 2.3 km^2 in the spring of 1999, determined 2 km^2 in the spring of 2000. The values of the area greater than 0.5 km^2 were found only in spring and these values were 2 km^2 in 2002, 2.3 km^2 in 2003, 2.1 km^2 in 2010, 0.8 km^2 in 2013, 1.6 km^2 in 2014 and 2 km^2 in 2017 respectively. The only exception to this situation is the value of 3 km^2 which was determined in December 2017. This is the highest calculated value of the lake.

As seen in the Figure 4.34 In the spring periods where the precipitation values were high, the lake area also reached the high values. These periods are periods in which evaporation also got low values (Figure 4.35).

Figure 4.36 shows the areal changes of the lake with images of 2 different years.

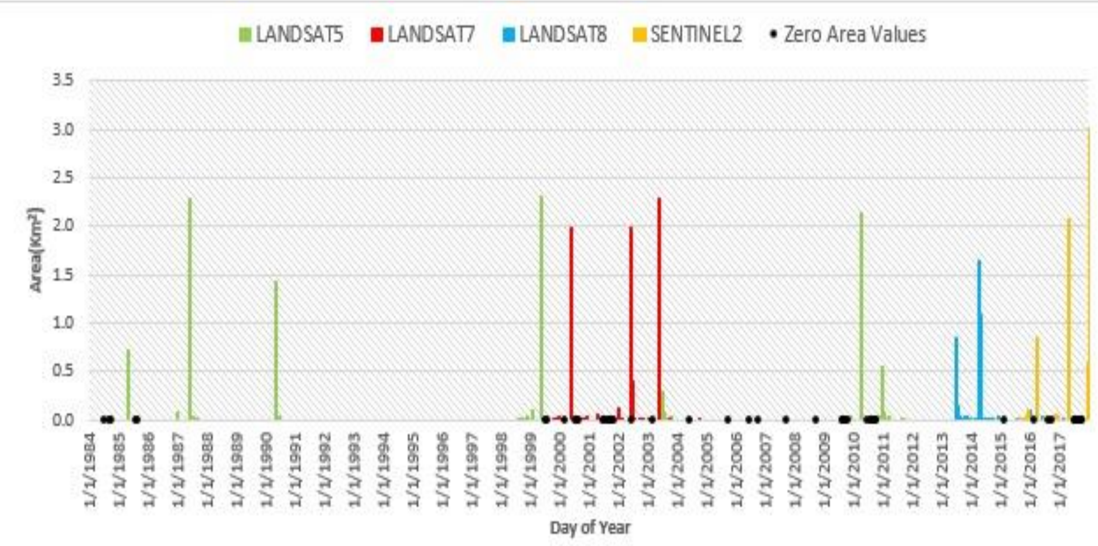

Figure 4.33. *Water Extent Change of Lake Gavur*

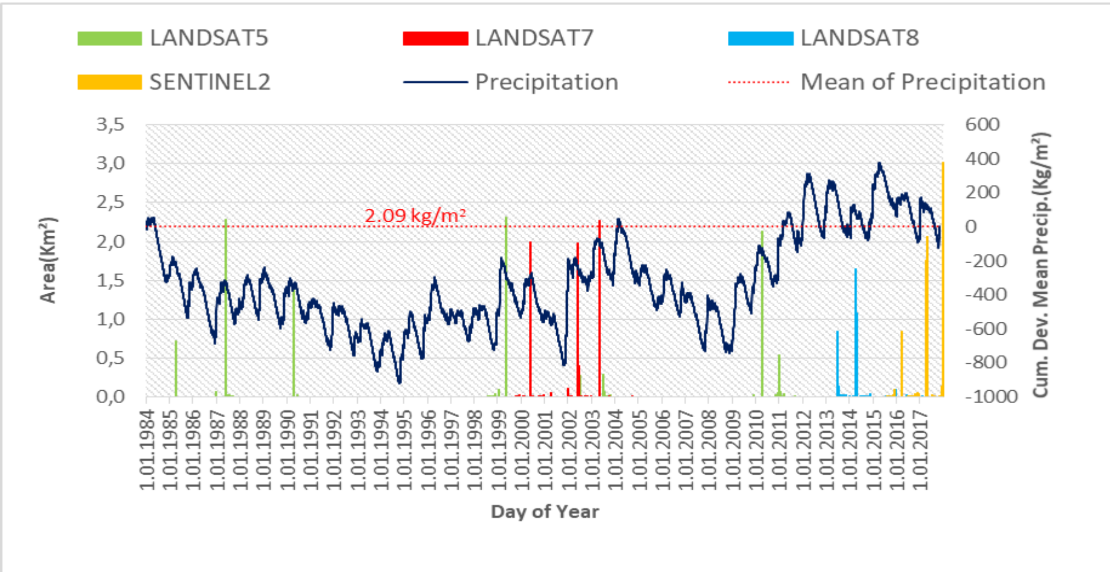

Figure 4.34. *Water Extent Change of Lake Gavur and Cumulative Deviation from Mean Daily Precipitation*

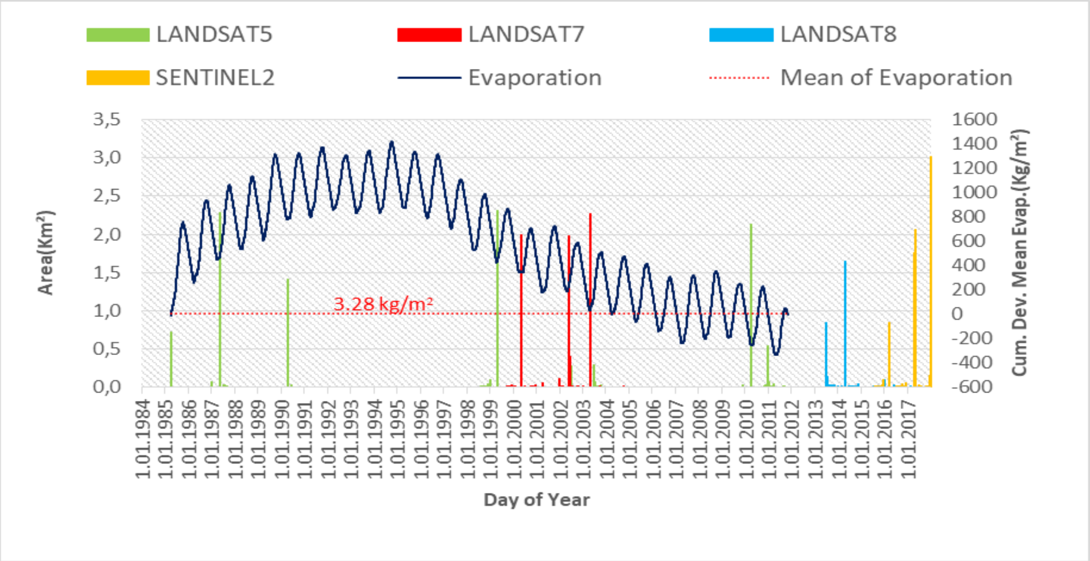

Figure 4.35. *Water Extent Change of Lake Gavur and Cumulative Deviation from Mean Daily Evaporation*

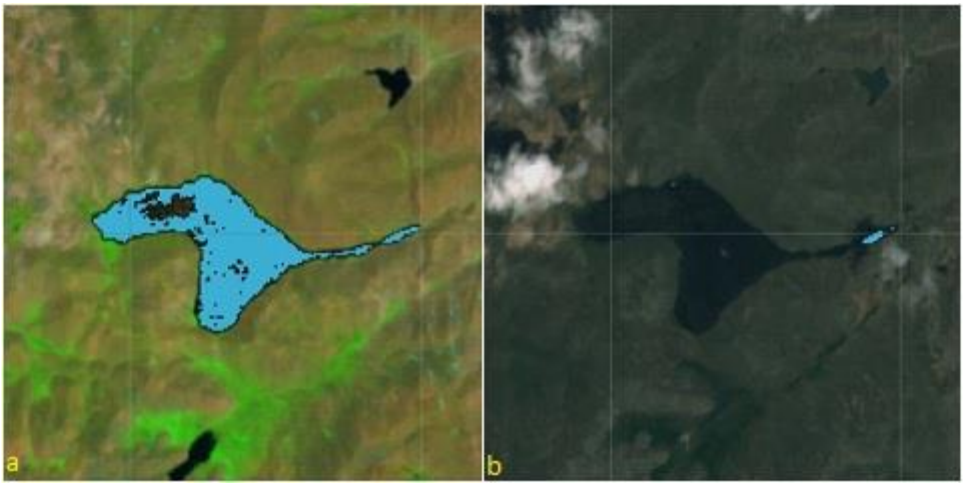

Figure 4.36. *Water Extent of Lake Gavur; (a) 10.05.2000 Area: 2 km² (Landsat 7), (b) 30.05.2016 Area: 0.02 km² (Landsat 8)*

4.1.10. Lake Burdur

The lake area, which was 235 km² in 1970 (General Directorate of Water Management, 2015), was determined 205 km² in the spring of 1984 as seen in Figure 4.37. The area of the lake, which was 204 km² in autumn 1984, fell to 201 km² in the autumn of 1986. At the beginning of 1987, the area value which was 201 km² decreased to 195 km² in summer and 199 km² in the autumn. From 1987 to 1998, there is only one area value, which is 170 km², which belongs to the summer of 1995. The lake area, which was 161 km² in the summer of 1998, determined 159 km² in the spring of 1999. The area value which was 157 km² at the beginning of 2000 decreased to 149 km² in summer and increased to 152 km² at the end of the year. Although the area value which was 152 km² at the beginning of 2001 increased to 160 km² in summer and 154 km² was determined at the end of the year. The area value of 154 km² at the beginning of 2002 showed small fluctuations and determined 151 km² at the end of the year. Although the area value which was 151 km² at the beginning of 2003 increased to 155 km² in summer and it was determined 151 km² in the autumn. According to the area values calculated between 2004-2009 by downloaded Landsat 7 images; 159 km² in the summer of 2004 and 156 km² in the autumn, 155 km² in the summer of 2005 and 151 km² in the autumn, 153 km² in the summer of 2006 and 150 km² in the autumn, 150 km² in the summer of 2007 and 147 km² in the autumn, 146 km² in the summer of 2008 and 144 km² in the autumn were identified. The area value, which was 142 km² in the spring of 2009, decreased by the end of the year and became 140 km². The area value of 143 km² in the spring of 2010 decreased by the end of the year and became 140 km². The lake area, which was 140 km² at the beginning of 2011, decreased by the end of the year and became 138 km². The lake area, which was 138 km² at the beginning of 2013, fell to 131 km² in the summer and increased to 136 km² at the end of the year. The lake area, which was 136 km² at the beginning of 2014, decreased by the end of the year and became 132 km². In the spring of 2015, the area of the lake, which was 132 km², increased to 136 km² in the summer and then fell again and became 133 km² at the end of the year. Although the area value of 136 km² at the beginning of 2016 showed small fluctuations throughout the year, it decreased regularly and became 130 km² at the end of the year. The area value, which was 131 km² at the beginning of 2017, showed fluctuations similar to 2016 and decreased to 127 km² by the end of the year.

In the lake which reached the highest area values in January-December period, the area value decreased by 35 % between 1984 and 2017.

Although the area of the lake shows some fluctuations during the year, it has decreased steadily from 1984 to the end of 2017. In the last 35 years, the surface area of Lake Burdur has lost one third (Sargin, 2012). The most important water loss from the Lake Burdur is due to evaporation (General Directorate of Water Management, 2015).

If the precipitation values are evaluated in the long term it is seen in Figure 4.38 that precipitation values decreased from 1984 to 1994 and then increased till 2004 except for the decrease in 2002. Then values decreased until 2009. After that, precipitation increased until 2011 and then it decreased until the end of 2017. Note that minor response of the lake to precipitation is observed for 1999-2017 period, however continuous decreasing trend in lake are dominates the behavior of the lake.

As seen in Figure 4.39 the evaporation values tended to decrease from 1984 to 2003, after which the trend tended to increase until 2017. Therefore, the DSİ report (General Directorate of Water Management, 2015) that relates the water loss of the lake to the evaporation is valid for the period after 2003. However, other possible factors, such as anthropogenic effect were not evaluated in this thesis.

Figure 4.40 shows the areal changes of the lake with images of 4 different years. It can be seen from these figures that the northeast part of the lake where most drying occurs.

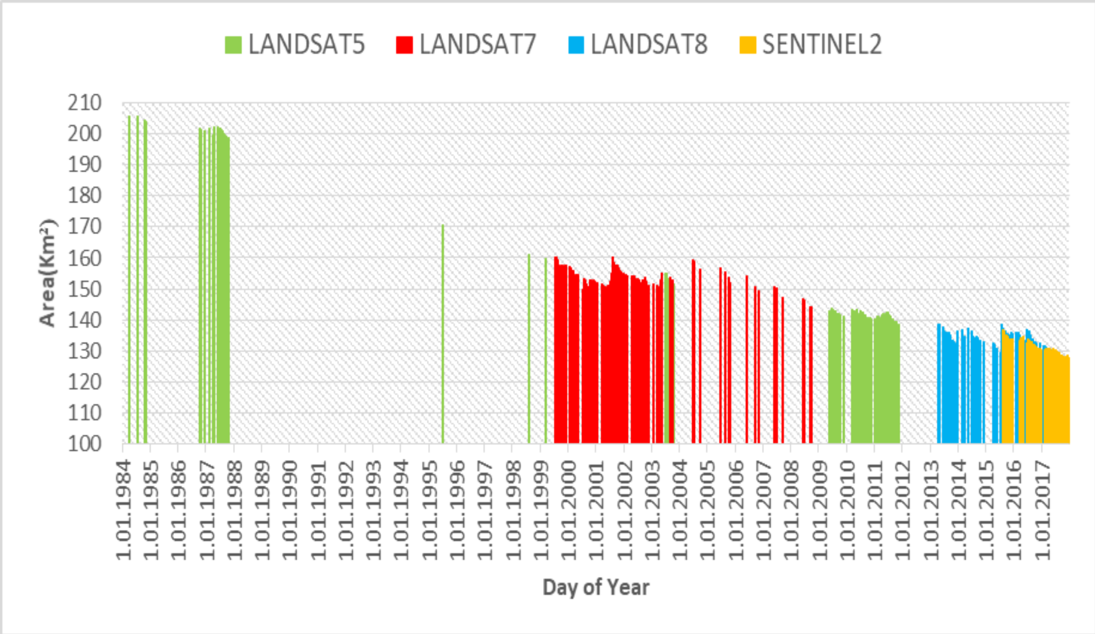

Figure 4.37. *Water Extent Change of Lake Burdur*

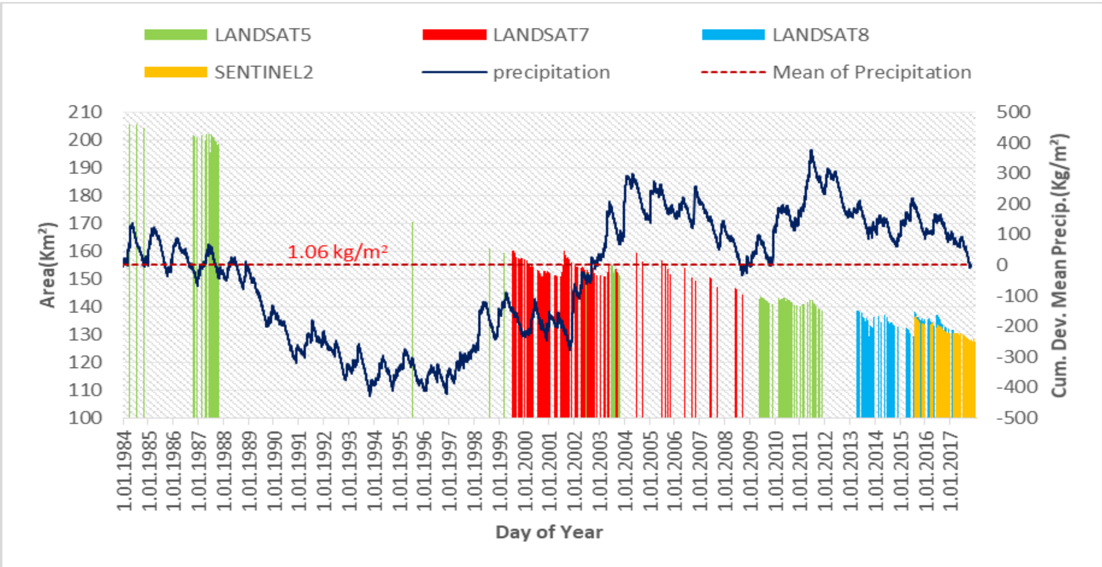

Figure 4.38. *Water Extent Change of Lake Burdur and Cumulative Deviation from Mean Daily Precipitation*

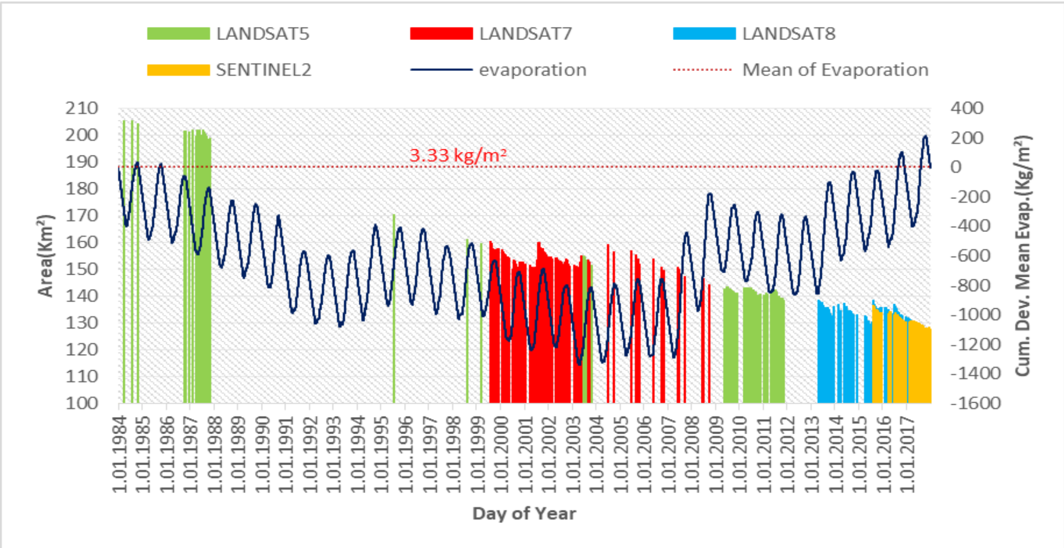

Figure 4.39. *Water Extent Change of Lake Burdur and Cumulative Deviation from Mean Daily Evaporation*

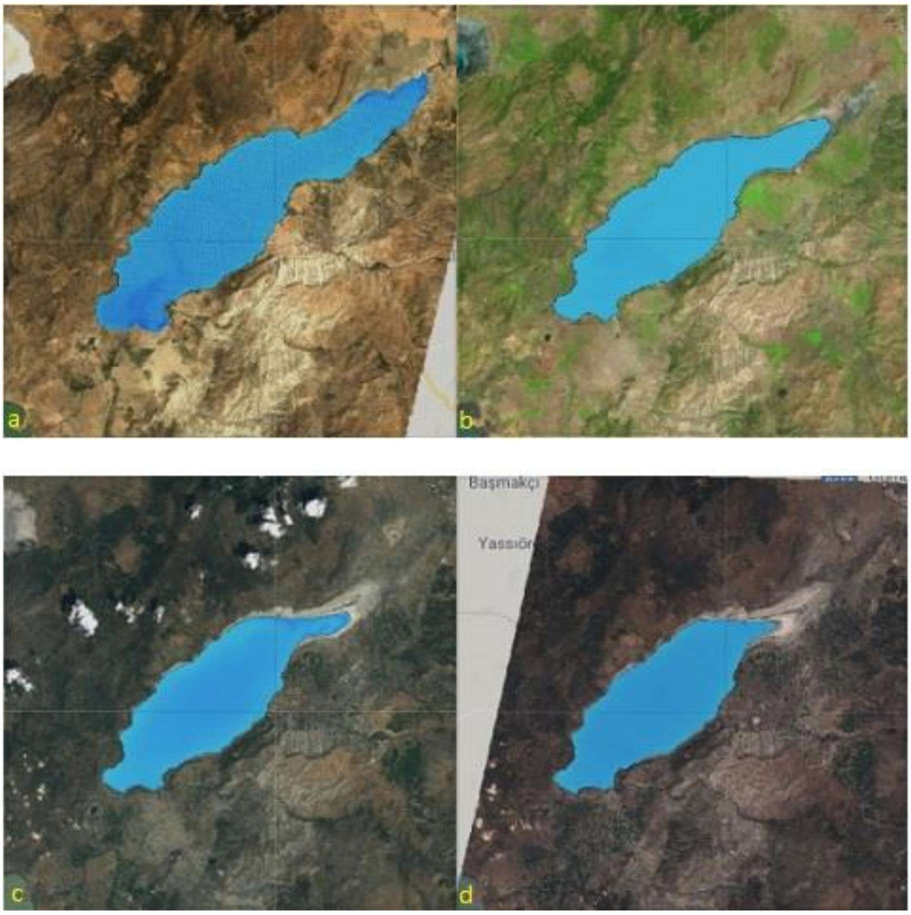

Figure 4.40. *Water Extent of Lake Burdur; (a) 27.8.1985 Area: 204 km² (Landsat 5), (b) 19.8.1999 Area: 157 km² (Landsat 7), (c) 17.8.2013 Area: 136 km² (Landsat 8), (d) 15.8.2017 Area: 129 km² (Sentinel 2)*

4.1.11. Lake Acigol

As seen in the Figure 4.41 in the spring of 1984, the area value of 143 km² was determined as 45 km² in the autumn of 1986. At the beginning of 1987, the area value of 78 km² decreased until the autumn and determined as 33 km². The most significant decrease in the Lake Acigol surface area was between 1984 and 1987 (Lake Acigol Wetland Management Plan, 2016). At the end of 1990, the area value of 32 km² was 46 km² in the summer of 1995. The area value, which was 52 km² in the summer of 1999, was 51 km² at the end of the year. The area value which was 68 km² at the beginning of 2000, increased to 119 km^2 in the spring but decreased to 42 km^2 at the end of the year. At the beginning of 2001, the area value which was 45 km^2 was reduced to 27 km^2 until autumn, but it increased again to 32 km^2 at the end of the year. The area value which was 114 km^2 in the spring of 2002 was reduced until the autumn and determined as 42 km^2. In the spring of 2003, the area value, which increased to 130 km^2, decreased towards the autumn and was determined to be 49 km^2.

Between 2004 and 2009, 2 Landsat 7 images per year were downloaded and the following values were calculated according to that images; in summer 78 km^2 and in autumn 44 km^2 for 2004, in summer 45 km^2 and in autumn 43 km^2 for 2005, in spring 58 km^2 and in autumn 45 km^2 for 2006, in spring 52 km^2 and in autumn 34 km^2 for 2007, in spring 52 km^2 and in autumn 33 km^2 for 2008. The area value, which was 73 km^2 in the summer of 2009, decreased to 46 km^2 by the end of the year. The area value, which was 84 km^2 in the spring of 2010, decreased to 47 km^2 in autumn, however it increased by the end of the year to a value of 58 km^2. The area value, which was 77 km^2 at the beginning of 2011, increased to 80 km^2 in spring then it decreased again in autumn and determined as 46 km^2. The area value of 79 km^2 in the spring of 2013 decreased to 46 km^2 in autumn. The area value, which was 61 km^2 at the beginning of 2014, increased to 66 km^2 in the spring and after that, it went down until the autumn and was determined to be 46 km^2. The area value, which was 84 km^2 at the beginning of 2015, increased to 130 km^2 in spring then it decreased again in autumn and determined 72 km^2. The area value, which was 73 km^2 at the beginning of 2016, decreased to 35 km^2 in the autumn, but it increased by the end of the year and determined 42 km^2. The area value, which was 52 km^2 at the beginning of 2017, was determined as 35 km^2 in summer.

In the lake which reached the highest area values in spring, there were no available images in spring for 2016 and 2017. Area values which increase in spring and fall in summer and autumn rose again at the end of the year. It is observed that the lake area shows a seasonal change. It can be seen from these figures that Lake Acigol is highly managed and mineral production ponds control significant portion of the water in the lake.

Figure 4.42 shows that the lake extent is highly responsive to precipitation pattern; spring season with high precipitation is the period with highest area values in the lake. The decrease in precipitation values in autumn periods is followed by the decrease in lake area. The seasonal character of the lake area is also depicted with the evaporation values given in Figure 4.43; the periods in which the area values are high, are the periods that evaporation values are the lowest and vice versa. The drying of lake in high evaporation summer season enables mineral production.

The most serious threat on the area is the interventions in the water regime of the area (Eken, Bozdogan, İsfendiyaroglu, Kilic, & Lise, 2006). It is aimed that the new dam and pond will not be allowed on the water resources feeding the lake (Lake Acigol Wetland Management Plan, 2016).

Figure 4.44 shows the areal changes of the lake with images of 2 different years.

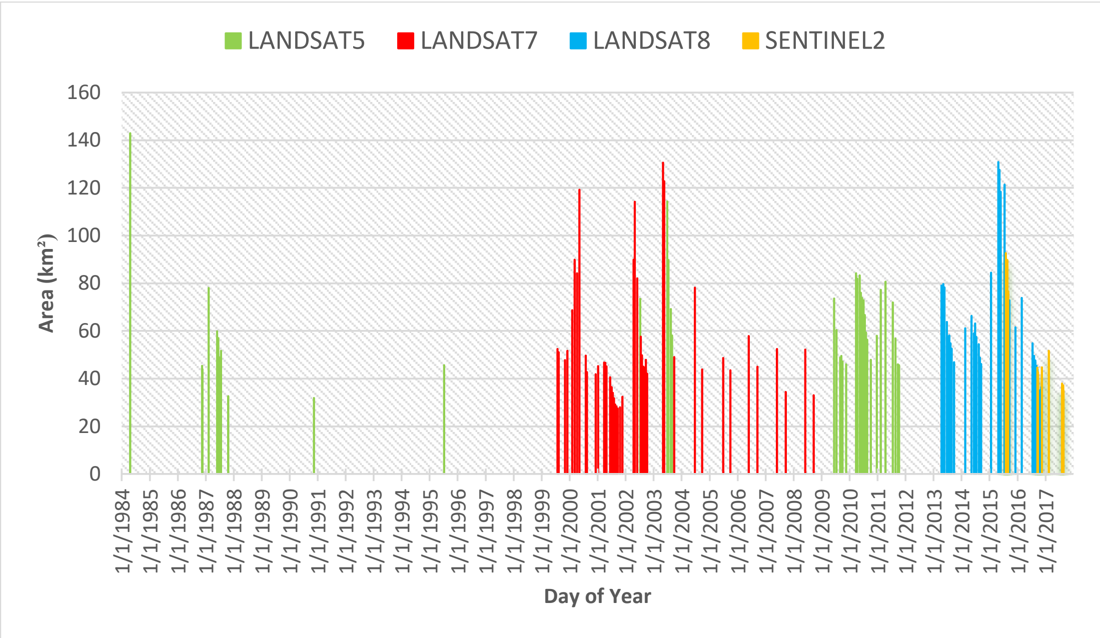

Figure 4.41. *Water Extent Change of Lake Acigol*

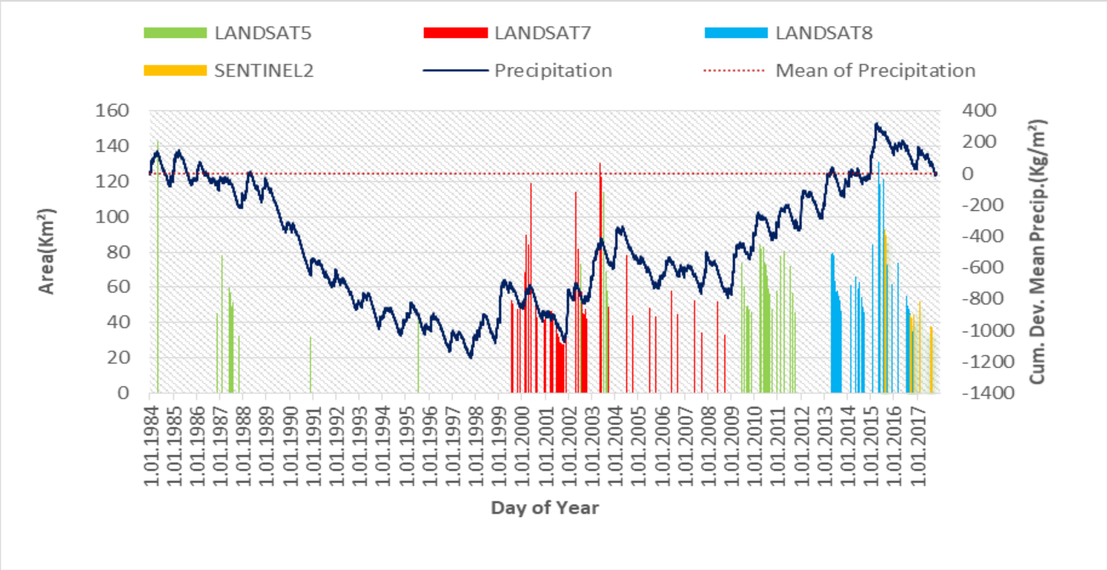

Figure 4.42. *Water Extent Change of Lake Acigol and Cumulative Deviation from Mean Daily Precipitation*

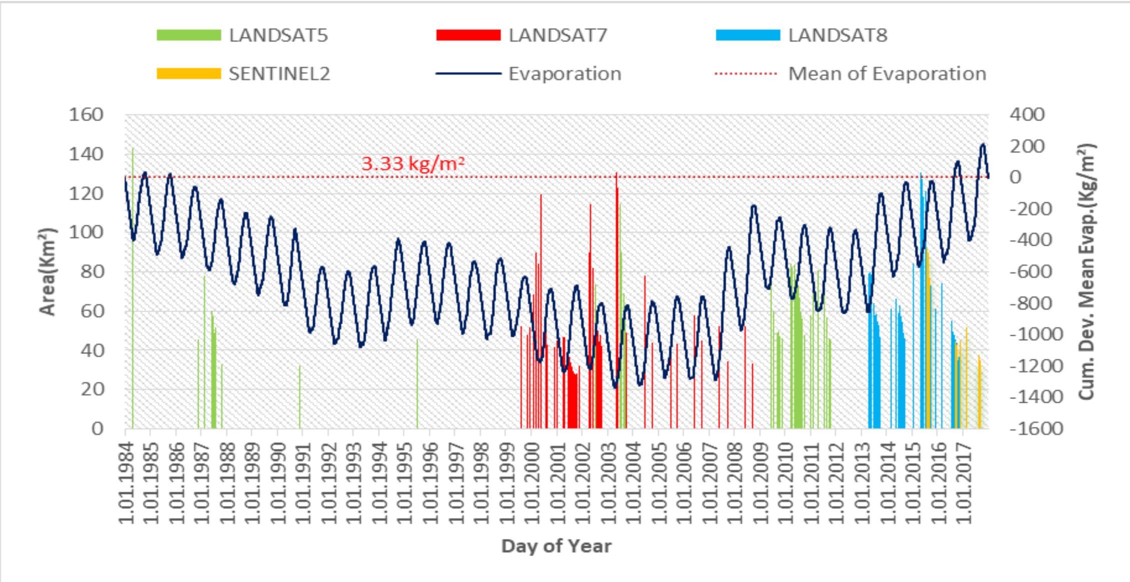

Figure 4.43. *Water Extent Change of Lake Acigol and Cumulative Deviation from Mean Daily Evaporation*

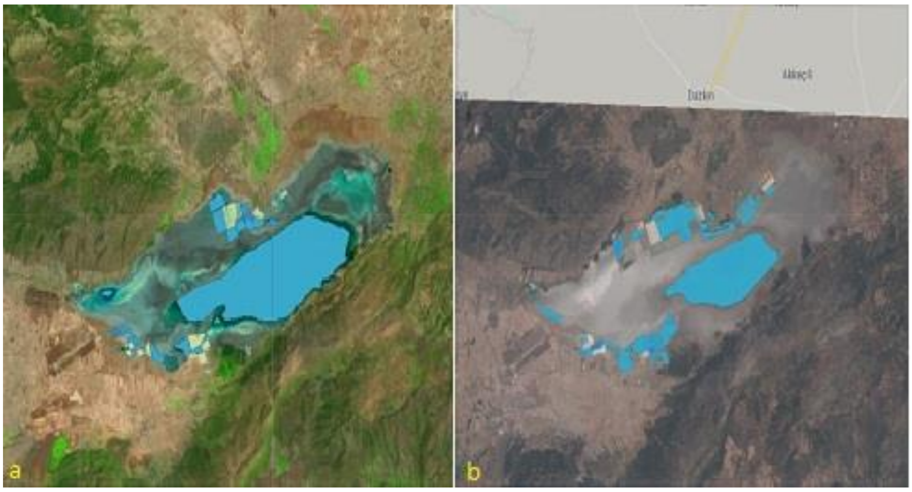

Figure 4.44. *Water Extent of Lake Acigol; (a) 25.07.1999 Area: 52 km² (Landsat7), (b) 03.08.2017 Area: 38 km² (Sentinel 2)*

4.1.12. Lake Isikli

As seen in the Figure 4.46 the area of the lake was determined 40 km² and 30 km² respectively in the autumn of 1984. The area value, which was 46 km² in the summer of 1986, decreased to 40 km² at the end of the year. The area value, which was 55 km² at the beginning of 1987, decreased until the autumn and was determined as 24 km². The area value, which was 27 km² at the end of 1990, was determined 31 km² in the summer of 1995. The area value, which was 37 km² in the summer of 1999, was determined 42 km² at the end of the year. The area value, which was 53 km² at the beginning of 2000, has fallen to 24 km² in the summer and then it increased to 45 km² at the end of the year. The area value which was 50 km² at the beginning of 2001 decreased to 10 km² in the summer, but reached to 42 km² at the end of the year. The area value, which was 58 km² at the beginning of 2002, decreased to 32 km² in summer and was 35 km² at the end of the year. The area value, which was 58 km² at the beginning of 2003, fell until the autumn and was determined 30 km². Area values calculated with downloaded Landsat 7 images between 2004 and 2009 were as follows; 35 km² in summer and 32 km² in autumn for 2004; 34 km² in summer and

23 km² in autumn for 2005; 35 km² in summer for 2006; 34 km² in summer and 13 km² in autumn for 2007; 33 km² in summer for 2008. The area value which was 55 km² in the spring of 2009 decreased to 34 km² in summer, but increased to 38 km² at the end of the year. The area value, which was 49 km² at the beginning of 2010, was 55 km² in spring, and the area value which was 35 km² in summer has increased to 48 km² at the end of the year. The area value, which was 48 km² at the beginning of 2011, increased to 54 km² in the spring and the area value which fell to 31 km² in the summer increased to 43 km² at the end of the year. The area value of 59 km² in the spring of 2013 decreased to 31 km² in summer and increased to 50 km² at the end of the year. The area value, which was 52 km² at the beginning of 2014, increased to 57 km² in the spring and then it was determined 25 km² in the autumn. The area value, which was 54 km² at the beginning of 2015, increased to 60 km² in spring, and the area value of 35 km² in the summer increased to 46 km² at the end of the year. The area value which was 54 km² at the beginning of 2016 decreased to 10 km² in summer and increased to 43 km² at the end of the year. The area value which was 48 km² at the beginning of 2017 decreased to 10 km² in summer and increased to 42 km² at the end of the year.

In the lake which mostly reached the highest values in spring, area values decreased to 10 km² in summer for last 2 years, however spring values were determined above 50 km². Seasonal variation in precipitation seems to be the main control on lake extent.

As seen in Figure 4.47 no relationship between precipitation values and area values in both long term and yearly values were determined. As seen in Figure 4.48 the periods in which the area values are high are the spring periods where the evaporation values are low.

Figure 4.49 shows the areal changes of the lake with images of 3 different years.

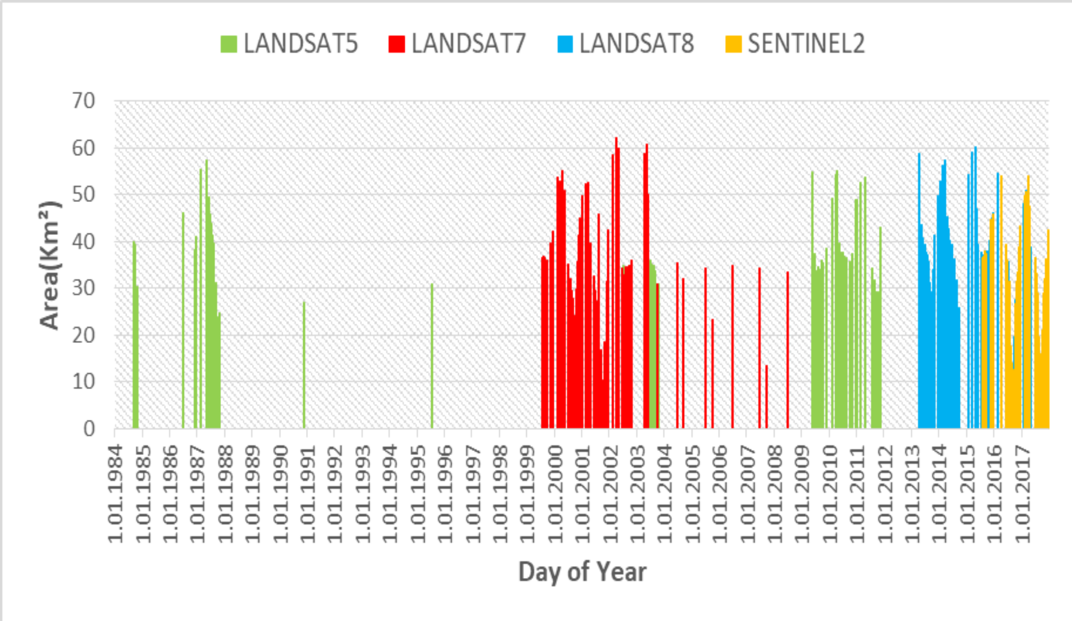

Figure 4.45. Water Extent Change of Lake Isikli

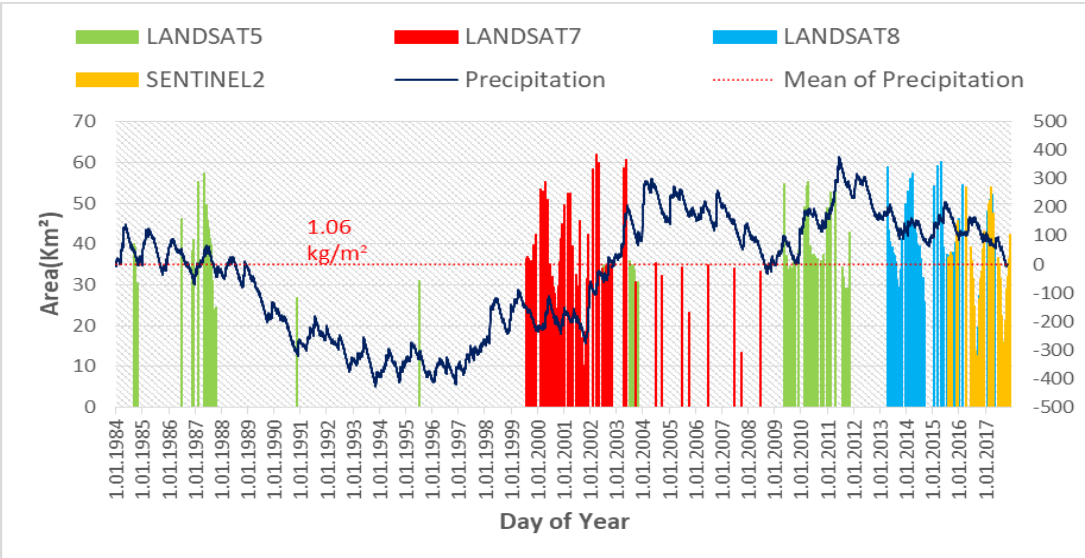

Figure 4.46. Water Extent Change of Lake Isikli and Cumulative Deviation from Mean Daily Precipitation

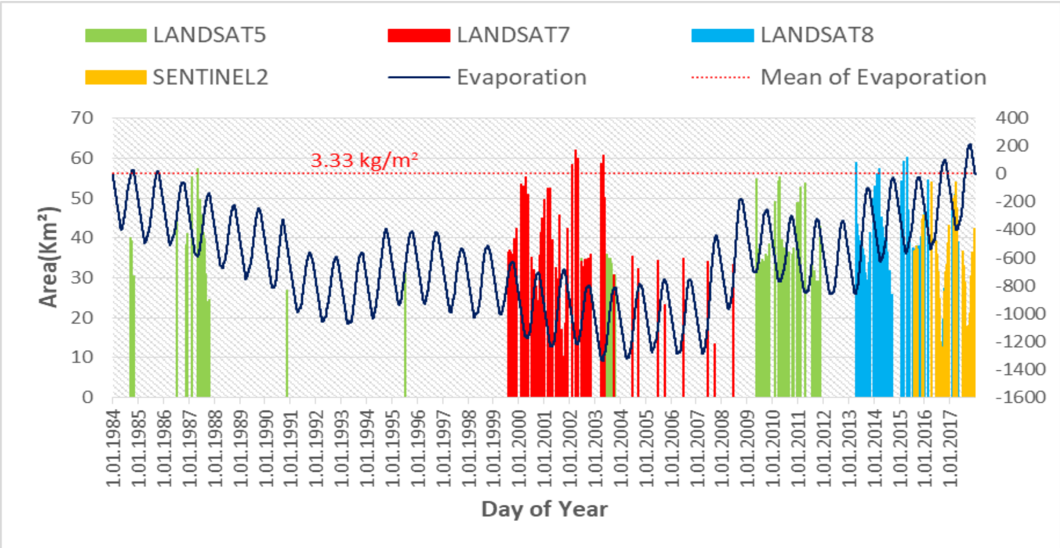

Figure 4.47. *Water Extent Change of Lake Isikli and Cumulative Deviation from Mean Daily Evaporation*

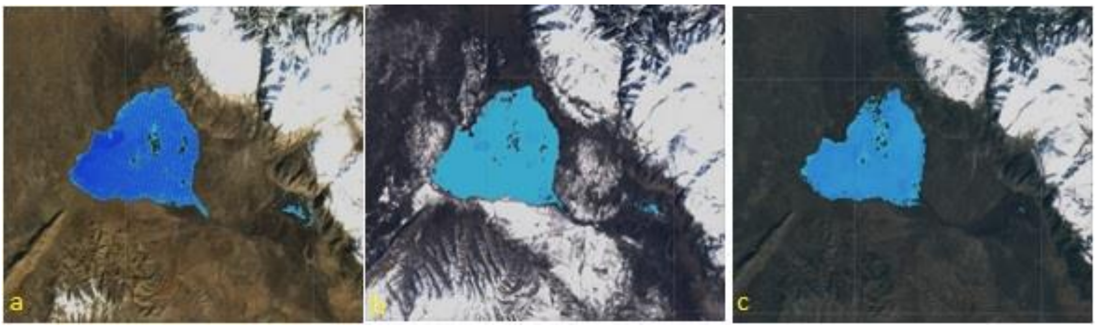

Figure 4.48. *Water Extent of Lake Isikli; (a) 06.02.1987, Area: 54 km² (Landsat 5), (b) 02.02.2000, Area: 54 km² (Landsat 7), (c) 23.1.2017 Area: 48 km² (Landsat 8)*

4.1.13. Lake Salda

As seen in Figure 4.50 the area value, which was 46 km² in the autumn of 1984, was also around this value at the end of 1986. The area value, which was 46.2 km² at the beginning of 1987, decreased to 45.8 km² in the summer and increased to 46.2 km² at the end of the year. The area value which was 45.3 km^2 in summer of 1990 was determined 44.2 km^2 in summer of 1995.

The area value, which was 44 km^2 in the summer of 1999, maintained its value until the end of the year. The area value which was 44 km^2 at the beginning of 2000 was determined 43.8 km^2 at the end of the year. At the beginning of 2001, the value of the area which was 43.7 km^2, decreased by the end of the year and determined 43.2 km^2. The area value, which was 43.7 km^2 in the spring of 2002, maintained this value until the autumn. The area value, which was 43.6 km^2 at the beginning of 2003, increased to 44 km^2 in spring and maintained this value until the autumn. Area values calculated with downloaded Landsat 7 images between 2004 and 2009 were as follows; 44.2 km^2 in summer of 2004; 44 km^2 in summer and 43.8 km^2 in autumn for 2005; 43.6 km^2 in spring and 43.8 km^2 in autumn for 2006; 43.6 km^2 in spring and 43.3 km^2 in autumn for 2007; 43.2 km^2 in spring and autumn for 2008. In the spring of 2009, the area value of 43.4 km^2 was 43.5 km^2 at the end of the year. The value of the area which was 43.7 km^2 in the spring of 2010 kept this value until the end of the year. The value of the area which was 43.8 km^2 in the spring of 2011 kept this value until the end of the year. The area value, which was 44 km^2 in the summer of 2013, maintained its value until the end of the year. The same area value remained at this level in 2014 as well. At the beginning of 2015, the area value which was 44.2 km^2 was reduced to 42 km^2 in summer, but it was determined 44.2 km^2 at the end of the year. In 2016, just like in 2015 the area value which was 44.2 km^2 was reduced to 42 km^2 in summer, but it was determined 44.7 km^2 at the end of the year. The area value, which was 44.1 km^2 at the beginning of 2017, was reduced to 35 km^2 in the summer and was 44 km^2 at the end of the year. Nowadays, area of Lake Salda is 44.7 km^2 and recharge from precipitation rather than evaporation has great influence on the changes of the lake water levels (Varol, et al., 2018).

The area value which was around 46 km^2 in 1984 and 1987 in the lake, decreased to 44 km^2 around from 2000s. Although there are small fluctuations, the lake has maintained this area value until the end of 2017.

As seen in the Figure 4.51 the precipitation values which decreased from 1984 to 1998 increased until 2005 except decreasing in 2002. After that these values increased until 2015 except for the decrease in 2009. Precipitation values decreased from 2015 to end of the 2017. It can be seen from this figure that the lake extent is responsive to precipitation more significantly at the long timescales.

As seen in Figure 4.52 evaporation values increased from 1984 to 2002 except in 1993 and 1999. Then values decreased from 2002 to 2012. There was no relationship between evaporation values and area values for both seasonal and long term scales.

Figure 4.53 shows the areal changes of the lake with images of 2 different years.

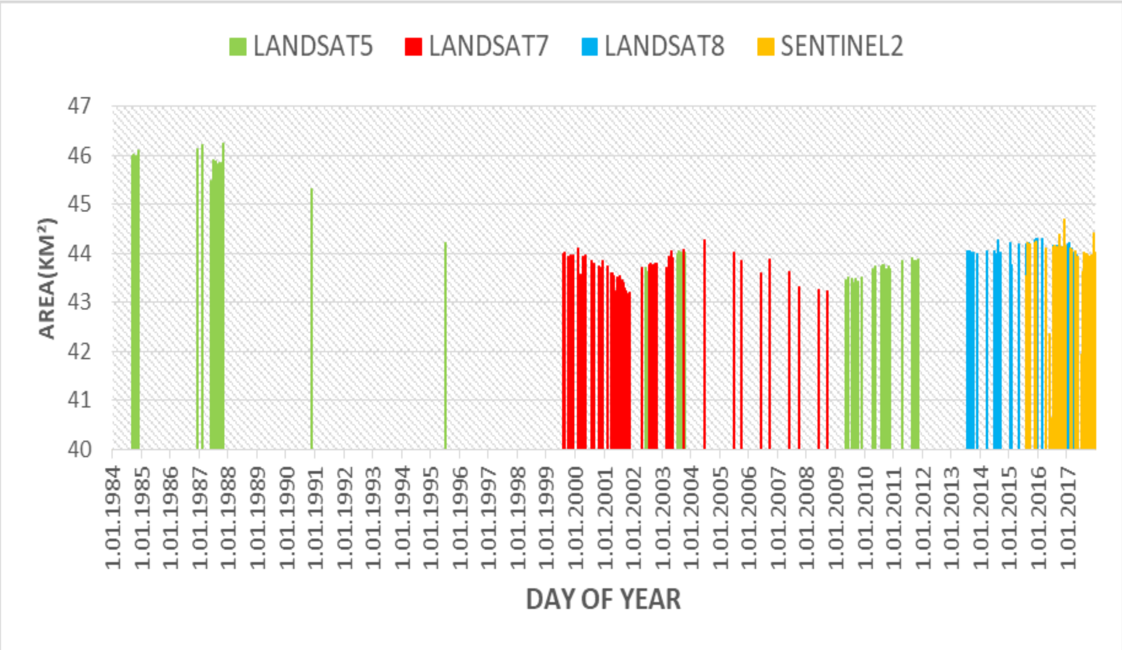

Figure 4.49. *Water Extent Change of Lake Salda*

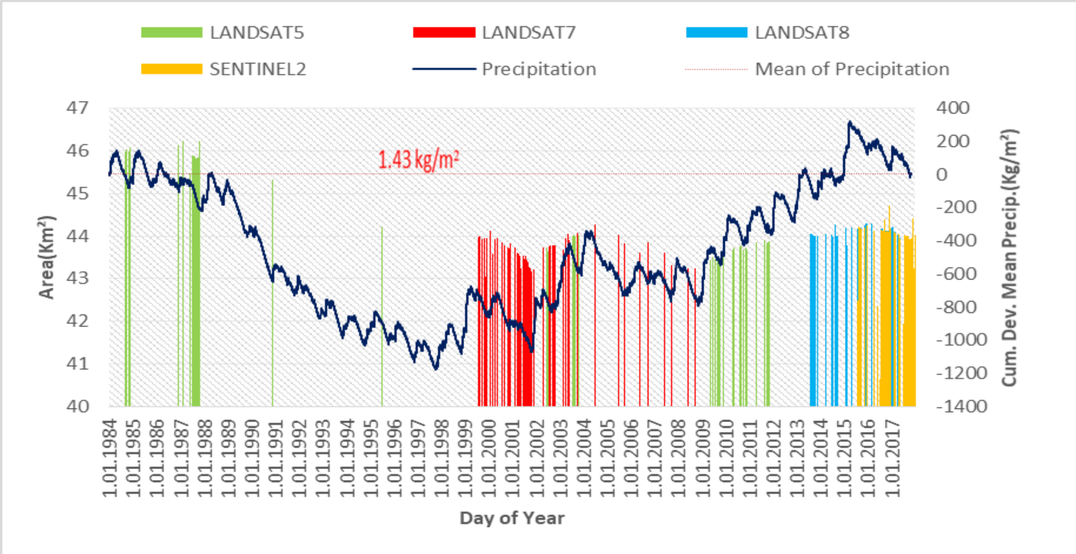

Figure 4.50. *Water Extent Change of Lake Salda and Cumulative Deviation from Mean Daily Precipitation*

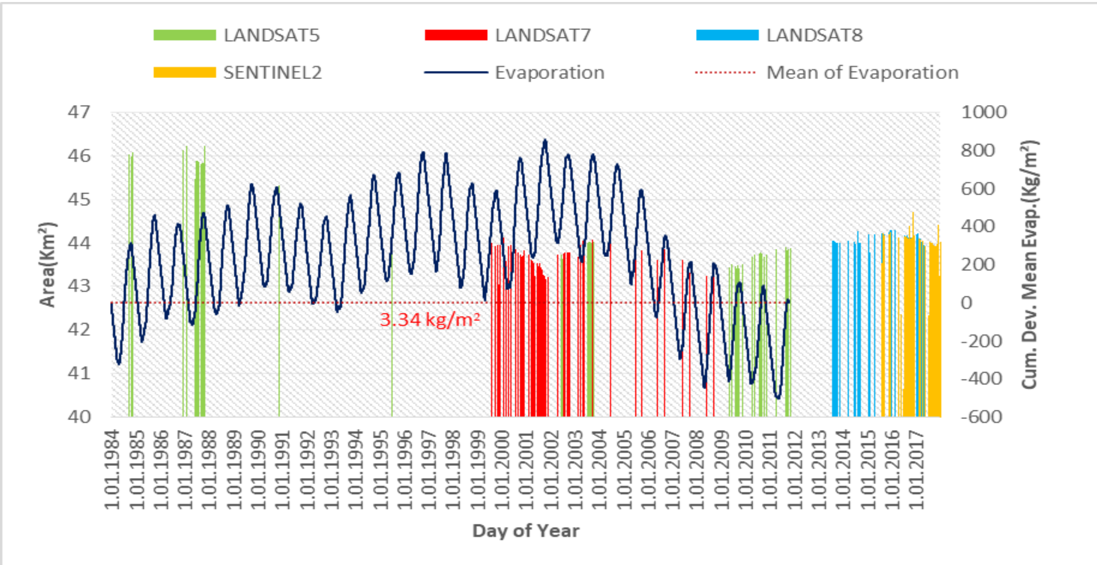

Figure 4.51. *Water Extent Change of Lake Salda and Cumulative Deviation from Mean Daily Evaporation*

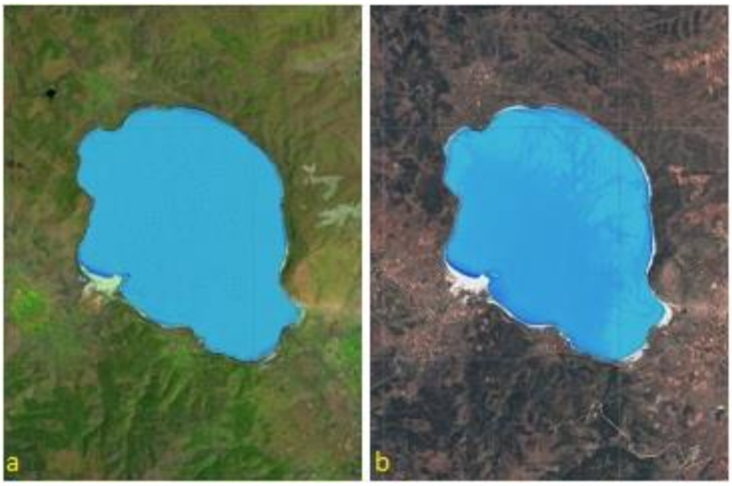

Figure 4.52. *Water Extent of Lake Salda; (a) 25.7.1999 Area: 44 km² (Landsat 7), (b) 24.7.2017 Area: 44 km² (Sentinel 2)*

4.1.14. Lake Yarisli

As seen in the Figure 4.54 during 1984, 1986 and 1987, the area value of the lake was around 16 km². The area value which was 6 km² in the autumn of 1990 was determined as 4 km² in the summer of 1998. The area value, which was 13 km² in the spring of 1999, decreased to 0 in summer and increased to 2.5 km² again at the end of the year. The area value which was 2.5 km² at the beginning of 2000 increased to 11 km² in the spring and the area value which decreased to 0 in summer increased to 1 km² at the end of the year. The area value, which was 5.2 km² at the beginning of 2001, increased to 6 km² in spring and the value which decreased to 0 in the summer, increased to 12 km² at the end of the year. The area value, which was 13 km² at the beginning of 2002, increased to 14 km² in spring and decreased to 0 in the autumn. In the summer of 2004, the area value was 14.8 km² and 14.3 km² in autumn. The area value that below 1 km² in the summer of 2005, was determined 12 km², 10 km² and 6 km² in the autumn of the same year. In the spring of 2006, the area value, which was 12 km², decreased to 9.3 km² in summer and to 2 km² in autumn. In the spring of 2007, the area value, which is 2.5 km², has fallen below 1 km² in summer and autumn. In the spring of 2008, the area value, which is below 1 km², decreased to 0 in autumn. The area value which was

12.6 km² in the spring of 2009, decreased to 0 in the summer and increased to 5 km² at the end of the year. At the beginning of 2010, the area value of 13.2 km² was increased to 13.8 km² in the spring and then decreased to 8 km² at the end of the year. The area value which was 13.7 km² at the beginning of 2011 increased to 14.1 km² in the spring and was around 13.6 km² until the end of the year.

The area value, which was 14.7 km² in the spring of 2013, showed a small decrease until the end of the year and was determined 13.5 km² at the end of the year. The area value which was 14.5 km² at the beginning of 2014 decreased to 11 km² in autumn and was determined 12.5 km² at the end of the year. In the spring of 2015, the area value, which was 14.6 km², decreased to 12.5 km² in summer and was determined as 14.5 km² at the end of the year. The area value, which was 14.7 km² at the beginning of 2016, remained at these levels until the end of the year and was determined 14.4 km² at the end of the year. The area value, which was 14 km² at the beginning of 2017, decreased to a value of less than 1 km² until the autumn and was determined 7.6 km² at the end of the year.

The lake area, which was around 16 km² in 1984, 1986 and 1987 years, showed fluctuations between 2000 and 2009. In this period, it was observed that the area decreased to 0 in the summer. After that, the lake area, which was around 14 km² until 2017, decreased again in 2017.

As seen in Figure 4.55 even if the relationship between area and precipitation was not observed in the long term, the decrease in the area values especially seen between 2013 and 2017 from spring to autumn is also valid for precipitation values.

As seen in Figure 4.56 although there is no long-term relationship between the area and the evaporation values, the periods with high area values are the spring periods where the evaporation values are low.

In order to maintain the amount of water in the lake, illegal water wells in the lake will be detected and the use of agricultural water will be controlled (Lake Yarisli Wetland Management Plan (2018-2022), 2017).

Figure 4.57 shows the areal changes of the lake with images of 2 different years.

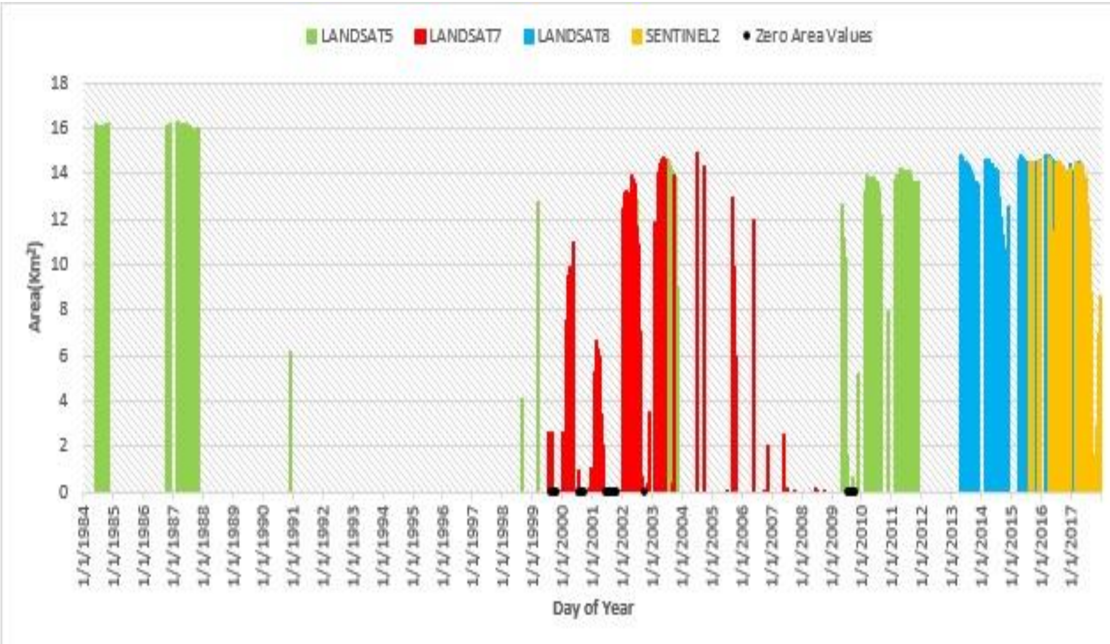

Figure 4.53. *Water Extent Change of Lake Yarisli*

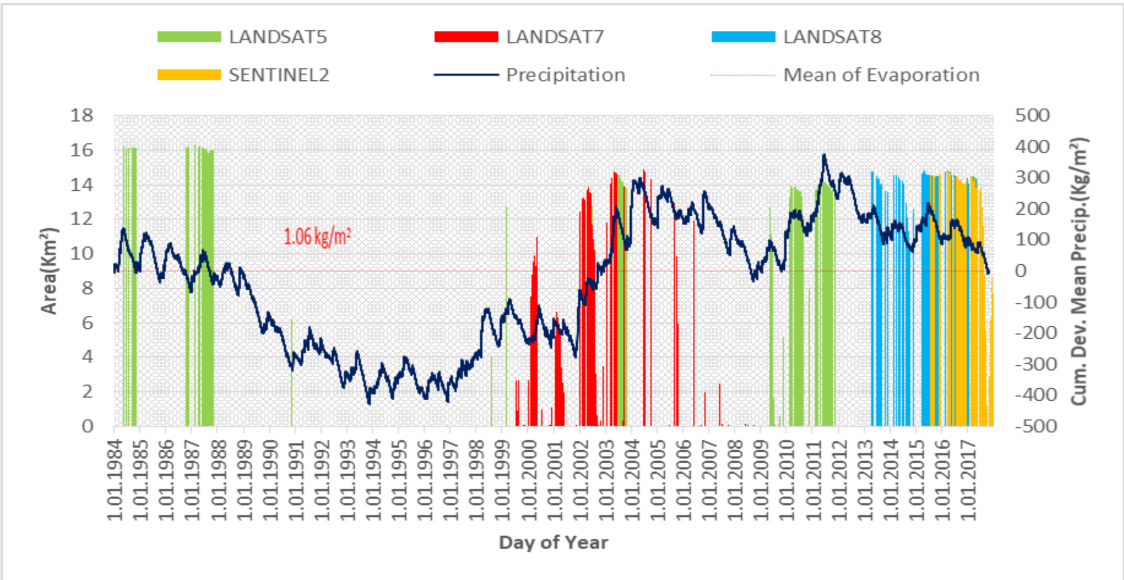

Figure 4.54. *Water Extent Change of Lake Yarisli and Cumulative Deviation from Mean Daily Precipitation*

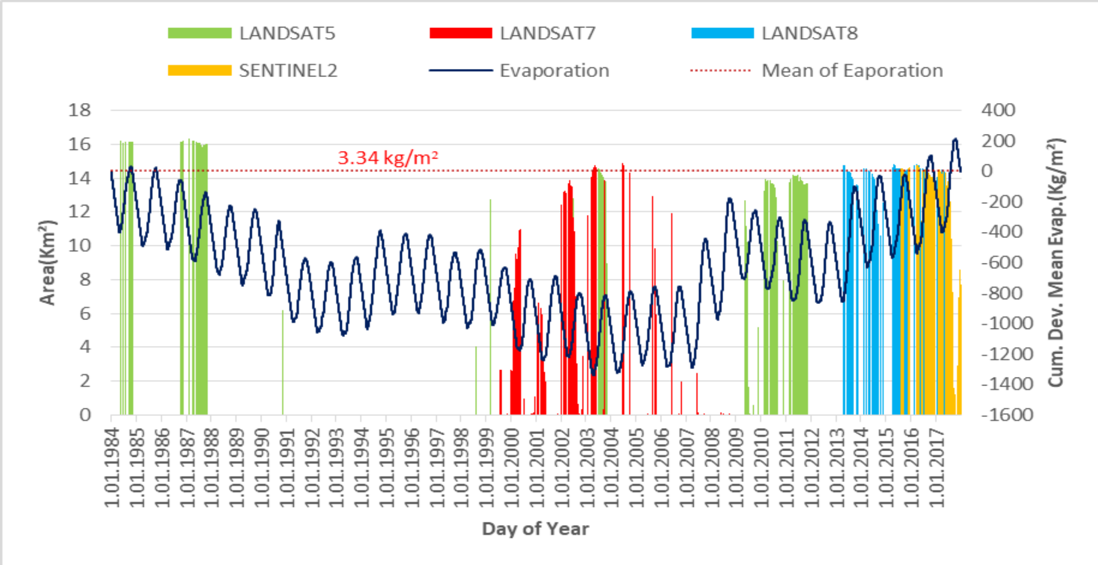

Figure 4.55. *Water Extent Change of Lake Yarisli and Cumulative Deviation from Mean Daily Evaporation*

Figure 4.56. *Water Extent of Lake Yarisli; (a) 10.6.1999 Area: 0 km² (Landsat 7) (b) 18.1.2003 Area: 12 km² (Landsat 7), (c) 26.12.2017 Area: 7,7 km² (Sentinel 2)*

4.1.15. Lake Karatas

As seen in the Figure 4.57 the area value which was 12 km^2 in the spring of 1984, decreased to 11 km^2 in summer and 9.3 km^2 in autumn. The area value which was 10.6 km^2 at the beginning of 1987 increased to 11.4 km^2 in spring, and the area value which was 9 km^2 in the summer decreased to 6.6 km^2 in autumn.

The lake area, which was 4.1 km^2 at the end of 1990, was determined as 4 km^2 in summer of 1995 and 1998. The area value of 6.5 km^2 in the spring of 1999 decreased to 4.2 km^2 in the autumn and increased to 4.5 km^2 at the end of the year. The area value, which was 6.5 km^2 in the spring of 2000, was determined around 4 km^2 from summer to the end of the year. The area value which was 4.5 km^2 in the spring of 2001 decreased to 3 km^2 at the end of the year. The area value which was 6.6 km^2 at the beginning of 2002 increased to 9.4 km^2 in the spring. The value of the area which decreased to 5.3 km^2 in summer of 2002, increased to 6.1 km^2 at the end of the year. At the beginning of 2003, the area value of 8.1 km^2 was increased to 12 km^2 in the spring and 11.1 km^2 was determined at the end of the year. The lake area which was under 1 km^2 in summer and autumn of 2004, was determined as 10.2 km^2 in the summer of 2005. The area value was 9.6 km^2 in the autumn of 2005 and it was 10.5 km^2 in the spring of 2006. In the autumn of the same year, the area was determined as 8.3 km^2. In the spring of 2009, the area value, which was 8.2 km^2, decreased to 5 km^2 in summer and it was determined 5.5 km^2 at the end of the year. The area value, which was 8.5 km^2 at the beginning of 2010, increased to 10.2 km^2 in spring and was 8 km^2 at the end of the year. The area value, which was 9.6 km^2 at the beginning of 2011, increased to 11 km^2 in the spring and got values around 10 km^2 until the end of the year. In the spring of 2013, the area value, which was 11.5 km^2, decreased until the autumn to a value of 8.8 km^2. In the spring of 2014, the area value which was 10 km^2 has fallen until the autumn and was determined 6.5 km^2. The area value, which was 8.3 km^2 at the beginning of 2015, increased to 10 km^2 in the spring and the area value which was 8 km^2 in the autumn was determined 8.7 km^2 at the end of the year. The area value, which was 9.3 km^2 at the beginning of 2016, was determined 9.5 km^2 in spring. The area value which was 4.8 km² in the autumn of 2016, was determined 6.1 km² at the end of the same year. The area value which was 6.6 km² at the beginning of 2017 was 7.5 km² in the spring and the area value which was 4 km² in the autumn, was determined as 4.8 km² at the end of the year. When the comparison is made by evaluating the spring periods of the year, it is seen that area values reached the highest vale in 1984 and lowest values in 2001. The values that are below 1 km² belong to summer periods. Lake area showed a decreasing trend after 2013. In summary, it can be seen that the lake extent is controlled by the seasonal variation in precipitation, taking the highest values in spring and the lowest values in summer (Figure 4.58).

As seen in the Figure 4.59, the periods with high area values are the spring periods where the evaporation values are low.

Figure 4.60 shows the areal changes of the lake with images of 2 different years.

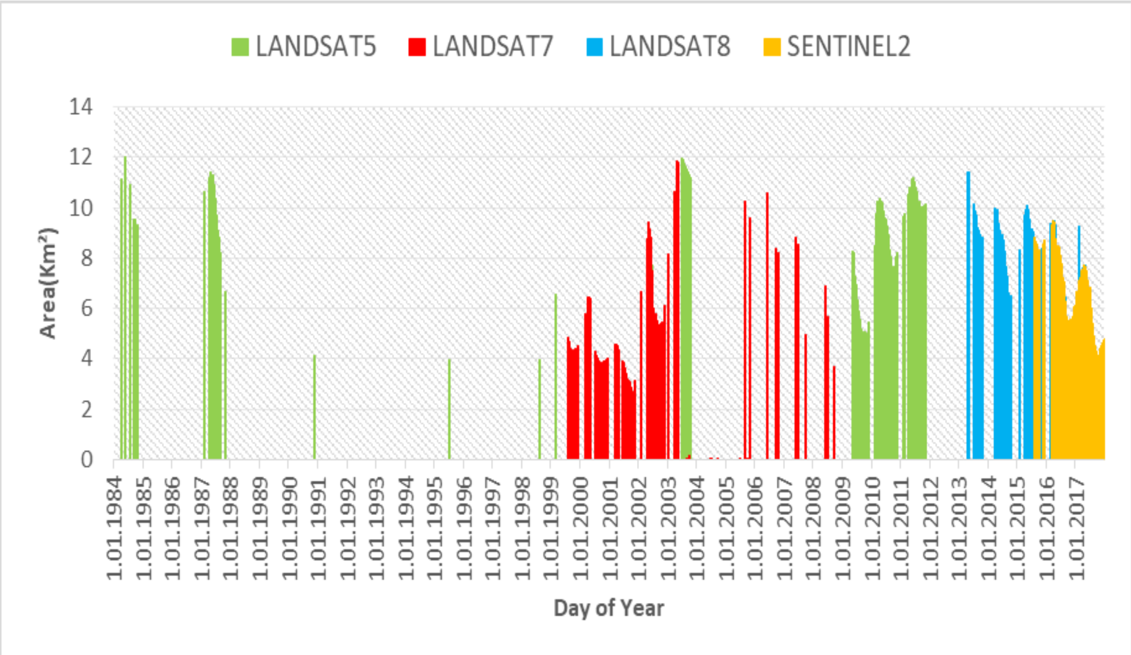

Figure 4.57. *Water Extent Change of Lake Karatas*

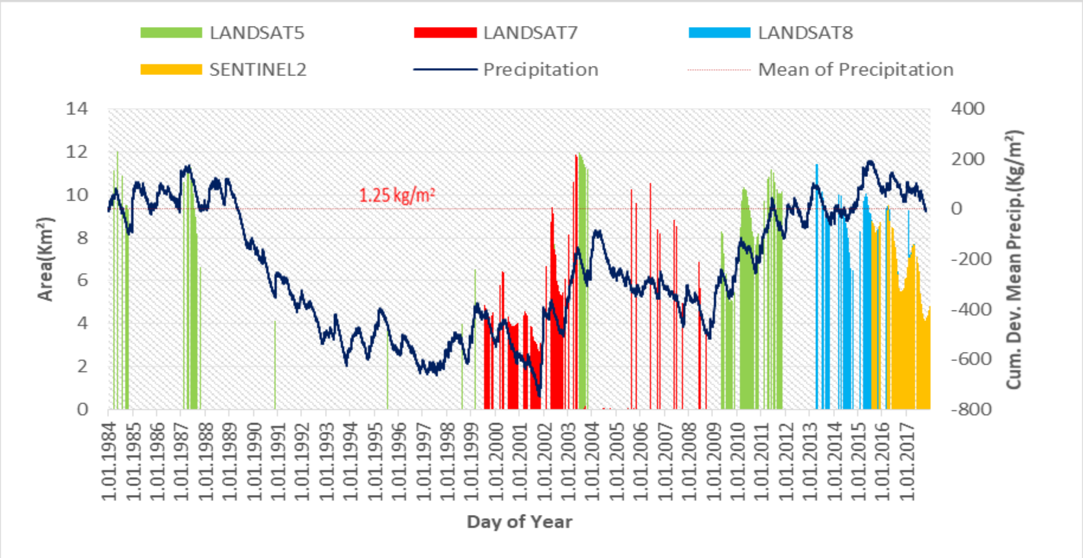

Figure 4.58. *Water Extent Change of Lake Karatas and Cumulative Deviation from Mean Daily Precipitation*

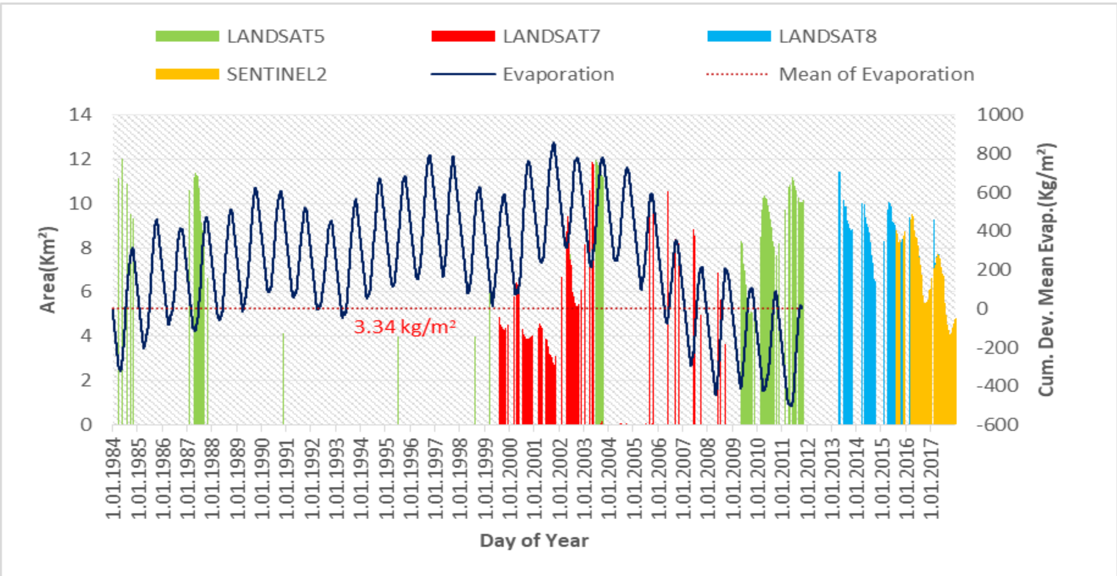

Figure 4.59. *Water Extent Change of Lake Karatas and Cumulative Deviation from Mean Daily Evaporation*

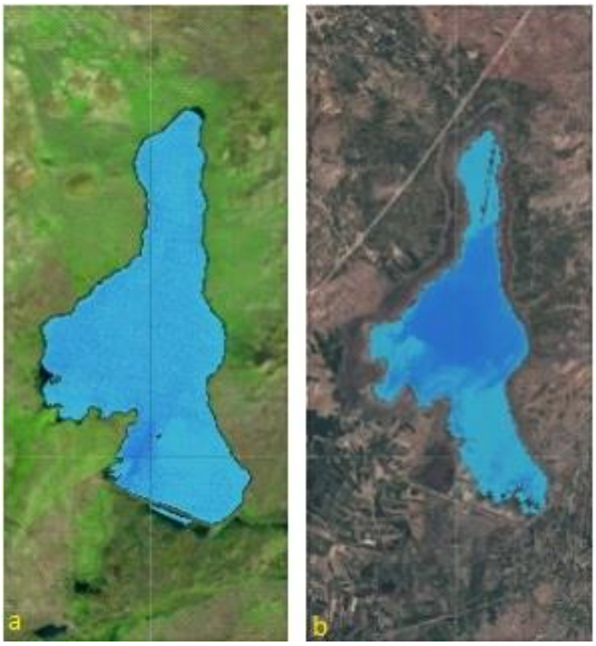

Figure 4.60. *Water Extent of Lake Karatas; (a) 1.5.2003 Area: 12 km² (Landsat 7), (b) 10.5.2017 Area: 7,5 km² (Sentinel 2)*

4.1.16. Lake Akgol

As seen in Figure 4.61 the lake area, which was determined at 10 km² in the autumn of 1984, was completely dry in the autumn of 1986. In 1987 the lake area which values determined as 7 km² and 5 km² in the spring, decreased to 0 km² in autumn. The lake was completely dry in the summer of 1995 and 1999. In the spring of 2000, the area of the lake, which was 5.1 km², fell to 0 km² in the summer. The area of the lake was determined as 0 km² from summer to autumn in 2001. In the spring of 2002, the area of the lake, which was 7.7 km², was determined 0 km² in summer and autumn. At the beginning of 2003, the lake area, with values as 3.7 km² and 2 km², increased to 8.8 km² in spring and the lake was completely dry in the autumn. In 2004, the area of the lake was determined 8 km² in summer and 0 km² in the autumn. In the summer and autumn of 2005, the lake area received values below 1 km². The area value of 1.4 km² in the spring of 2006 fell below 1 km² in autumn. In 2007 and 2008, both in spring and autumn, the lake area received values below 1 km². The values of the lake from

2004 to 2008 were calculated by downloaded Landsat 7 images. The lake area, which was 6.5 km^2 in spring 2009, remained dry in the summer and in the autumn and was determined as 0 km^2. In the spring of 2010, the lake area, which was 7.5 km^2, fall below 1 km^2 in summer, and was determined 0 km^2 in autumn and end of the year. The lake area, which was 7.3 km^2 in spring 2011, was completely dry in autumn. The lake area, which was 7.5 km^2 in spring 2013, decreased to 2 km^2 in summer and was completely dry in autumn. In the spring of 2014, the area value of 5.5 km^2 has fallen until summer and was completely dry then the lake area was determined 0.5 km^2 at the end of the year. The area value which was 6.7 km^2 at the beginning of 2015 increased to 10.5 km^2 in the spring, and the area value which was 7 km^2 in the summer was determined as 3.7 km^2 at the end of the year. The area value, which was 8.8 km^2 at the beginning of 2016, was dry in summer and remained at 0 km^2 until the end of the year. The area value, which was 1.7 km^2 at the beginning of 2017, increased to 2.5 km^2 in spring and then declined and was determined as 0 km^2 at the end of the year.

When the comparison is made by referring the same periods of the year, it is seen that the lake reached the highest values in spring and completely dried in most years during summer. The lake area which values were above 8 km^2 in 2003, reached its maximum extent of 10.4 km^2 in April 2015 and then values decreased until the end of 2017.

As seen in the Figure 4.62 precipitations values reached the highest values in 2015 similar to the lake area values. Then both area and precipitation values decreased until the end of 2017. At the seasonal scale, the lake area follows the high precipitation pattern in spring. In the long time scales, the precipitation controls the lake extent. Figure 4.63 shows the seasonal variation of lake extent, with higher extent during spring with lower evaporation values.

Figure 4.64 shows the areal changes of the lake with images of 3 different years.

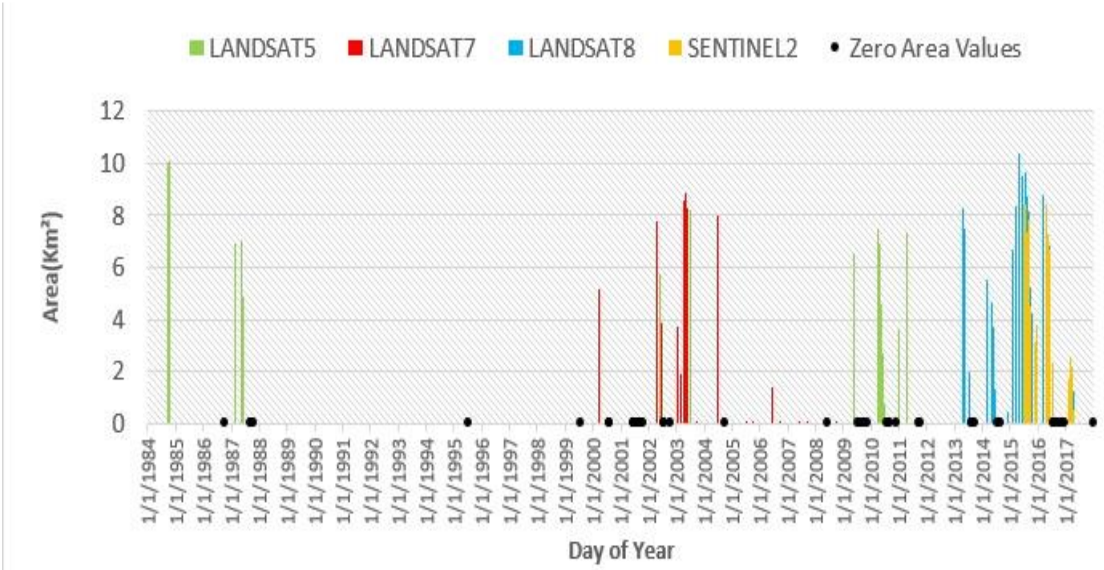

Figure 4.61. *Water Extent Change of Lake Akgol*

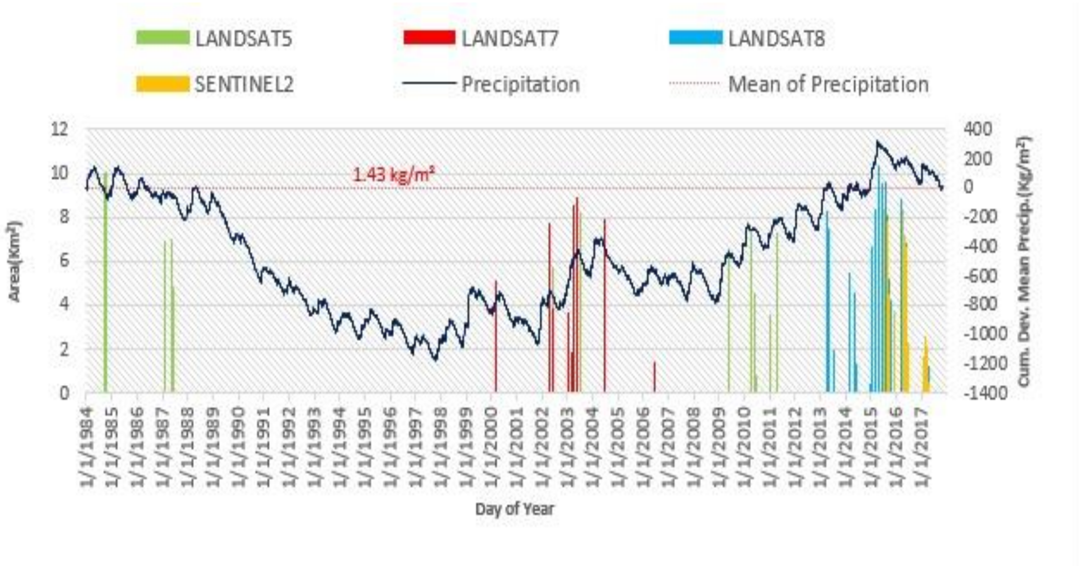

Figure 4.62. *Water Extent Change of Lake Akgol and Cumulative Deviation from Mean Daily Precipitation*

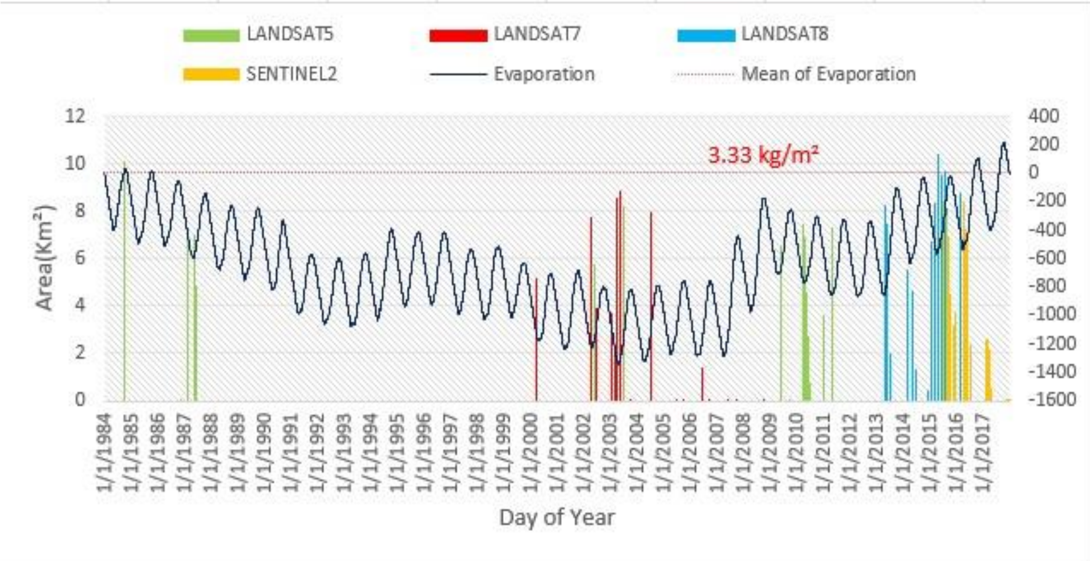

Figure 4.63. *Water Extent Change of Lake Akgol and Cumulative Deviation from Mean Daily Evaporation*

Figure 4.64. *Water Extent of Lake Akgol; (a) 12.06.2001 Area: 0 km² (Landsat 7), (b) 30.3.2003 Area: 8.5 km² (Landsat 7), (c) 21.3.2017 Area: 2.1 km² (Sentinel 2)*

In summary, maximum and minimum area values of the lakes between 1984 and 2017 together with the year of occurrence is listed in Table 4.1. To enable comparison between lake extents, the time period was chosen as the lakes reached the maximum area values in a year. For Lake Burdur, Lake Sugla and Lake Kovada this period was

December-January period but for all the other lakes this period was spring period that includes March, April and May. The maximum and minimum values of the lakes that are shown in the Table 4.1 are the average lake extent for the reference periods. For example, in Lake Egirdir, maximum average value of the area that belong to spring period is 469.3 km² which was in 1987 and the minimum value is 452.4 km² which was in 2002. Table 4.1 also shows the recent value that belongs to 2017 and the percentage of the recent value compared to the maximum value. In this way, the percentage of the area of the lake relative to the maximum extent is shown. Moreover, character of lake area variation during the study time period is listed in last column in Table 4.1. Note that the area of Egirdir and Beysehir lakes did not change significantly and hence variation in area could not be characterized.

Table 4.1. Maximum and Minimum Area Values of the Lakes and their character of area variation

Lake	Max. Area Value (km²)	Date of Max. Area Value	Min. Area Value (km²)	Date of Min. Area Value	Area in 2017 (km²)	% of area value in 2017 compared to Max. Value	Character of area variation
Egirdir	469.3	1987	452.4	2002	457.1	97.4	-
Salda	45,5	1987	43.3	2008	44	96.8	Seasonal
Beysehir	670.1	2013	625.8	2001	641.6 (2016)	95.7	-
Sugla	37.4	2015	0	1988,1993,1994, 2006	35.2	94	Dam controlled
Yarisli	16.2	1984	4	2001	14.3	88	Seasonal
Kovada	8.3	2002	7.3	2017	7.3	88	Seasonal
Acigol	143	1984	46.2	2001	125.6 (2015)	87.9	Seasonal (Salt Pans)
Gavur	2.3	1999	0	2011	1.9	82.6	Mostly dry
Isikli	60.4	2002	46	2001	49.4	81.9	Seasonal
Ilgin	26.8	1984	18.3	2001	21.8	81.3	Seasonal
Burdur	201.3	1987	130.8	2017	130.8	65	Decreasing
Karatas	11.6	1984	4.5	2001	6.8	58.8	Seasonal
Karamik	22.7	2011	1.7	2009	13	57.3	Seasonal (marshes)
Eber	82.4	2000	6.2	2009	45.9	55.7	Seasonal (marshes)
Aksehir	328.9	1984	53.6	2017	53.6	16.3	Decreasing
Akgol	9.4	2015	1.3	2017	1.3	14.2	Seasonal (dry in summers)

4.2. Elevation – Area – Volume Relations

As stated in Chapter 3.5, bathymetric measurements collected in the lake consist of points that have elevation data. In this chapter it is aimed to show volume of the lakes calculated by digital elevation models which was produced using bathymetric measurements as shown in Chapter 3.5.5. Thus elevation-area-volume relations could be revealed. The bathymetric measurements reveal the lake area and lake volume corresponding to a certain lake level. Hence in-situ lake level measurements can be used together with the bathymetric measurements to obtain lake extent values that can be compared to lake extent obtained from remote sensing for the same date. Note that lake bathymetry may change in time due to sedimentation or other factors. However, lake bathymetry data provided by DSİ was utilized throughout the study time period. In this study lake area and lake volume calculations from in-situ lake level measurements were made only for 5 lakes (Lake Aksehir, Lake Beysehir, Lake Burdur, Lake Egirdir and Lake Kovada) that have both bathymetric measurements and lake level measurements as shown in Table 2.3. Note that Section 3.5 discusses the reason why the area and volume calculation for Lake Eber is missing despite the fact that both bathymetric and lake level measurements exist.

The relationship between lake level, lake area and lake volume was examined using elevation-area-volume graphs (Figure 4.65-4.69). Note that if the area never increases or increases slightly, while the volume increases uniformly, it means that the lake has a U-shaped structure. However, if the increase in the area in the lake is more significant compared to the increase in volume, this means that the lake has a V-shaped structure.

For all the 5 lakes studied in this chapter; it is seen that the slope of the area curve decreased with elevation, while the slope of the volume curve increased. Just one exception to this situation is Lake Burdur for which slope of area curve increased second time after elevation of 833 m (Figure 3.18 and Figure 4.67).

Elevation-area-volume relationship for Lake Aksehir is shown in Figure 4.65. For elevation values between 952 m and 953 m, area increased sharply and then the slope gradually decreased. In contrast to the area, slope of the volume values increased after 953 m. Figure 4.66 shows area-volume-elevation relations for Lake Beysehir. As seen in this figure the curve of the area value decreased after 1120 m. and after 1123 m, it became almost completely horizontal. Decrease in slope of area curve indicates that the lake area does not change significantly as a function of elevation and hence presents difficulty in optical remote sensing observation of lake water quantity. The slope of the volume curve is almost constant after 1117 m.

Figure 4.67 shows the elevation-area-volume relationship for Lake Burdur. As seen in this figure the slope of the area curve increased after 832 m. After this value slope of area and volume curves are almost parallel.

Figure 4.68 shows elevation-area-volume relationship for Lake Egirdir. As seen in the figure that the slope of the area curve decreases after 914 m and the slope volume curve is almost horizontal until 908 m and increase at higher elevations.

Figure 4.69 shows elevation-area-volume relationship for Lake Kovada. As seen in the figure the slope of the area curve at 902 m has gradually decreased and after 905 m it has become almost horizontal. By contrast, the slope of the volume curve is almost horizontal up to 902 and then become almost linear.

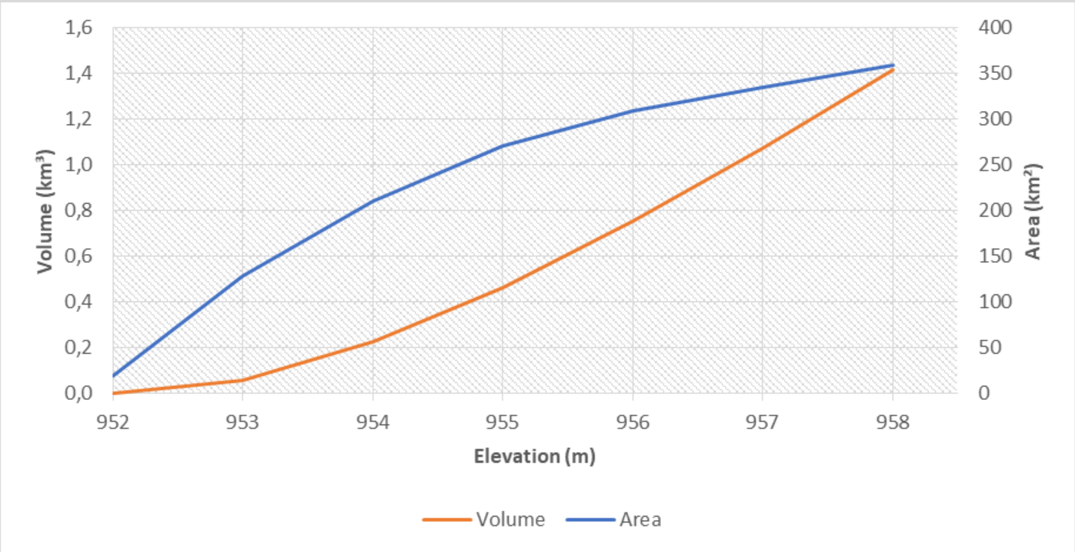

Figure 4.65. *Area-Volume Relation According to Elevation in Lake Aksehir*

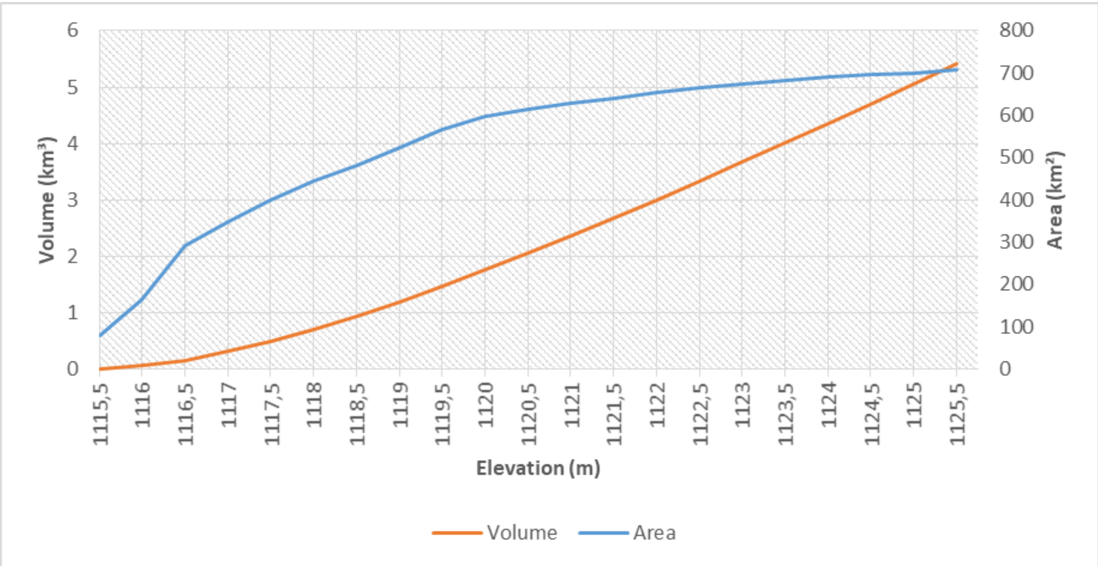

Figure 4.66. *Area-Volume Relation According to Elevation in Lake Beysehir*

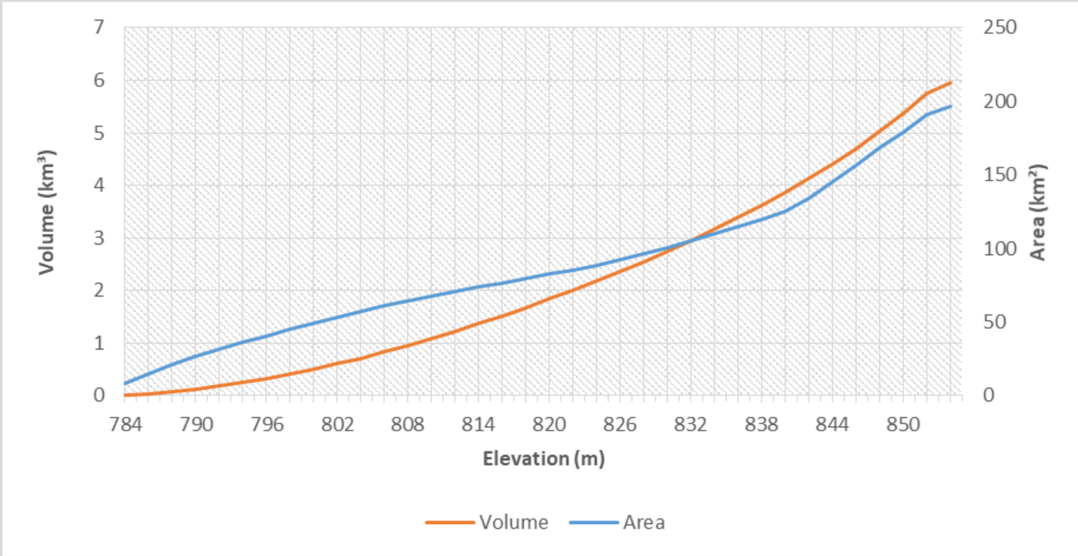

Figure 4.67. *Area-Volume Relation According to Elevation in Lake Burdur*

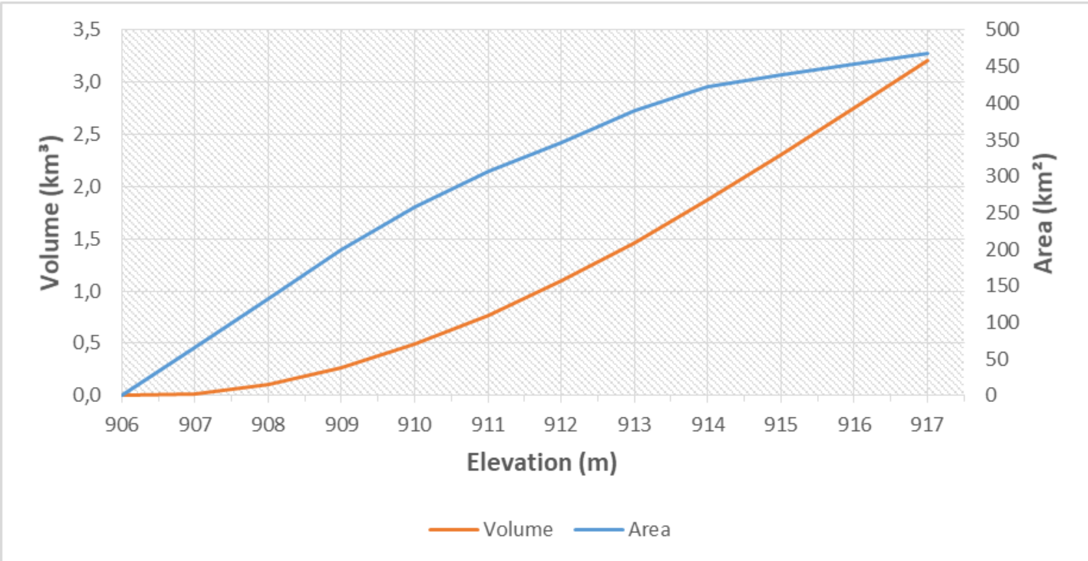

Figure 4.68. *Area-Volume Relation According to Elevation in Lake Egirdir*

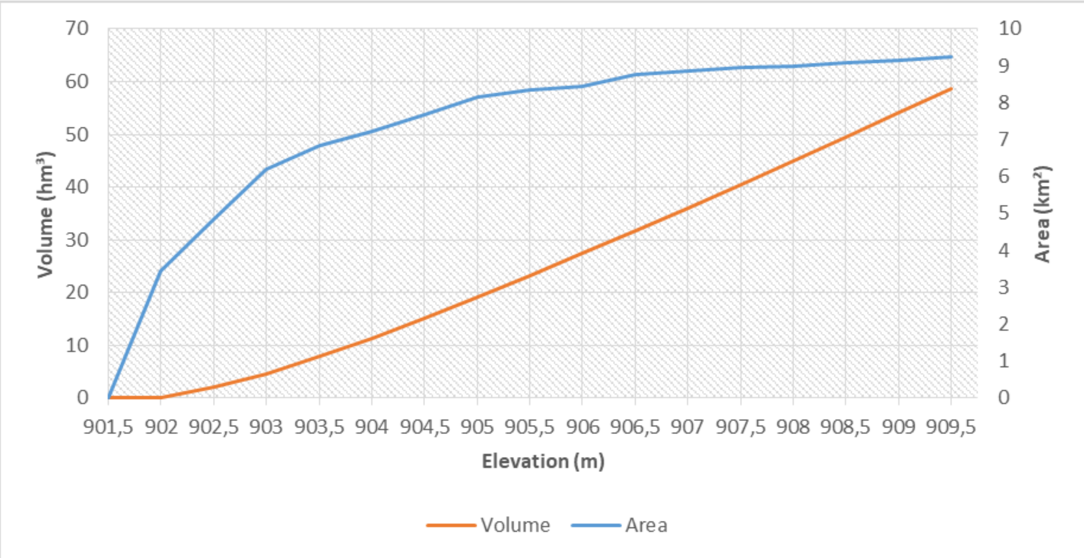

Figure 4.69. *Area-Volume Relation According to Elevation in Lake Kovada*

4.3. Comparison of Remotely Sensed and Ground Based Water Extent Measurements

In previous studies focusing on the Lakes Region (see Chapter 1.3), the accuracy of the remotely sensed lake area values was performed by comparing with the lake area values calculated by manual digitizing from the lake images. Referencing the image could be reliable especially if it is digitized precisely. However, digitizing the image manually is a laborious and time-consuming task. If the study consists of only a few images like mentioned in chapter 1.3, this effort can be tolerated. However, in this study, it was not possible to use the digitization method for the validation, because there were more than 4000 images that was included in the analyses. Therefore, in-situ lake level measurement time series together with bathymetric measurements were used to calculate lake area information and then compared with remotely-sensed lake area information for the overlapping dates. These operations were made by coding as described in Chapter 3.5.4.

Surface area of the lakes calculated from remotely sensed images and in-situ lake level measurements were compared using scatterplots and coefficient of determination (Figure 4.70). It can be seen from these scatterplots that surface area of the lakes obtained from remote sensing is consistently less than that of obtained from in-situ measurements. This bias could be due to mismatch between elevation of the in-situ measurement and the bathymetry survey. Moreover, additional uncertainty arises due to the 30-meter resolution of the Landsat imagery – although consistently low values were not expected due to this uncertainty alone. High linear correlation values were obtained for Lake Aksehir R^2=0.86, Lake Beysehir R^2=0.75, Lake Burdur R^2=0.93, whereas low linear correlation values were obtained for Lake Egirdir R^2=0.28 and Lake Kovada R^2=0.04. The best match is obtained for Lake Burdur both in terms of correlation and in terms of bias.

As shown in Table 3.1 the lake area values that were calculated from digitized lake images were used for determining the threshold values used in NDWI. The accuracies of the 5 lakes that referenced in Table 3.1 are 97.6% for Lake Aksehir, 98.9% for Lake Beysehir, 98.6% for Lake Burdur, 97.2% for Lake Egirdir and 96.4% for Lake Kovada. High accuracy obtained from digitized images gives reliability to the NDWI-based lake area detection used in this study. A few data points were marked as outliers (red markers) in these scatterplots. The reason of outliers in Lake Egirdir was the cloud cover. Note that a %10 cloud cover threshold was applied to the image collections to remove cloudy pixels as much as possible while increasing the number of images in the analysis. In some cases, although the cloud cover in the image were less than the selected threshold, cloud cover concentrated over the lake caused lower than expected surface area values.

In addition, even though some images were cloud free and clear, NDWI method failed to identify water due possibly to several reasons including chlorophyll content in water, whitening due to calcite solution in lake water as well as sun angle (Figure 4.71). The images far from the scatter were screened visually for these characteristics and positive instances were considered as outliers (red markers in scatterplots).

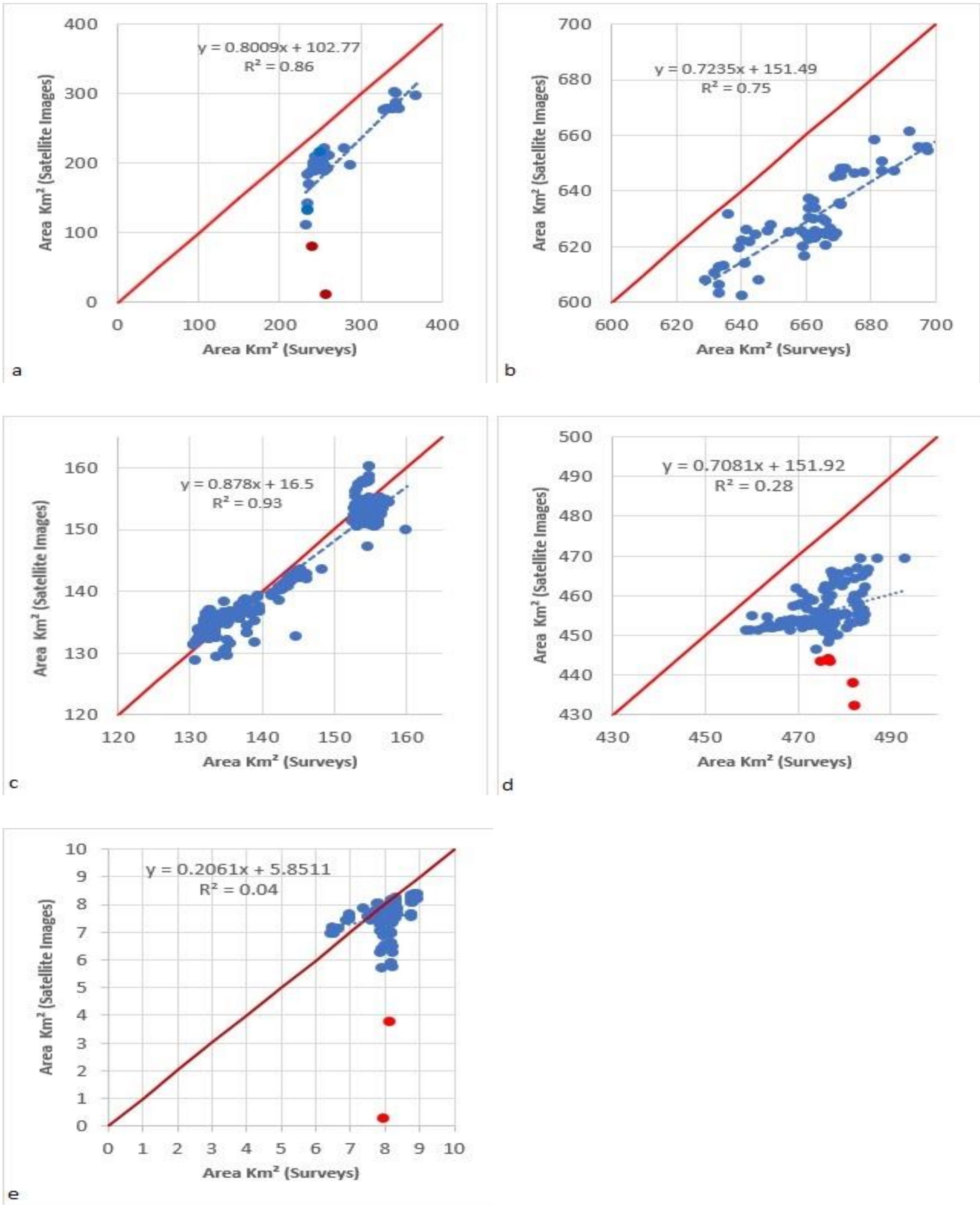

Figure 4.70. *Scatterplot comparing surface area of (a) Lake Aksehir, (b) Lake Beysehir , (c) Lake Burdur , (d) Lake Egirdir, (e) Lake Kovada obtained from in-situ lake level measurements and remote sensing. Note that red markers are outliers*

Figure 4.71. *Examples of cloud-free images for (a) Lake Aksehir and (b) Lake Kovada showing pixels that were not considered as water by NDWI*

CHAPTER 5

CONCLUSIONS AND RECOMMENDATIONS

The main objective of this study is to analyze the spatio-temporal variations in lake water extents of sixteen lakes located in the Lakes Region, Turkey using remotely sensed images. The changes in water extents were further evaluated using in-situ water level measurements through bathymetric surveys (elevation-area-volume relationships). The relationship between water extent changes and meteorological variables were also investigated to better understand the drivers of water extent change.

Remote sensing analysis was performed within Google Earth Engine Platform to enable fast and efficient processing of large number of satellite images within the Google cloud environment. In this way, analyzes were performed on the platform without downloading images. Remote sensing images were provided from Landsat 5 TM, Landsat 7 ETM+ and Landsat 8 OLI/TIRS collections and Sentinel-2 MSI: MultiSpectral Instrument, Level-1C collection in the Lakes Region. A %10 cloud threshold was applied to these images according to determined lake boundaries between 1984 and 2018 by using Fmask bands and Q60 band provided in Google Earth Engine. The imagery from different platforms were available for the following time periods: Landsat 5 for 1984-2012, Landsat 7 for 1999-2003, Landsat 8 for 2013-2018 and Sentinel 2 for 2015-2018. A total of 4031 images, including 2601 Landsat family and 1430 Sentinel-2, were included in the analysis. Normalized Differential Water Index (NDWI) was used to determine the pixels to be evaluated as water. NDWI > 0.1 was accepted as water. A function that uses green and NIR bands were used to calculate NDWI values in Earth Engine Code Editor for all images in the collection. Time series of remotely sensed lake water extent, station precipitation and evaporation as well as in-situ lake level and bathymetric datasets were used in the analysis.

According to these analysis the following results are found:

- In Lake Burdur and Lake Aksehir water extents decreased continuously since 1984, reaching in 2017 to %65 and %16 of their maximum extents respectively. This continuous decrease could not be explained by meteorological variables. Therefore further investigation is needed for other factors, such as anthropogenic impacts on these lakes.
- Seasonal fluctuations in water extents were identified for Lake Salda, Lake Beysehir, Lake Yarisli, Lake Kovada, Lake Acigol, Lake Ilgın, Lake Karatas, Lake Karamik, Eber and Lake Akgol. While Lake Gavur, smallest lake studied (maximum extent 2.3km^2), was mostly dry in analyzed imagery, Lake Akgol was dry in almost all summers.
- In Lake Egirdir, Lake Salda, Lake Beysehir and Lake Sugla water extent did not fall below %90 of their maximum extent at the end of the study period (2017). This result could be due to the bathymetrical features of these lakes. If the elevation-area curve for a lake has a gentle slope then changes in water level will not be reflected in water extent. Actually, this was the case for Lake Egirdir and Lake Beysehir for which bathymetry data is available.
- Remotely-sensed water extents were consistently lower than the water extents obtained by in-situ lake level measurements and lake bathymetry information that are available for five lakes. This situation could be due to the coarse resolution of satellite images (30m for Landsat and 10m for Sentinel-2) or due to discrepancy between reference lake level measurement and bathymetry dataset.

Google Earth Engine provided an efficient Cloud Platform for analysis of large number of images from various missions, such as Landsat and Sentinel-2. The lack of an algorithm in Google Earth Engine to fill the gaps in Landsat 7 satellite imageries corresponding to 2003-2008 period were solved by downloading and digitizing representative number of Landsat 7 images. Finding a software solution within Google

Earth Engine for this problem could be a further extension of this work. A limitation of the optical sensors used in this study is their inability to penetrate clouds. A further extension of this work would be to utilize synthetic aperture radar (such as Sentinel-1) or satellite altimetry (such as Topex-poseidon) to monitor lake extents and lake levels, respectively. Another difficulty encountered in this study stems from factors affecting the reflectance properties of water such as marshes, chlorophyll content and calcite deposition. Further investigation is recommended to identify images affected by these factors.

REFERENCES

(2013). Retrieved from Burdur Province Nature Tourism Master Plan 2013 - 2023: http://bolge6.ormansu.gov.tr

(2014). Retrieved from Provincial Directorate of Culture and Tourism: http://burdurkulturturizm.gov.tr/

(2019). Retrieved from Burdur Governor of the Republic of Turkey: http://www.burdur.gov.tr/

(2019). Retrieved from USGS: https://earthexplorer.usgs.gov/

Altinsacli, S. (2000). A Preliminary Study on the Ostracoda (Crustacea) Fauna of Lake Aksehir. *Turkish J. Zoology*, 9-16.

Atalay, İ., & Efe, R. (2008). Ecoregions of the Mediterranean Area and the Lake Region of Turkey. *Environment and Culture in the Mediterranean Region* . International Symposium on Geography.

Ataol, M. (2010). The water level changings in Burdur Lake . *Journal of Geographical Sciences*, 77-92.

Ayhan, E. (2016). Multi-Temporal Water Extent Analysis Of A Hypersaline Playa Lake Using Landsat Imagery. Ankara: Master Thesis, METU.

Bahadir, M. (2013). Determination of Spatial Changes of Aksehir Lake with Remote Perception Techniques. *Marmara Geography Jornal*, 246-275.

Cevik, M. (2009, 12 5). *Lake Beysehir*. Retrieved from National Nature and Culture Documentaries Association: https://dogabel.wordpress.com/

Doganer, P. D. (2015). *Geography of the Mediterranean Region*. Retrieved from istanbul.edu.tr.

Erdem, O. (2007). *Wetland Management Planning Directory*. Ankara: General Directorate of Nature Conservation and National Parks Bird Research Association.

ESA Sentinel Online. (2019). Retrieved from https://sentinel.esa.int/web/sentinel/missions/sentinel-2

Feyisa, G. L., Meilby, H., Fensholt, R., & Proud, S. R. (2014). Automated water extraction index: A new technique for surface water mapping using Landsat imagery. *Remote Sensing of Environment*, 23-35.

Google Earth Engine. (2018, 10 17). Retrieved from Google Earth Engine: https://developers.google.com/earth-engine/datasets/

Gorcelioglu, E. (1976). The Importance and Widspread of sedimentation of Burdur Lake in Lakes Region. *The Journal of Istanbul University Faculty of Forestry*, 57-58.

Gorelick, N. (2017). Google Earth Engine: Planetary-scale geospatial analysis for everyone. *Remote Sensing of Environment*, 18-27.

Healy, R. W., Winter, T. C., & Franke, J. W. (2007). Water Budgets: Foundations for Effective Water-Resources and Environmental Management. *U.S. Geological Survey Circular 1308*, 90.

Huang, C., Chen, Y., Zhang, S., & Wu, J. (2018). Detecting, Extracting, and Monitoring Surface Water From Space Using Optical Sensors: A Review. *Reviews of Geophysics*, 333-360.

Instruments and Devices Used in Meteorology. (2019). Retrieved from Turkish State Meteorological Service: https://www.mgm.gov.tr/genel/meteorolojikaletler.aspx?s=9

IPCC. (2013). *Climate Change 2013*. Warsaw: IPCC.

Kaplan, G., Avdan, U., Yavdan, Z., & Yildiz, N. (2016). Drought Monitoring Using Landsat Satellite ImagesS (Case Study Aksehir Lake). *UZAL-CBS 2016*, (pp. 535-540). Adana.

Kesici, E. (2015). Effects of Interventions on the Natural Structure of Lake Egirdir (Isparta) on the Ecological Structure of the Lake. *Ege Journal of Fisheries and Aquatic Sciences*.

Kole, M. M., Ataol, M., & Erkal, T. (2016). Spatial changes of Eber and Akşehir lakes between 1990 and 2016. *International Geography Symposium* (pp. 859-872). Ankara: International Geography Symposium.

Komeil Rokni , Anuar Ahmad , Ali Selama , Sharifeh Hazini. (2014). Water Feature Extraction and Change Detection Using Multitemporal LandsatImagery. *Remote sensing*, 2317–2335.

Kriegler, F.J., Malila, W.A., Nalepka, R.F., Richardson, W. (1969). Preprocessing transformations and their effects on multispectral recognition., (pp. 97-131).

(2008). *Lake Aksehir and Lake Eber Wetland Management Plan (2008-2012).* General Directorate of Nature Protection and National Parks.

(2013). *Lake Karatas.* General Directorate of Nature Protection and National Parks Wetlands Branch.

Lake Yarisli. (2014). Retrieved from dogadernegi.org

Landsat Science. (2019). Retrieved from Technical Details: https://landsat.gsfc.nasa.gov/about/technical-information/

Lucas, C. S. (1998, 9 12). *Multispectral Pattern Recognition*. Retrieved from http://maps.unomaha.edu/Peterson

McFeeters, S. K. (1996). The use of the normalized difference water index (NDWI) in the delineation of open water. *International Journal of Remote Sensing*, 1425–1432.

Ministry of Forestry and Water Affairs, T. S. (2018). *Environmental Indicators.* Retrieved from https://environmentalindicators.csb.gov.tr/precipitation-i-85992

NOAA. (2018, 6 25). *How is bathymetric data used?* Retrieved from National Ocean Service: https://oceanservice.noaa.gov/facts/bathyuses.html

Ozden, S. (2010, 01 04). Climate change and drought: the case of Istanbul and regulations studies in Turkey.

Ozturk, M. (2005). An investigation of metazoan parasites of common Carp (Cyprinus carpio L.) in Lake Eber, Afyon, Turkey. *Turkish Society for Parasitology*, 204.

Sapcilar, E., & Fakioglu, M. (2004). Hydrographic Map Works at General Directorate of State Hydraulic Works. Chamber of Survey and Cadastre Engineers.

Schwarb, M., Acuna, D., Konzelmann, T., Rohrer, M., Salzmann, N., B. Serpa, L., & Silvestre, E. (2011). A data portal for regional climatic trend analysis in a Peruvian High Andes region. *Advances in Science & Research*, 219-226.

Sciences. (2001). *A Beginner's Guide to Water Management - Lake Morphometry.* Department of Fisheries and Aquatic Florida Lakewatch.

Sener, E., Davraz, A., & Sener, S. (2010). Investigation of Aksehir and Eber Lakes (SW Turkey) Coastline Change with Multitemporal Satellite Images. *Water Resour Manage*, 727-745.

Sener, S. (2016). Hydrogeochemical Investigation of the Lake Kovada (Isparta). *Journal of Engineering Sciences and Design*, 49-58.

Sisay, A. (2016). Remote Sensing Based Water Surface Extraction and Change Detection in the Central Rift Valley Region of Ethiopia. *American Journal of Geographic Information System*, 33-39.

Sobek, S., Nisell, J., & Folster, J. (2011). Predicting the depth and volume of lakes from map-derived parameters. *Inland Waters*, 177-184.

Stagl J., Mayr E., Koch H., Hattermann F.F., Huang S. (2014). Effects of Climate Change on the Hydrological Cycle in Central and Eastern Europe. Springer, Dordrecht.

Taylan, D., & Aydin, T. (2018). The Trend Analysis of Lakes Region Precipitation Data in Turkey. *Cumhuriyet Science Journal*, 258-273.

Tri Dev Acharya , Anoj Subedi , Dongha Lee. (2018). Evaluation of Water Indices for Surface Water Extraction in a Landsat 8 Scene of Nepal. *Sensors*, 2580.

Uyan, U. (2014). An endemic in Acigol.

Uzun, N. (2007). *Environmental Status Report.* Afyonkarahisar Governorship.

Varol, S., Davraz, A., Sener, S., Sener, E., Aksever, F., Kırkan, B., & Tokgozlu, A. (2018). Application of A Conceptual Water Budget Model For Salda Lake, (Burdur/ Turkey). *Journal of Engineering Sciences and Design*, 29-37.

Wenbo Li , Zhiqiang Du , Feng Ling. (2013). A Comparison of Land Surface Water Mapping Using the Normalized Difference Water Index from TM, ETM plus and ALI. *Remote Sensing*, 5530-5549.

Wetlands of Turkey. (2016). Retrieved from http://www.turkiyesulakalanlari.com/wp-content/uploads/sulak-alan-kartlar%C4%B1-6x9-01.pdf

Wetlands of Turkey. (2016). Retrieved from http://www.turkiyesulakalanlari.com

Xu, H. (2006). Modification of normalised difference water index (NDWI) to enhance open water features in. *International Journal of Remote Sensing*, 3025–3033.

Xu, H. (2006). Modification of normalised difference water index (NDWI) to enhance open water features in remotely sensed imagery. *International Journal of Remote Sensing*, 3025–3033.

Zedef, V. (1995). Hydromagnesite stromatolites and sediments in an alkaline lake, Salda Golu, Turkey. *Journal of Sedimentary Research*, 991-1002.

Zhu, Z., & Woodcock, C. E. (2012). Object-based cloud and cloud shadow detection in Landsat imagery. *Remote Sensing of Environment*, 83-94.

CURRICULUM VITAE

PERSONAL INFORMATION

Surname, Name	: Peker, Emin Atabey
Nationality	: Turkish (TC)
Date and Place of Birth	: 26 January 1982, Kayseri
Phone	: +90 312 207 55 29
E-mail	: atabey.peker@metu.edu.tr

EDUCATION

Degree	Institution	Year of Graduation
BS	ITU Geomatic Engineering	2008
High School	Kucukcalik Anatolian High School, Kayseri	2000

WORK EXPERIENCE

Year	Place	Enrollment
2012-Present	Ministry of Agriculture and Forestry	Expert
2011-2012	General Directorate of Mining Affairs	Survey Engineer
2008-2009	Bechtel-ENKA Joint Venture - Albania	Survey Engineer

FOREIGN LANGUAGES

Advanced English, German (A1)

HOBBIES

Chess, Philosophy